

# *Abnormal Grain Growth*

27-750

Texture, Microstructure & Anisotropy

A.D. Rollett

Contributors: E.A. Holm<sup>1</sup>, D.J. Srolovitz<sup>10</sup>, Y. Arita<sup>2</sup>, L. Chan<sup>6</sup>, S.D. Sintay<sup>3</sup>, T. Bennett<sup>9</sup>, S. Wilson<sup>1</sup>, S. Wang<sup>1</sup>, M. Miodownik<sup>5</sup>, C. Roberts<sup>7</sup>, S.L. Semiatin<sup>8</sup>, K.-J. Ko<sup>4</sup>, W. Frazier<sup>1</sup>, S. Dillon<sup>11</sup>, M.P. Harmer<sup>12</sup>, G.S. Rohrer<sup>1</sup>, S. Bojarski<sup>1</sup>

<sup>1</sup>Carnegie Mellon University, <sup>2</sup>Nippon Steel, <sup>3</sup>Los Alamos Natl. Lab., <sup>4</sup>Seoul National Univ., <sup>5</sup>University College, London, <sup>6</sup>Tescan, <sup>7</sup>Cartech Inc., <sup>8</sup>Air Force Research Lab., <sup>9</sup>Univ. Ghent, <sup>10</sup>U. Penn., <sup>11</sup>UIUC, <sup>12</sup>Lehigh

*Last revised: 21<sup>st</sup> April 2016*



## *Outline*

- Review of possible causes of Abnormal Grain Growth (AGG)
- Variation in stored energy (from plastic deformation)
- Particle and pore pinning
- Complexion transitions
- AGG theory based on energy & mobility
- Coarsening of subgrain structures (giving rise to recrystallization nuclei)
- Appendix: computer codes: MMSP, MEV, SPPARKS



# *Possible Causes of AGG*

- Abnormal grains maintain high mobility on their perimeters:  
Example 1 – the GBs acquire impurities and transition from one structure to a different one, *aka* they undergo a *complexion transition*.  
Requires propagation of the complexion transition from one GB to another. See work by Dillon, Harmer, Rohrer, Frazier *et al.*
- Example 2 – in a subgrain network, a highly misoriented (compared to the matrix) subgrain has high angle, mobile boundaries. See papers by Holm, Wang.
- Matrix pinned from faceting of majority of grain boundaries: abnormal grains escape by de-faceting. However, do the abnormal grains maintain a majority of defaceted boundaries? See work by Henry, Yoon *et al.*
- Matrix pinned with second phase particles: abnormal grains escape how? Or, how do they maintain high mobility?
- A possible explanation of AGG in the presence of pinning particles is where the matrix is stabilized at a size below the Zener-Smith limit because all the particles are on the boundaries, then a grain that can get away will grow abnormally. Roberts, Holm, Hoffman *et al.*
- Matrix grains have a non-trivial stored energy (but nucleation of recrystallization somehow not possible, e.g. insufficient strain): abnormal grains have lower stored energy. Antonione, Bennett, *et al.*
- Special case: AGG in grain-oriented electrical steels has been ascribed to wetting of matrix grains by low angle boundaries in Goss grains. Hwang *et al.*

# Abnormal grain growth microstructure

- Abnormal grain growth is dramatically obvious in Fe-3Si steels.
- The  $\{110\}\langle 001\rangle$  grains are much larger than the matrix grains.
- Pinning of the matrix grains can be achieved with either MnS or AlN particles

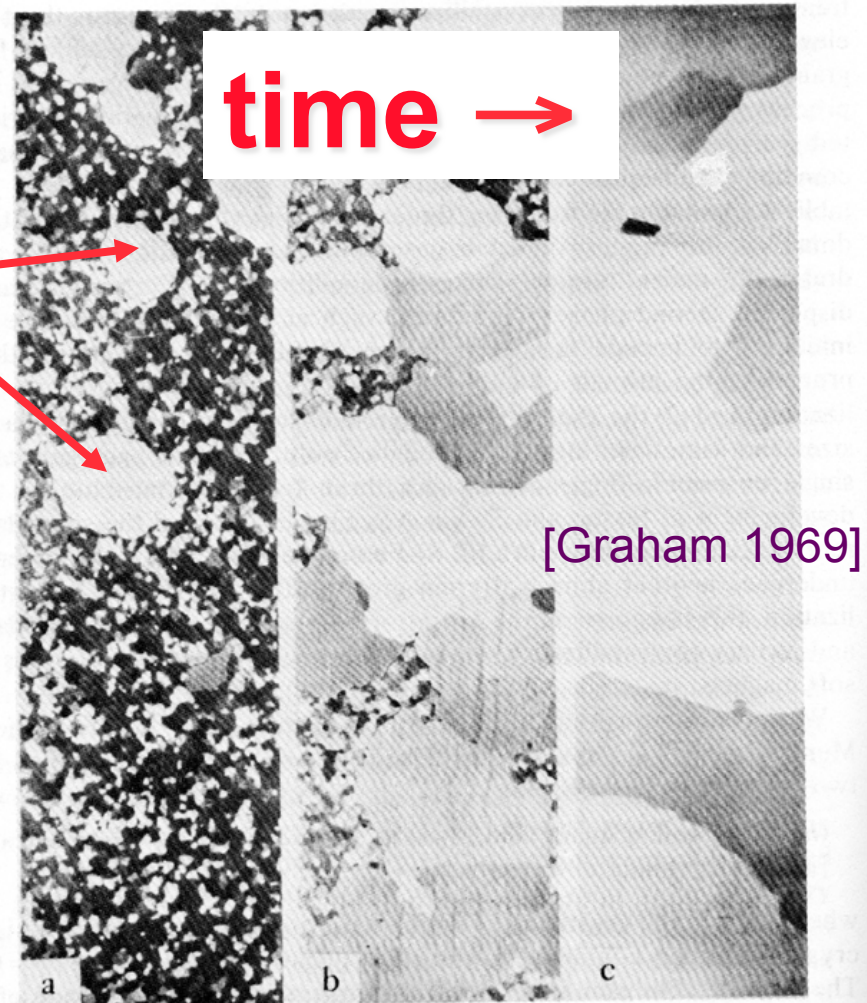
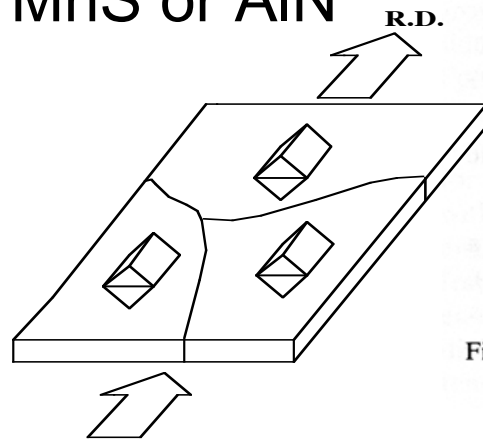
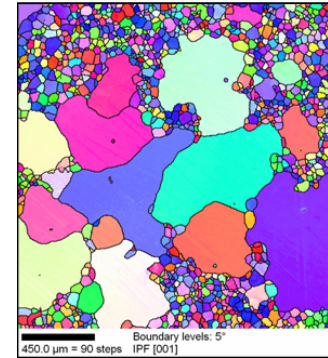
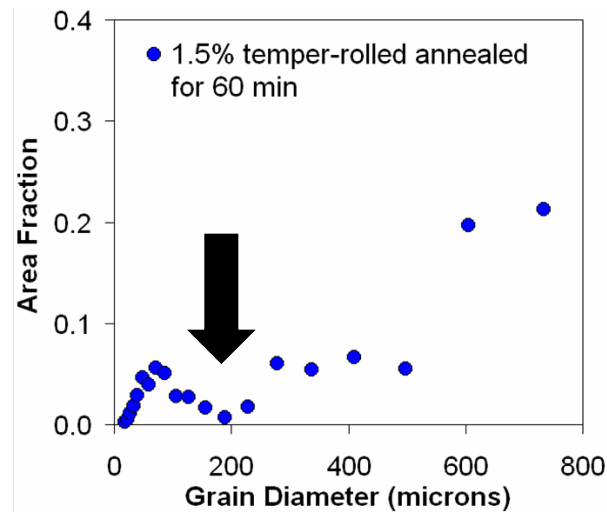


Fig. 5.48. Evidence for the preferential formation of  $(110)[001]$ -oriented grains by secondary recrystallization in 5% Si-Fe (Graham [1969]).

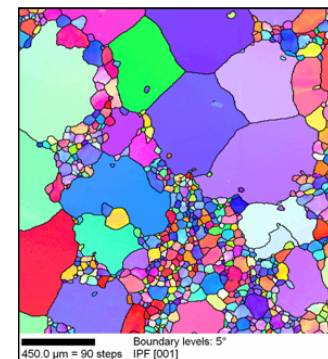
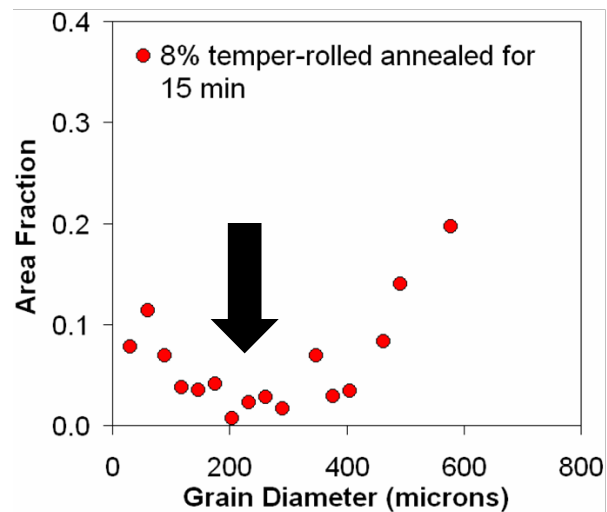
# AGG: Definition

- AGG has occurred when a minority of grains grow much larger than the majority (“matrix”).
- AGG has occurred when the grain size distribution is clearly **bi-modal**.
- Definition above works best when the upper set is a **minority** by number (and then **area-weighting** helps).
- In this material, AGG is a consequence of non-uniform stored energy from the low strain.



1.5% temper-rolled material annealed for 60 min. at 787°C in air.

Bimodal feature typical of AGG



8% temper-rolled material annealed for 15 min. at 787°C in air.

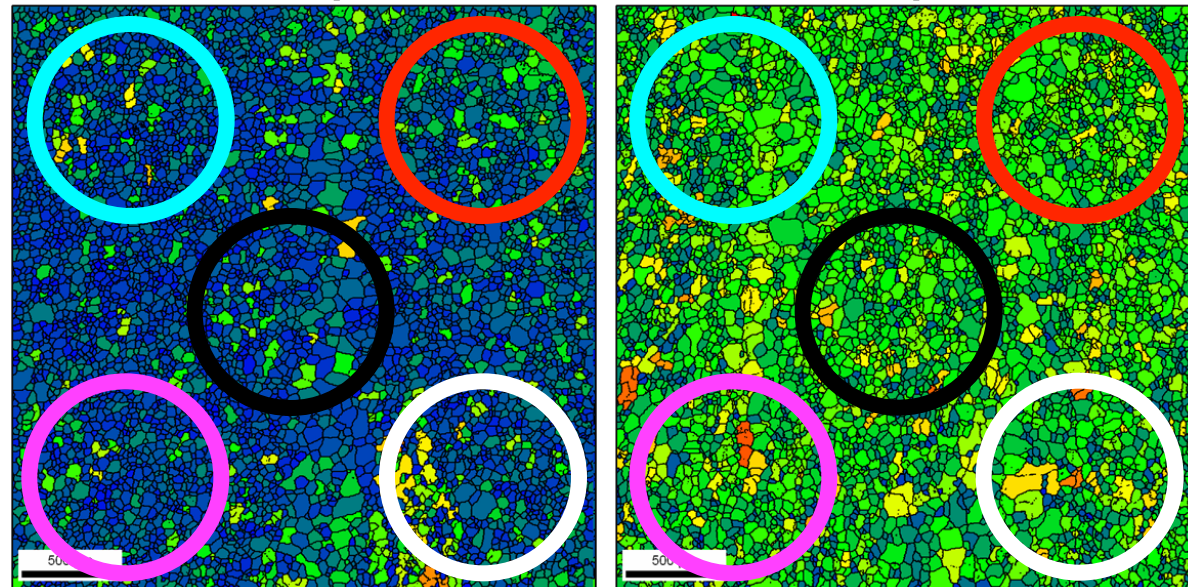
[Bennett 2011]



# *As-deformed Fe-1%Si*

As 1.5% temper-rolled

As 8% temper-rolled



Intergranular variations in GOS greater in 8% temper-rolled material.

AGG is a local phenomenon.

AGG occurs more readily in 8% material because of greater local intergranular orientation gradients.

Density of abnormally large grains will be higher in the 8% material.

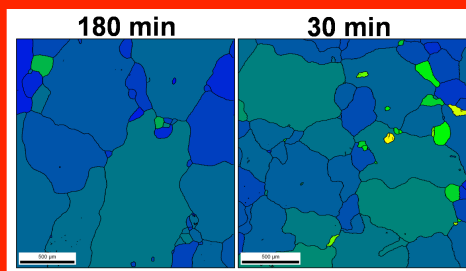
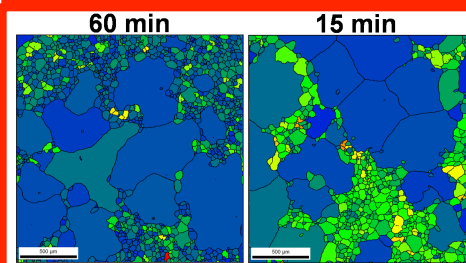
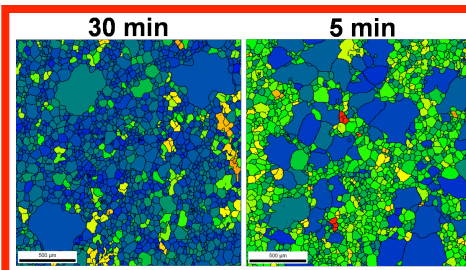
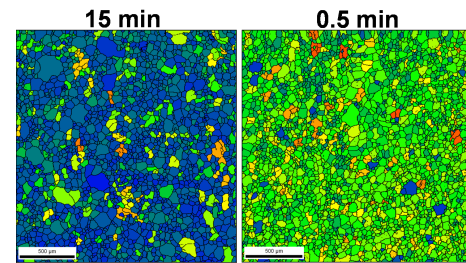
Presence of several same-stored-energy regions in 1.5% material leads to lower density of abnormally large grains.

Maps shaded according to GOS.

Grains that grow abnormally already exist in the as-deformed material.

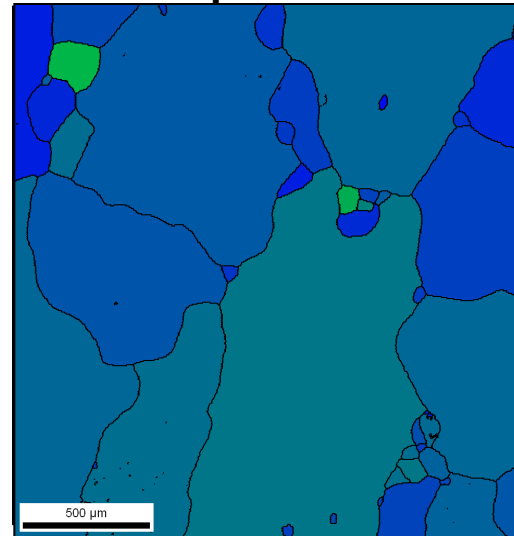
[Bennett 2011]

# Orientation Spread, Fe-1%Si



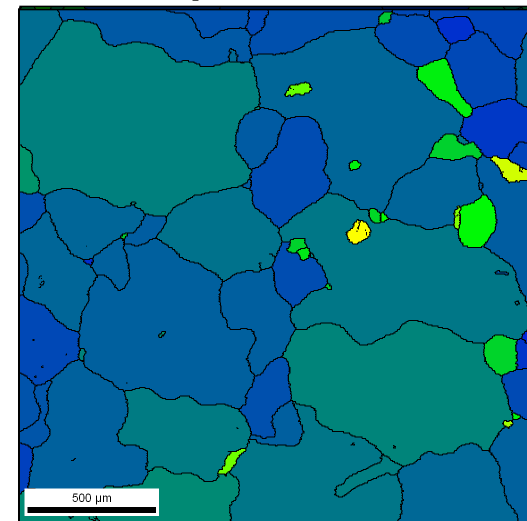
1.5% and 8% temper-rolled Fe-1%Si, annealed in air at 787°C for various times.

1.5% temper-rolled

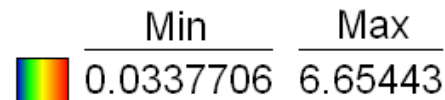


180 min.

8% temper-rolled



30 min.



[Bennett 2011]

AGG proceeds by low GOS, soft grains, consuming their high GOS, deformed neighbors. Overall GOS decreases with annealing time.

# Pinning & AGG

Calvet J and Renon C  
(1960) "Discontinuous  
grain growth in Al-Cu  
alloys" *Mémoires  
Scientifiques Revue de  
Métallurgie* 57 3

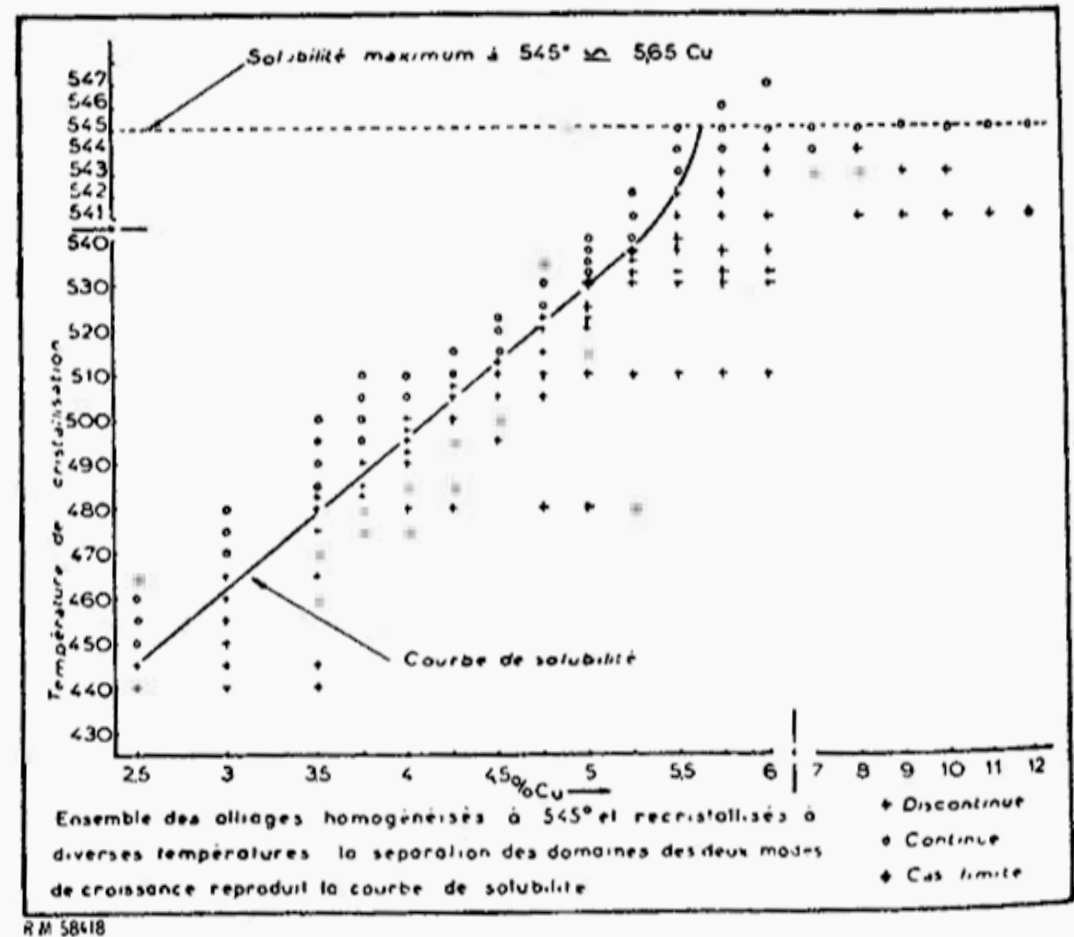
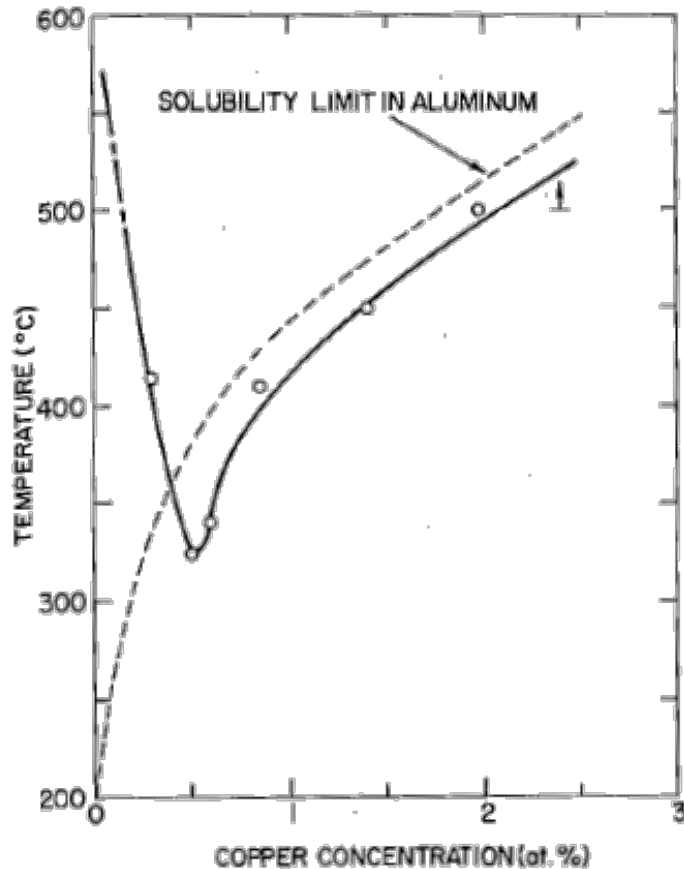


Fig. 4.

- Still to be explained is the role of particles in AGG. Why is it that the phenomenon is so often (but not always) associated with annealing in the proximity of a solvus?

# Background



**Effect of Cu concentration on the temperature at which AGG starts in Al-Cu films. Gangulee et al. (1972).**

## Pinned microstructures

In pinned microstructures, the onset of AGG has been strongly correlated to the solution solvus.

*Traditional explanation:*

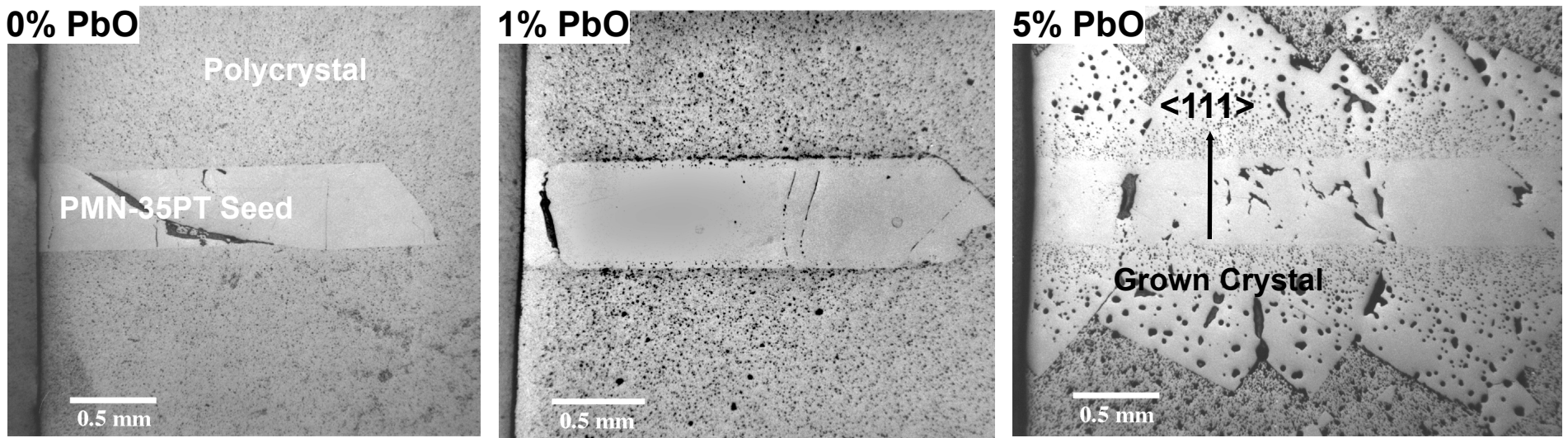
- Second-phase particles begin dissolving
- The pinning force is decreased due to smaller particle size
- Select boundaries are then able to break free.

*However, simulations have shown that AGG can occur:*

- ... in particle-pinned microstructures without particle dissolution (Roberts et al.)
- ... in solute-pinned microstructures without particles (Kim et al.)



# Crystal Growth in $Pb(Mg_{1/3}Nb_{2/3})O_3$ - $PbTiO_3$ [PMN-PT]



**{111} seeds PMN-35PT + xPbO 1150°C 10hrs**

\*Courtesy E. Gorzkowski (PhD thesis 2005), M. Harmer, Lehigh Univ.;  
J. Amer. Ceramic Society, **89**, 2286-2294



## *Role of Particle Pinning*

- Well dispersed second phase particles (including voids) are well known to be efficient at stabilizing grain networks.
- Smith-Zener analysis provides the basic theory but is based on randomly placed particles, with respect to the boundaries.
- Particle pinning investigated in Waspaloy\*: 2 key observations were that (a) the density of particles on boundaries was higher than random, and (b) AGG occurred.

Zener, C. (1948). Private communication to C.S. Smith.  
*Trans. Metall. Soc. AIME* **175**: 15.

- Roberts, C. G. 2007, 'Grain Growth and the Zener Pinning Phenomenon: A Computational and Experimental Investigation', .PhD thesis, Carnegie Mellon Univ. 2007

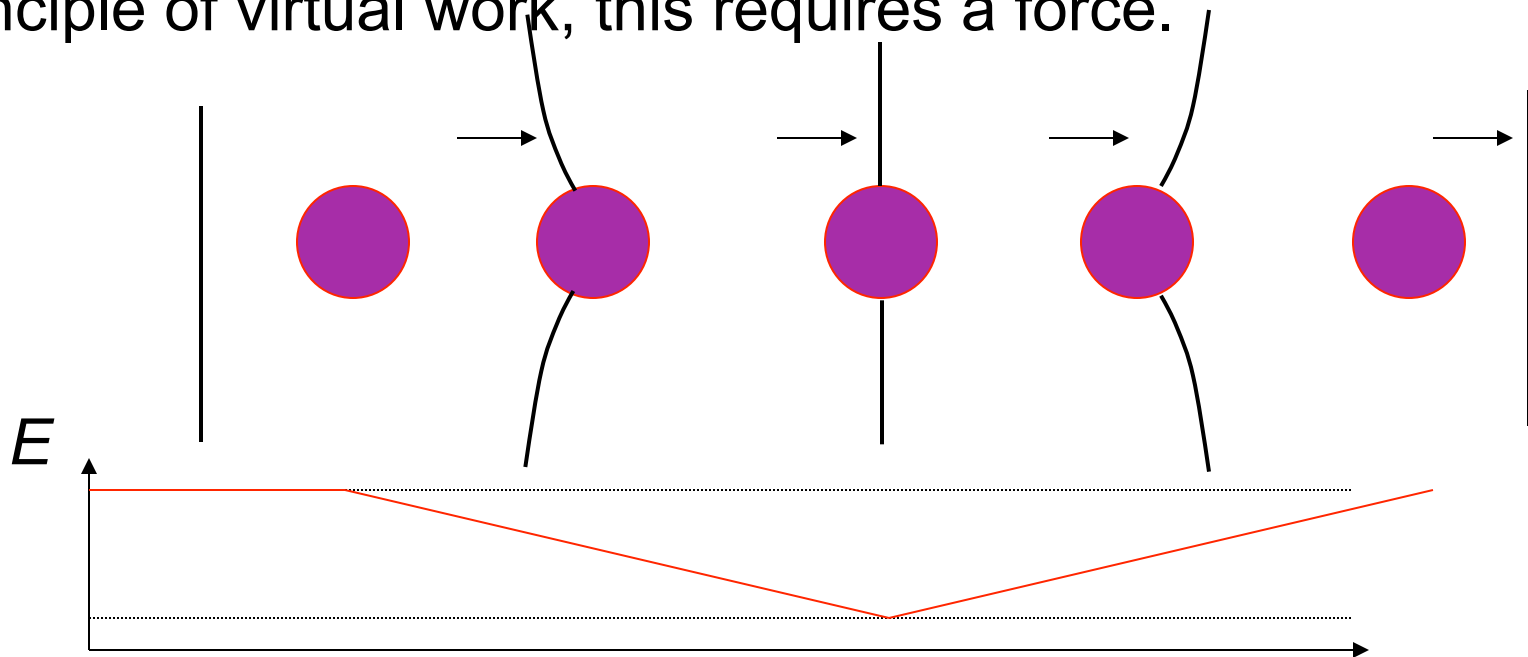
D.A. Porter and K.E. Easterling, *Phase Transformations in Metals and Alloys*, (1981) Van Nostrand Reinhold Co: New York.  
P.A. Manohar, M.Ferry and T. Chandra, *ISIJ Intl.*, **38** (1998), 913.

## *Notation*

- $r$  particle radius
- $R$  grain size (or domain size)
- $R_{max}$  maximum (limiting) grain size (or domain size)
- $f$  or  $v_f$  volume fraction (of particles)
- $\gamma$  grain boundary energy (or domain wall energy)
- $\theta$  angle made by boundary at pinning point
- $P_{drag}$  drag force
- $\Delta E$  Energy trap
- $\Delta U$  Change in energy of system
- $N_V$  Number density of voids
- $N_A$  Voids per unit area of domain wall

## *Smith-Zener: Basics*

- Why do particles have a pinning effect?
- Answer: once a boundary has intersected with a particle, a certain amount of boundary area is removed from the system. In order for the boundary to move off the particle, the “missing area” must be re-created. This restoration of boundary area requires an energy increase. Through the principle of virtual work, this requires a force.



## *Analogy to Pinning Effect*

- Remember how to blow bubbles?
- You take a ring on the end of a stick, dip the ring into a soap solution to get a film inside the ring, and then blow bubbles out of the ring.
- The soap+water film “sticks” to the ring for the same reason as a grain boundary (or domain boundary) sticks to a particle: it is simply trying to minimize its surface area.

# Boundary-particle interaction

- The drag effect of the particles can be quantified by considering a force balance at the (immovable) particle surface.
- Length of boundary attached to a particle  
 $= 2\pi r \cos \theta$ .
- Force per unit length exerted by boundary on particle  $= \gamma \sin \theta$ .
- Total force =  
 $\text{length} * \text{force} \cdot \text{length}^{-1}$ .
- For  $\theta=45^\circ$ , the reaction force on the boundary is at a maximum.
- *Maximum force =  $\pi\gamma r$*

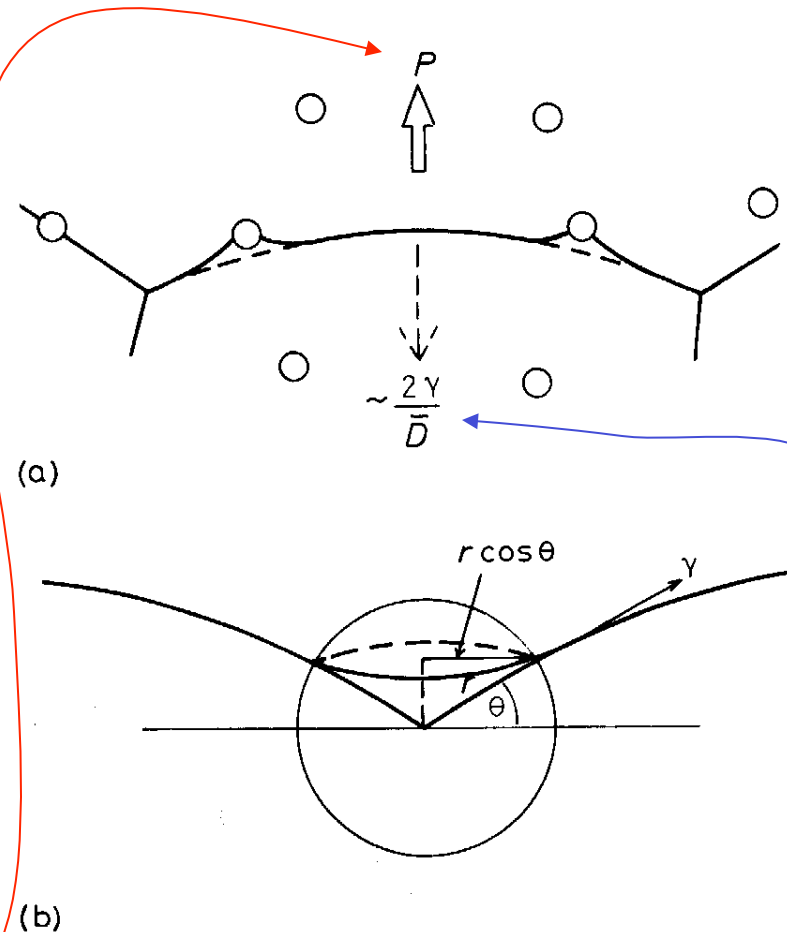


Fig. 3.30 The effect of spherical particles on grain boundary migration.

*grain growth pressure*

## *Drag pressure*

- To find the point at which grain growth stagnates, we have to equate the driving force (pressure, really) to the drag pressure.
- We cannot equate a per-particle force to a pressure, so we must make an assumption about the fraction of boundary area that intersects with particles.
- Smith-Zener assumption was that the boundaries can be assumed to intersect randomly with the particles (not always true, but a good place to start!).
- Stereology (again!): the fraction of particles with radius  $r$  and volume fraction  $f$  that intersect unit area of a random oriented section plane is  $3f/2\pi r^2$ .
- Multiply the maximum force per particle by the number per unit area of boundary to obtain the drag pressure:

$$P_{\text{drag}} = \pi\gamma r * 3f/2\pi r^2 = 3f\gamma/2r$$

## *Stagnation of grain growth*

- The point at which grain growth will stop is (approximately) determined by a balance between the driving force (pressure) for grain growth,  $\gamma/D$ , and the drag force (pressure).

$$3f\gamma/2r_{particle} = \gamma/R_{stagnation} = \gamma/R_{max}$$

$$\Leftrightarrow R_{max} \leq 2r/3f, \text{ or,}$$

$$D_{max} \leq 4r/3f \text{ (Smith-Zener Equation)}$$

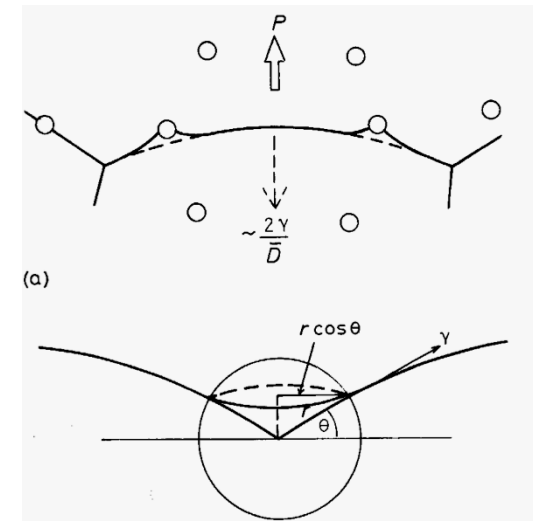
- Note that Underwood gives a more precise analysis and arrives at a *larger* limiting grain size (in fact, double the above estimate),

$$R_{max} \leq 4r/3f$$

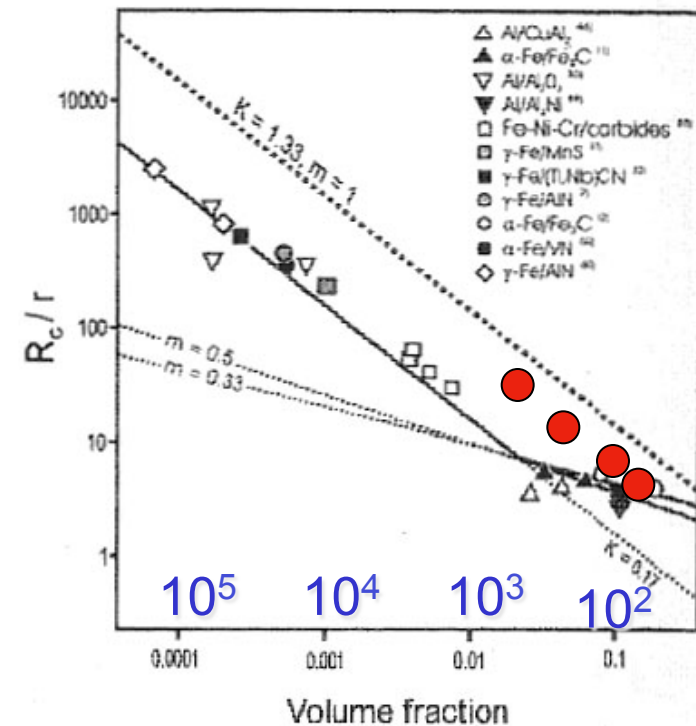
which illustrates the approximate nature of the derivation given.

# Grain Size Control

- Upper right panel illustrates the physics of boundary-particle interaction:  $D_{\text{pinned}} \sim d_{\text{ppt}}/V_f$
- Lower right panel shows summary of experimental data, together with only available parallel calculations w/Monte Carlo in 3D
- Investigating the significant range of particle volume fraction drives us into the petascale; linear sizes of the required mesh indicated on graph
- Monte Carlo method (Potts) offers only practical algorithm



● Previous parallel results: Miodonwik



Experimental review: Manohar et al. ISIJ 1998



## Grain growth kinetics

- The effect of the presence of fine particles is to slow down, and eventually stop grain growth.

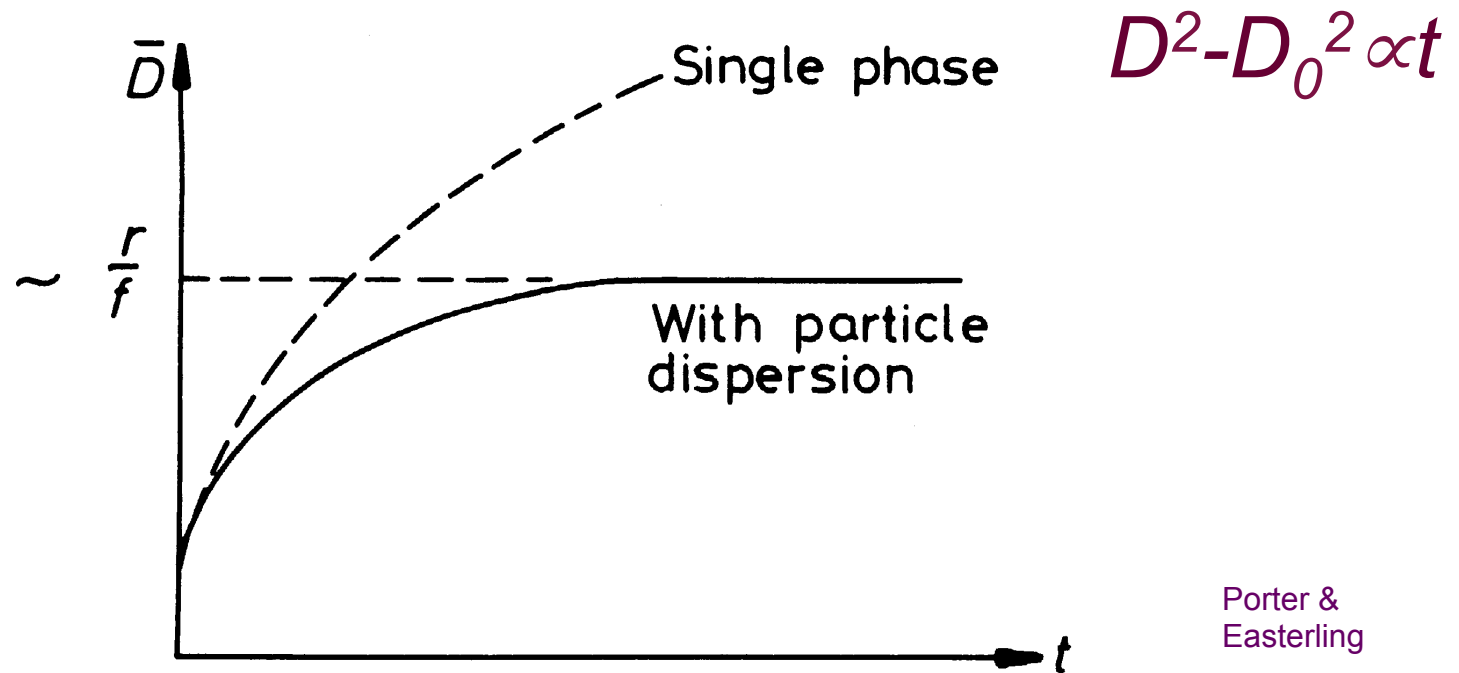


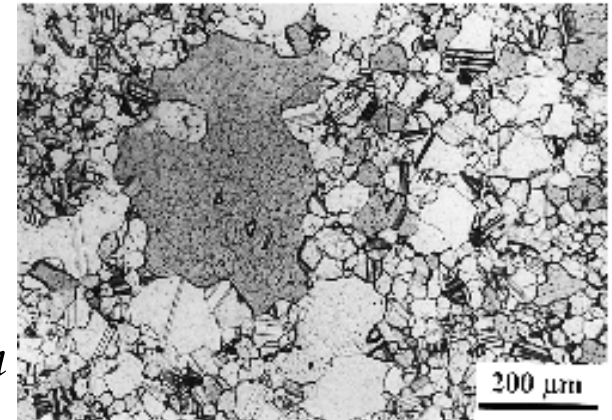
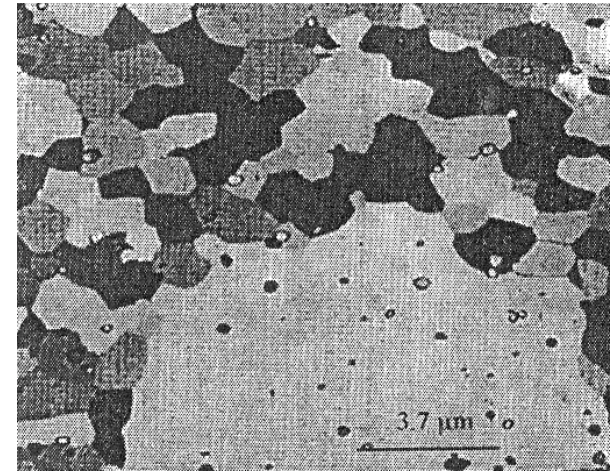
Fig. 3.31 Effect of second-phase particles on grain growth.

## *Pinning: technological impact*

- The technological impact of particle pinning is considerable.
- Most commercial structural materials, especially for elevated temperature service, rely on fine second phase particles to maintain a fine grain size.
- Limitations: particle dispersions are less effective when not stable, or not fully stable.
- A common observation: abnormal grain growth frequently occurs in materials annealed close to a solvus, where a particle dispersion is barely stable.
- Pinning of GBs by pores is equally effective. However, pores can also coarsen via diffusion along GBs. Therefore grain growth in ceramics is normally limited by pinning at pores, which in turn is limited by pore densification and/or coarsening. If, however, GBs escape from the pinning effect then abnormal grain growth can occur. This tends to leave pores behind in the matrix, which becomes a signature of AGG (in ceramics at least).

# Particles and AGG

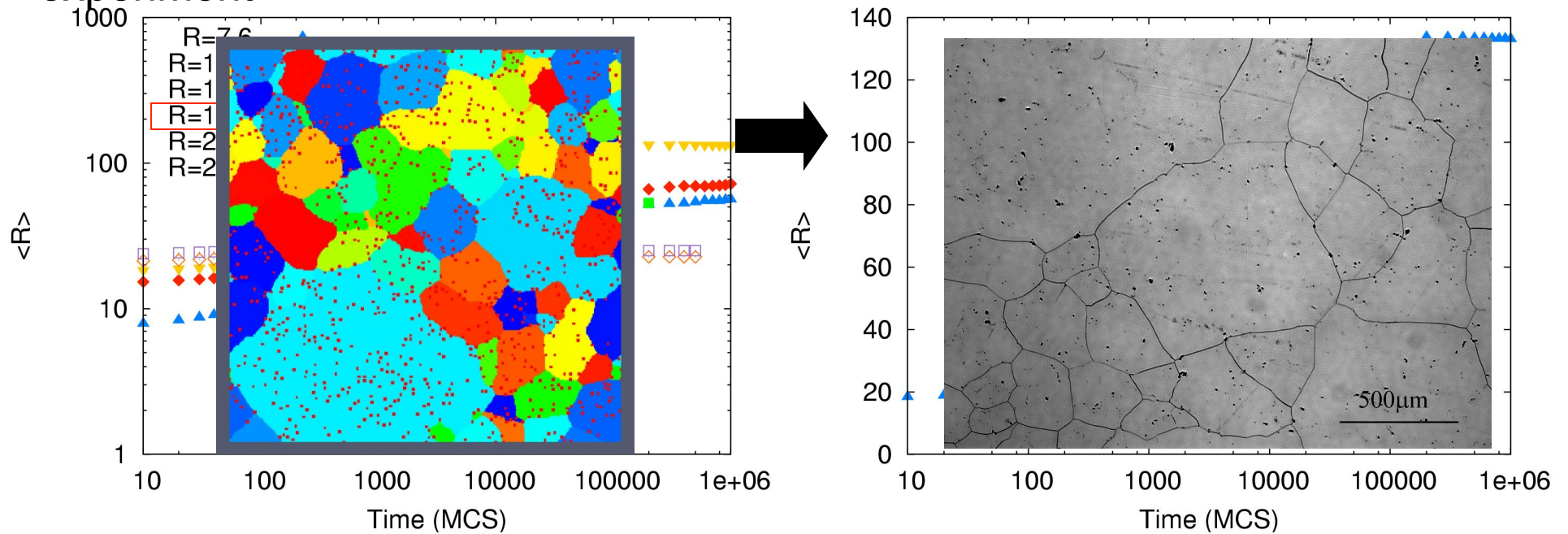
- AGG is often observed in particle-containing systems
  - Near the particle solvus  $\Rightarrow$  local dissolution?
  - Far from the particle solvus  $\Rightarrow$  inhomogeneous particle distribution?
  - In both cases, theories center around how *disruptions* in the Zener-pinned structure cause AGG.
- Large-scale simulations of pinned systems - *with no disruptions* - showed AGG at very long times (Roberts - CMU).



$\Rightarrow$  How do static particles affect the growth of abnormal grains?

# Comparison of Expt. with Simulation

A transition from NGG to AGG was observed in both the simulations and experiment



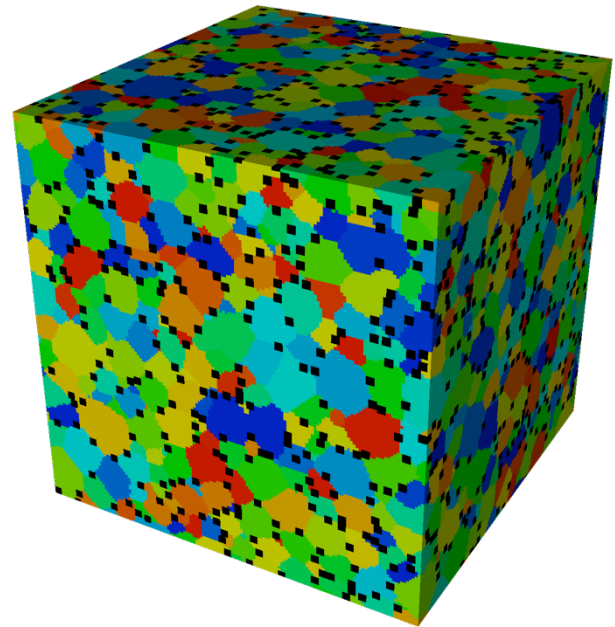
Initiation of AGG was caused by grain size advantage and/or non-random particle distributions on grain boundaries. More specifically, if the grain size is smaller than the Smith-Zener limit, but the structure is pinned by the larger-than-random density of particles on boundaries (to match expts.), then it is possible for a large grain to escape and become “abnormal”.

Simulation: isotropic GB properties; temperature = 1.5; particles size = 27 voxels; volume fraction of particles = 6%, 70% of particles were located *on boundaries*; image taken at 100,000 MCS.

Roberts (2007), PhD thesis, CMU

## *Simulation parameters, take 2*

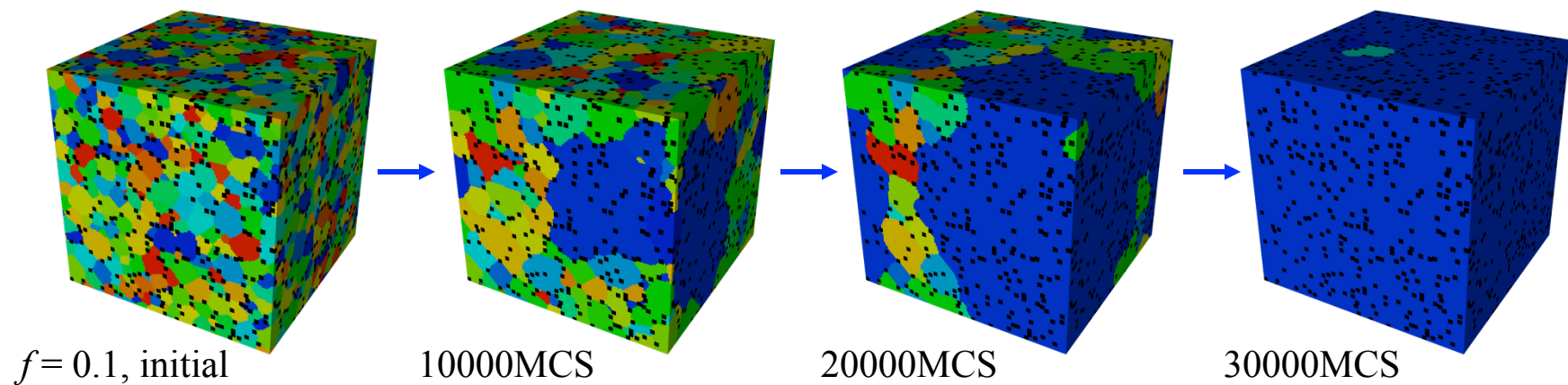
- Begin with an equiaxed polycrystalline microstructure
  - Boundary properties are uniform and isotropic, random grain texture
  - Note that there *AGG is never observed in the absence of particles*
- Deposit particles at random on the grain boundaries
  - At sufficiently high particle fractions, the system will be pinned
  - Note that this is a *stronger pinning situation than Zener pinning* because of the non-random spatial correlation of particles and boundaries
- Allow grains to evolve via normal grain growth physics





## *Results: Microstructural evolution*

- AGG occurs
- The abnormal grain size far exceeds the Zener pinned grain size

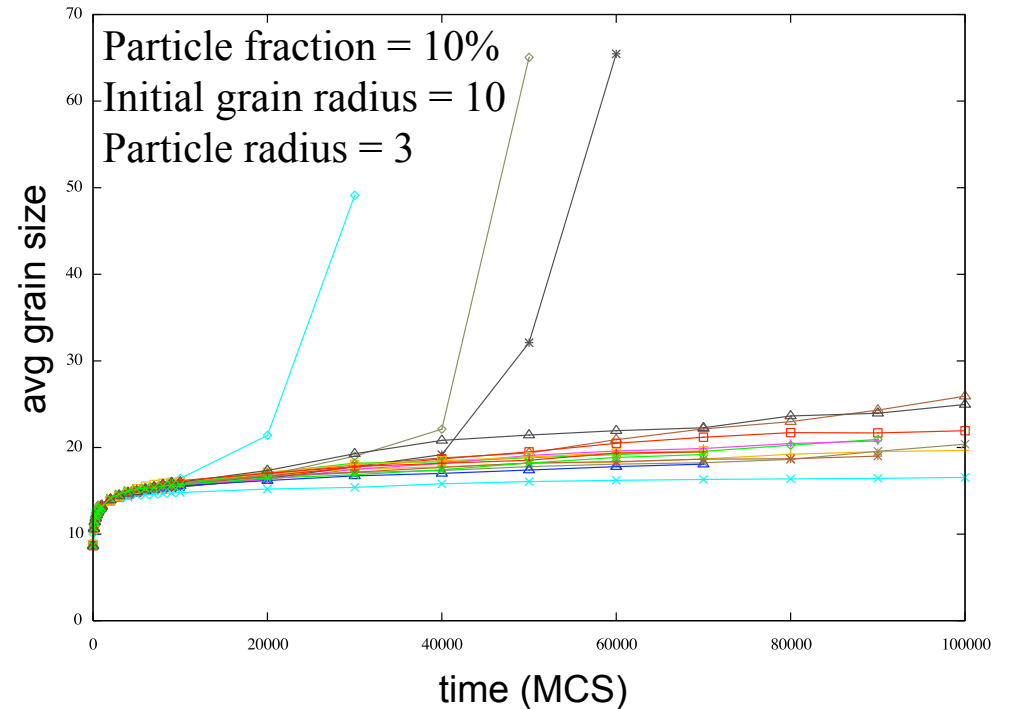


- This growth mode would not occur in the absence of particles.

⇒ A static particle dispersion inhibits normal grain growth but causes abnormal grain growth!

## Results: Growth kinetics and frequency

- The system initially grows to its Zener pinned grain size.
- AGG incubation time is long and variable; all of these runs eventually grow abnormally (by  $10^6$  MCS).
- AGG is rare: In this system, about 1 in 22,000 grains grows abnormally.
- The abnormal grain consumes all others, so we see only one event per system.



“Particle-Assisted Abnormal Grain Growth”, E.A. Holm, T.D. Hoffmann, A.D. Rollett, and C.G. Roberts (2015), in S. Fæster *et al.* (eds.): Proceedings 36<sup>th</sup> Risø Intl. Symp. Materials Sci.

# *The causes of abnormal grain growth*

- What permits a particular grain to grow abnormally?
  - **Energy** advantage (i.e. greater driving force for growth)
    - Elastic or plastic strain energy
    - Surface energy
  - **Mobility** advantage (i.e. grows faster than competitors)
    - Intrinsic – boundary structure
    - Extrinsic – solutes, particles
- Abnormal growth can occur only when the growth advantage can persist as the grain grows into new neighborhoods.

*Abnormal grain growth requires a **growth advantage** and a **persistence mechanism**.*



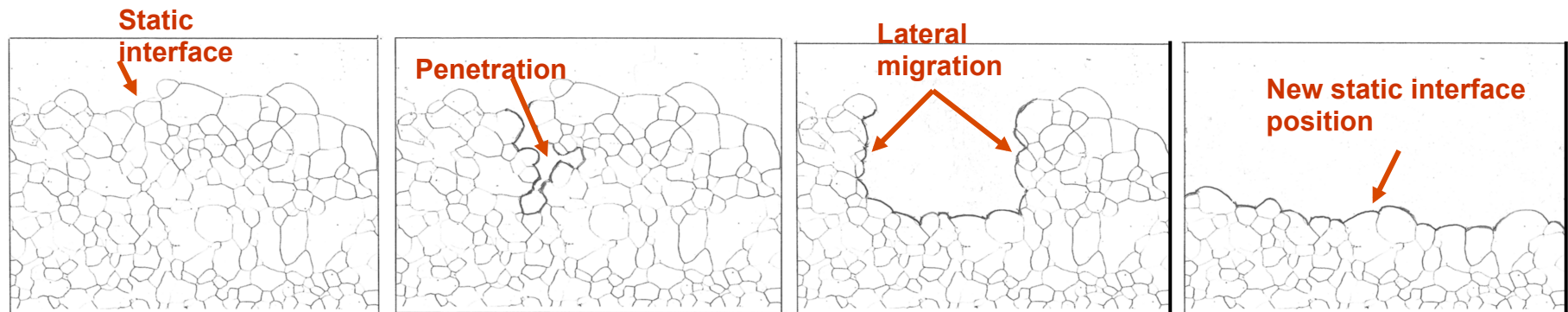
# Model for particle-mediated AGG

- All grains – *but not all grain boundaries* – are initially pinned; however, thermal fluctuations of the boundaries can occur.
- A grain boundary that fluctuates off of its pinning particles can move freely, consuming other unpinned boundaries and destabilizing pinned boundaries.

⇒ Mobility advantage.

- If the free boundary belongs to a grain that is inclined to grow, it will grow at the expense of its pinned neighboring grains.
- As the growing grain increases in size, it accesses ever more avenues for growth.

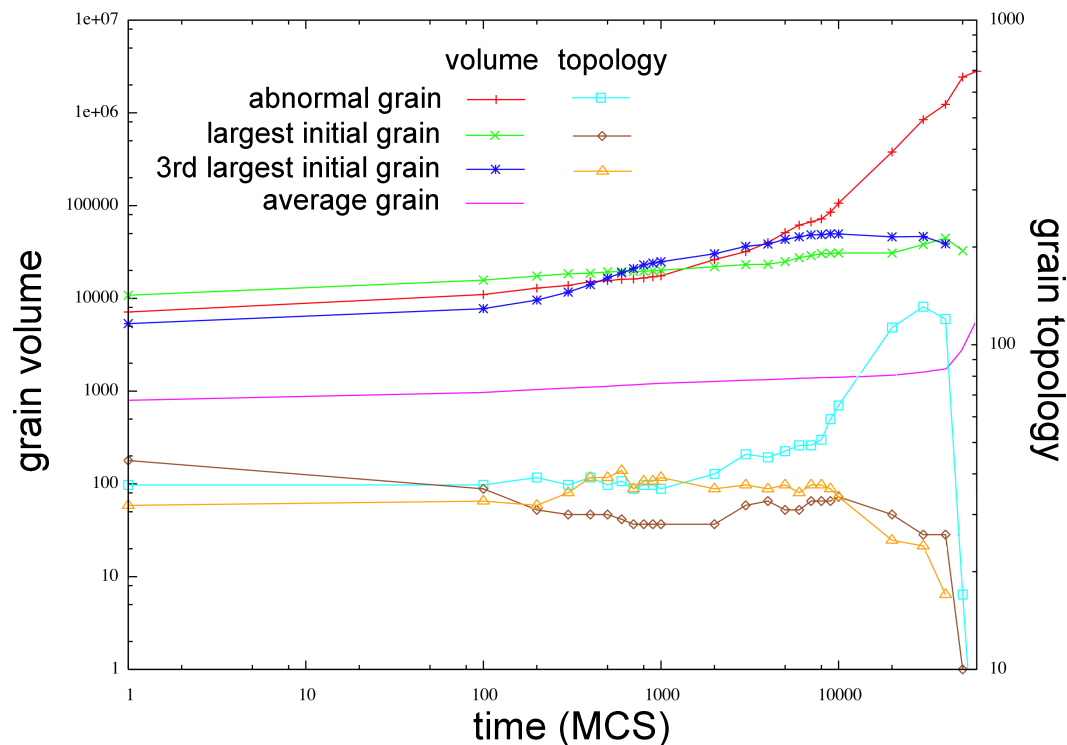
⇒ Persistence mechanism.



[courtesy Prof. Bevis Hutchinson]

# Effect of initial grain size on particle-mediated AGG

- For particle-assisted AGG, the abnormal grains should begin as grains with a high driving force for growth, i.e. large grains.
- Simulations confirm that the abnormal grains are usually among the largest initial grains.



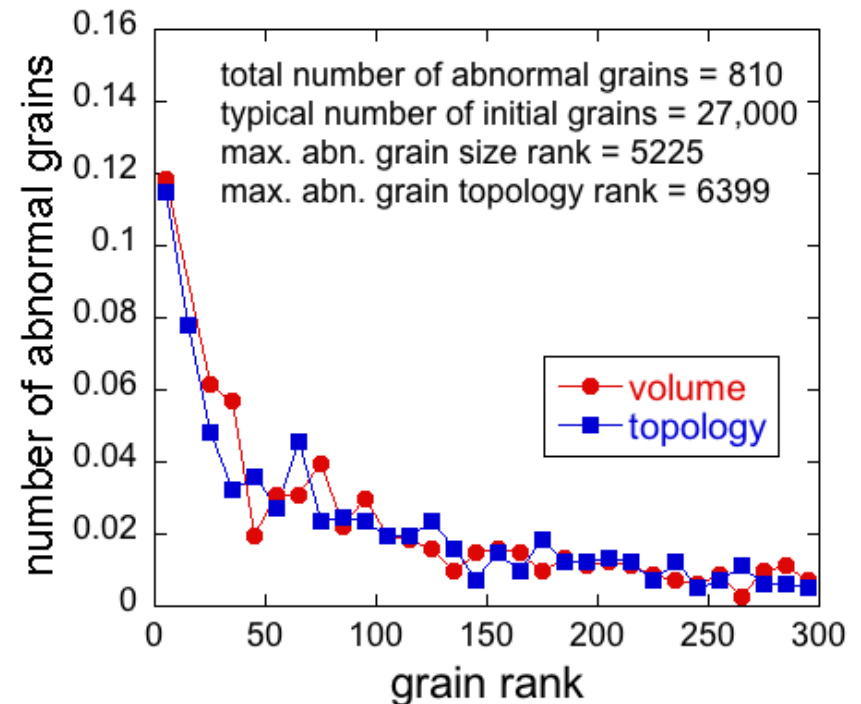
In this particular microstructure, the abnormal grain begins as the second largest grain, in both size and number of neighbors.

\* Note: In normal GG, even a large size advantage does not guarantee AGG.  
"Particle-Assisted Abnormal Grain Growth", E.A. Holm, T.D. Hoffmann, A.D. Rollett, and C.G. Roberts (2015), in S. Fæster *et al.* (eds.): Proceedings 36<sup>th</sup> Risø Intl. Symp. Materials Sci.

# *Which grains become abnormal?*

- Abnormal grains are typically among the largest – in volume and number of neighbors.
- There is a substantial spread:
  - We cannot predict which grain grows abnormally.
  - We cannot even predict which group of grains likely contains the incipient abnormal grain

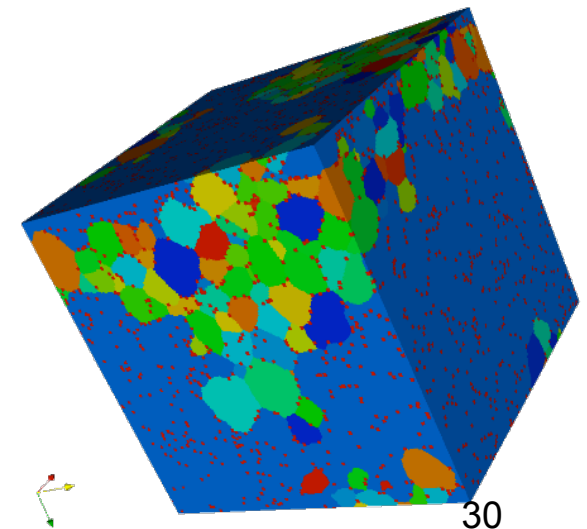
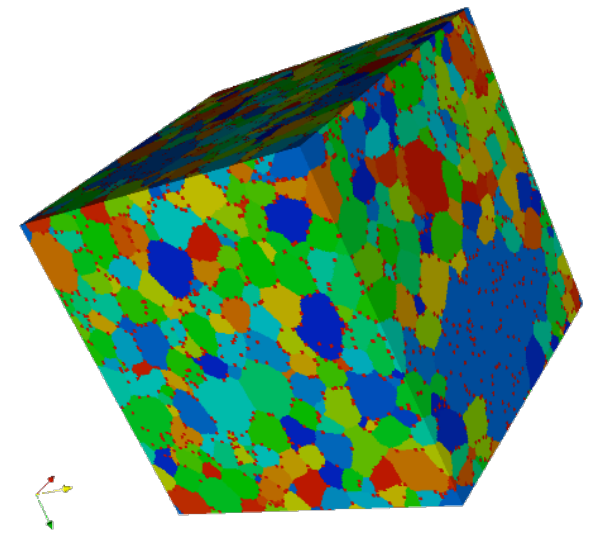
⇒ Abnormal grain growth depends on more than individual grain characteristics: The neighborhood is critical as well.



# System scaling

- This system scales with the area fraction of the particles on the boundaries, which is given by  $fR_0$
- We have examined  $f = 0.1$ ,  $R_0 = 10$
- In extending the simulations to  $f = 0.05$ ,  $R_0 = 20$ , the system grew to a pinned state then stopped.
- However, after  $29 \cdot 10^6$  MCS abnormal grain growth occurred.
- Because the initiating event is fluctuational, the incubation time scales exponentially with grain size.

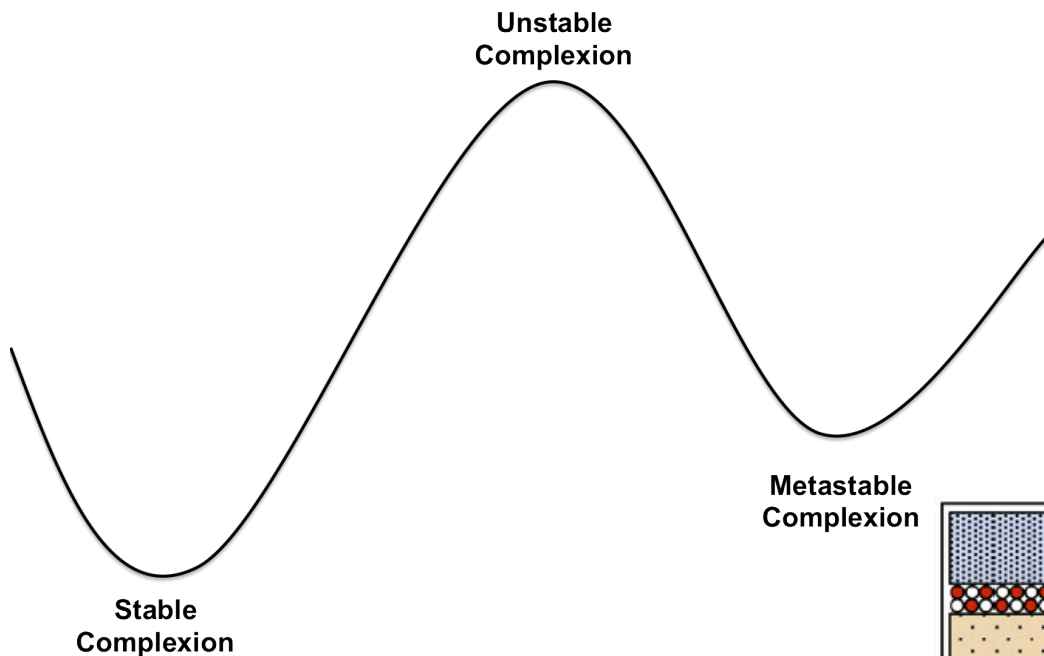
⇒ We expect particle-stimulated AGG to increase as grain size decreases, consistent with experimental observations.



# *GB Complexions and AGG*

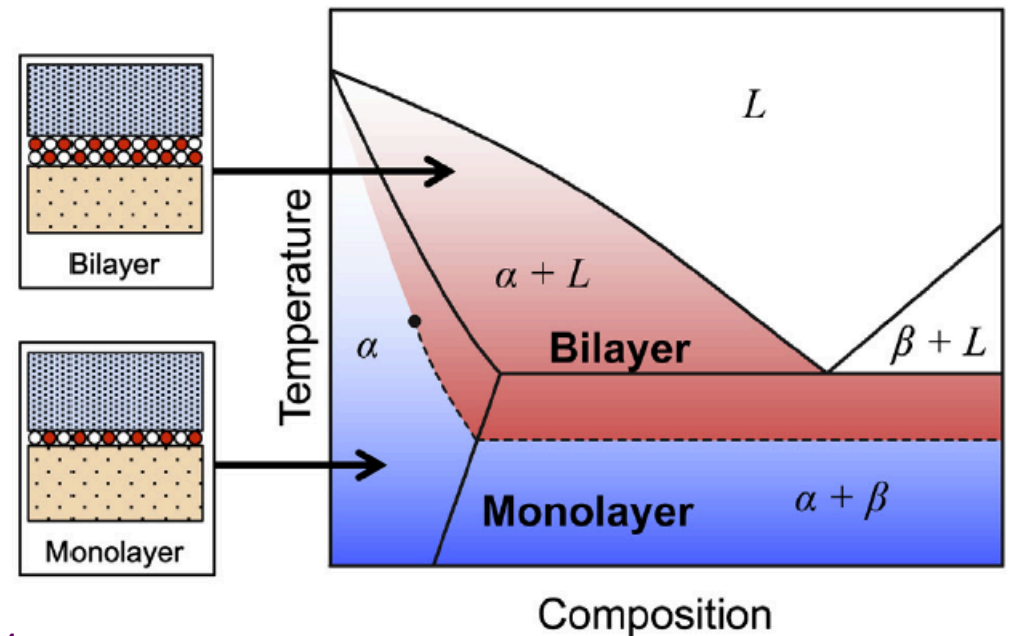
- A notable achievement by Dillon, Harmer *et al.* has been to delineate several types or “complexions” of grain boundary according to impurity content and structure. *J. Amer. Ceram. 89 3885 (2006)*.
- Note that it is commonly accepted that segregation of impurities to GBs, in metals, results in solute drag, i.e. lower effective mobility. For many solutes, increases in recrystallization temperature are apparent above a few parts per million.
- Counter to (metallurgical) intuition, for sufficiently high loading, boundaries in certain ceramics can be significantly more mobile than in the pure material.
- A “complexion” denotes a definite grain boundary structure (e.g., 1, 2 or 3 layers of impurity atoms) that is in equilibrium with the adjoining material. It is *not* the same as wetting, which simply means penetration of a boundary by the impurity with no limit on volume fraction.
- Just as in the model, if a small fraction (1%?) of GBs are highly mobile then AGG ensues. The crucial feature of the situation is, however, that the abnormal growth of a given grain cannot be sustained unless the complexion transition propagates from one grain boundary to (a reasonable fraction) of its adjoining boundaries. *Frazier et al. (2015), 'Abnormal grain growth in the Potts model incorporating grain boundary complexion transitions that increase the mobility of individual boundaries', Acta Mater., 96 390.*

# Grain Boundary Complexions



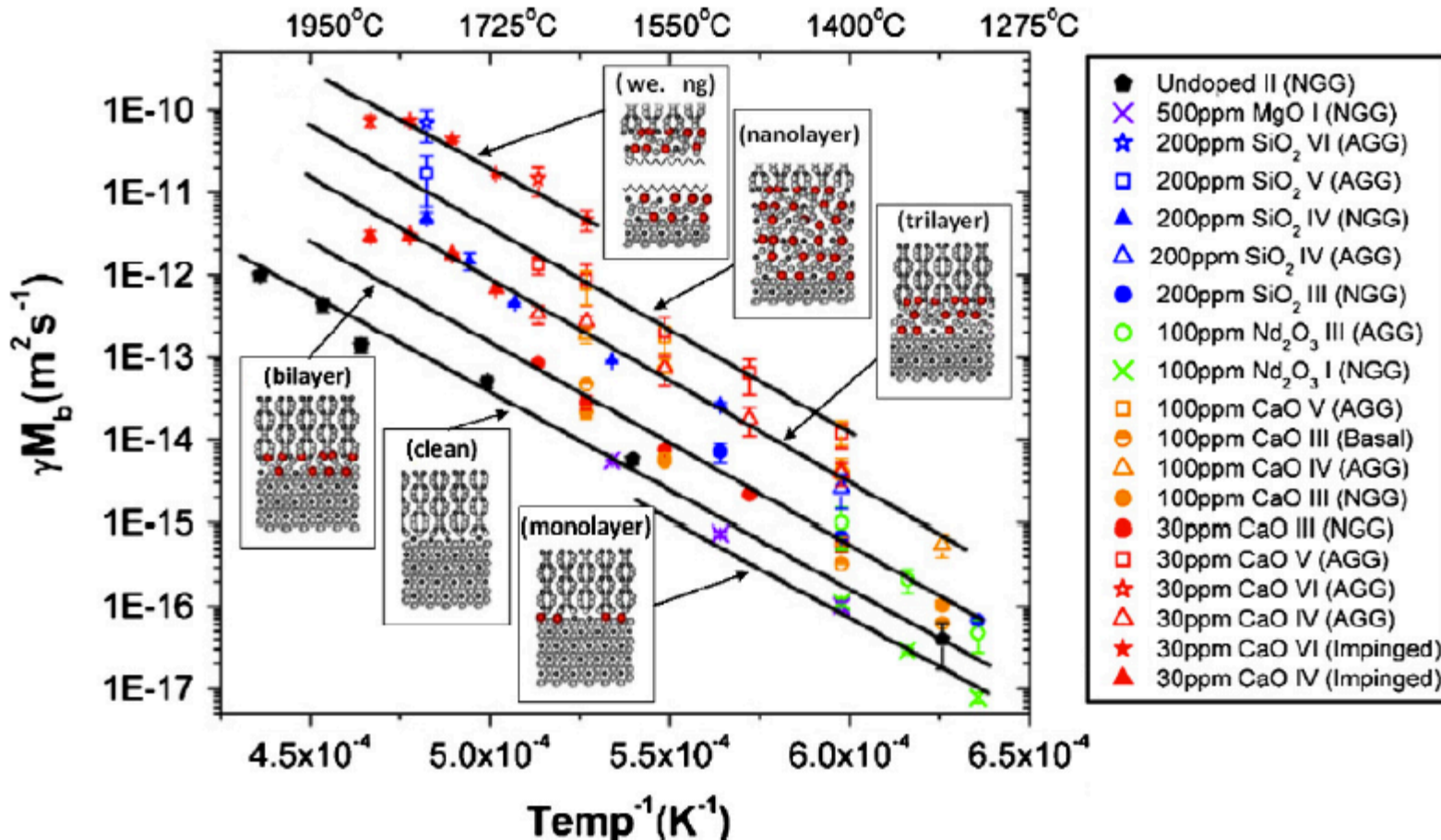
Complexion transitions occur when temperature and composition change such that one complexion becomes metastable with respect to another.

This can change some grain boundary properties drastically, especially mobility and energy





# Complexion Transitions and AGG



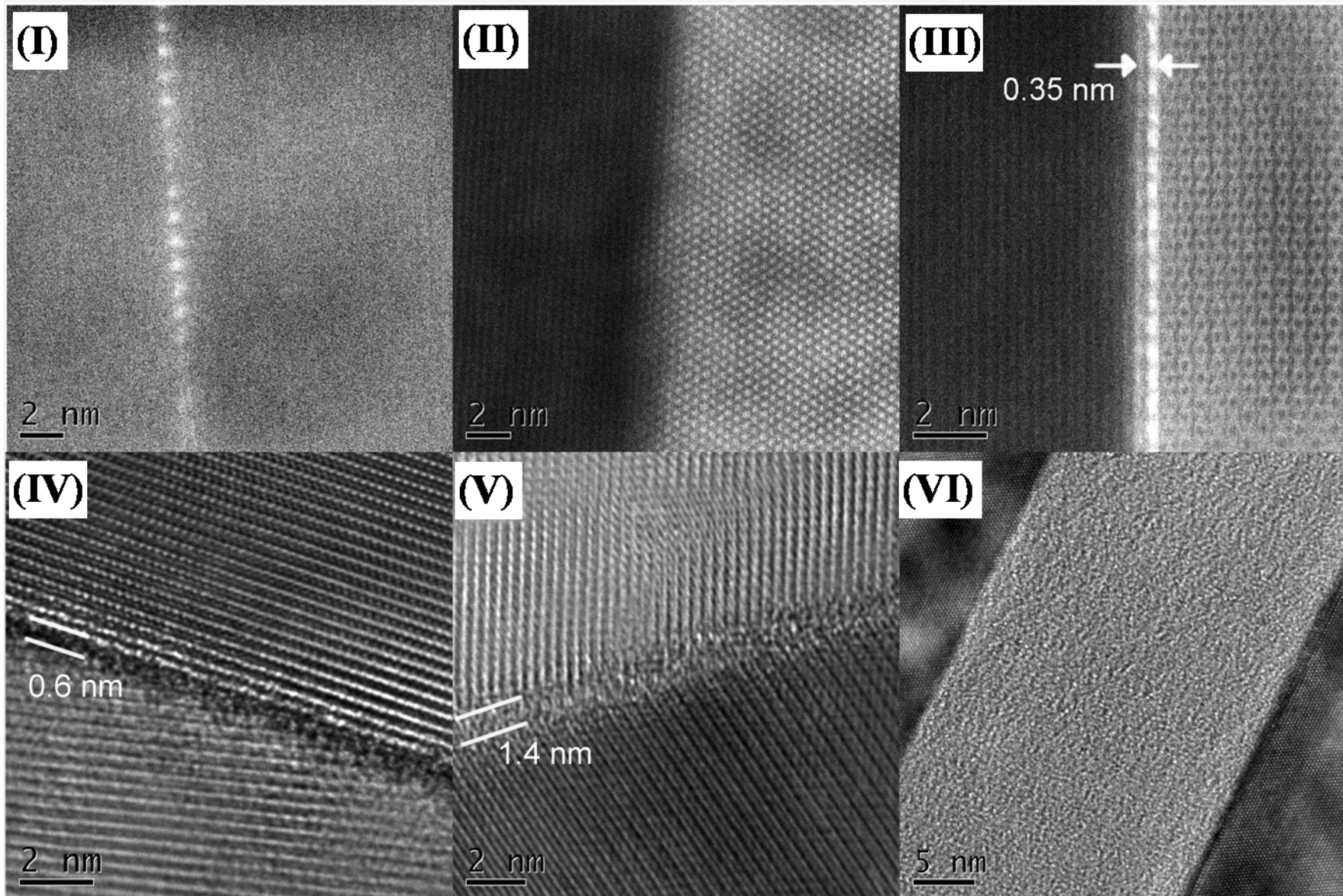
Grain Boundary Mobility Increases as Complexions Get Closer to Complete Wetting, but the Slope with Respect to Temperature Remains the Same!

Why?

Dillon & Harmer, *J. Amer. Ceram. Soc.* 2008 **91** 2304

S.J. Dillon, M. Tang, W.C. Carter, M.P. Harmer, "Complexion: A new concept for kinetic engineering in materials science," *Acta Mater.* **55** 6208-6218 (2007).

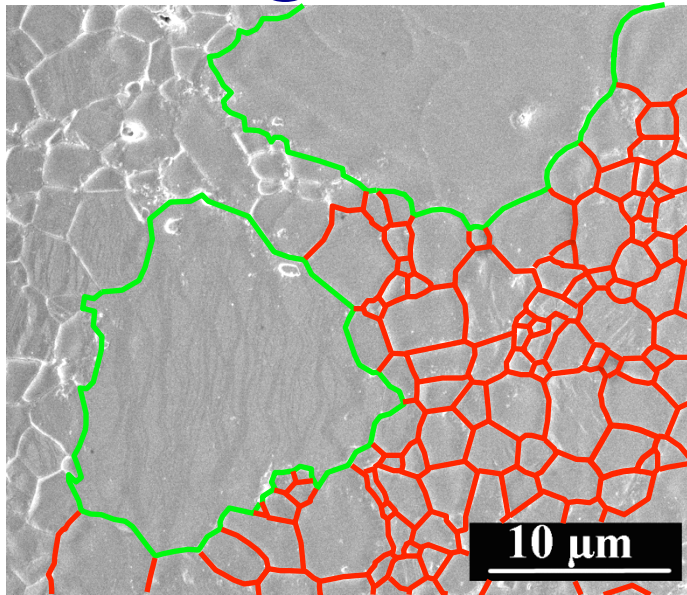
# *Aberration-Corrected Electron Microscopy*



*Courtesy: M.P. Harmer*

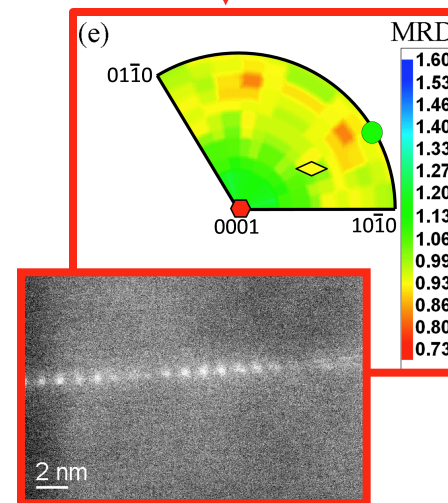
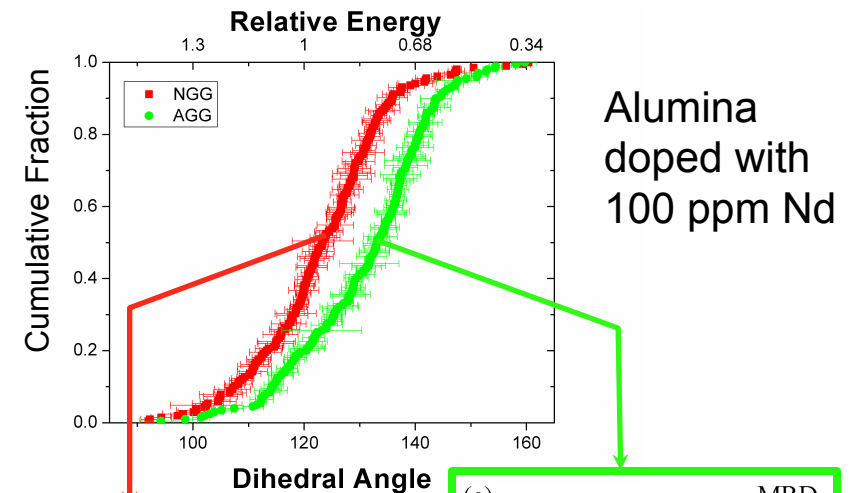


# Complexion: Energy and Mobility Changes

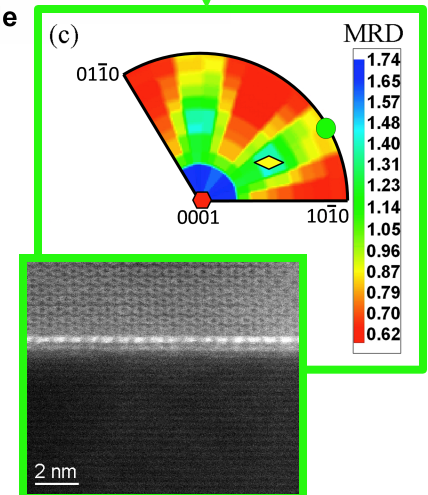


Grain boundary composition, structure, energy, mobility, and distribution linked.

Controlling complexion transitions offers possibility of microstructure control



Complexion I:  
mono layer  
segregation, low  
mobility



Complexion III:  
bilayer  
segregation,  
higher mobility

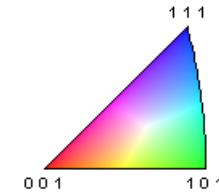
Dillon *et al. Acta Mater.* **55** (2007) 6208-18.

Dillon *et al. Int. J. Mat. Res.*, **101** (2010) 50-56. Dillon *et al. J. Am. Ceram. Soc.*, **93** (2010) 1796-802.

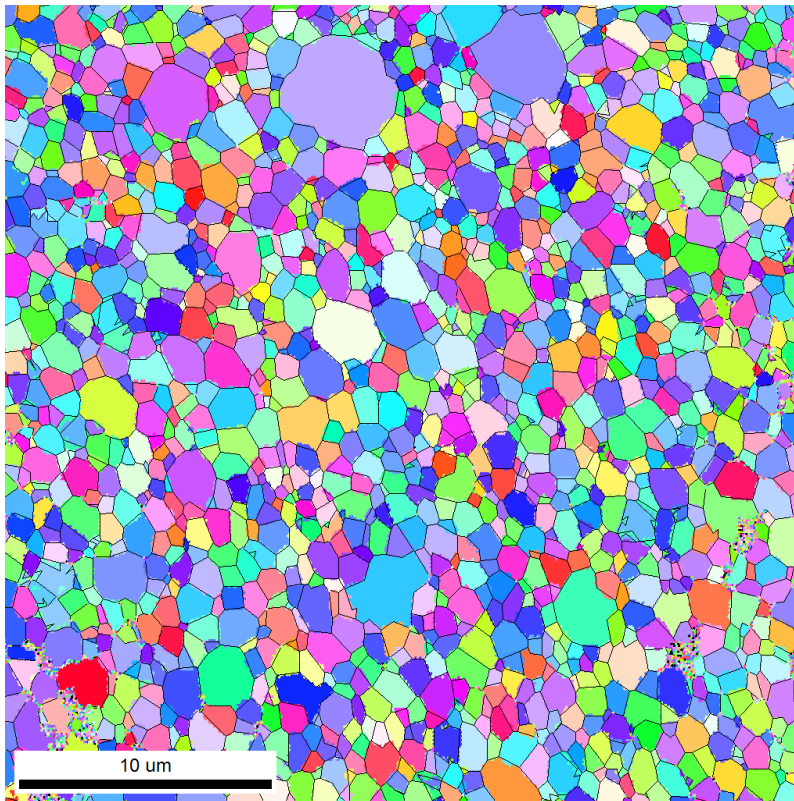
# *Doped Yttria - EBSD*

Color Coded Map Type: Inverse Pole Figure [001]

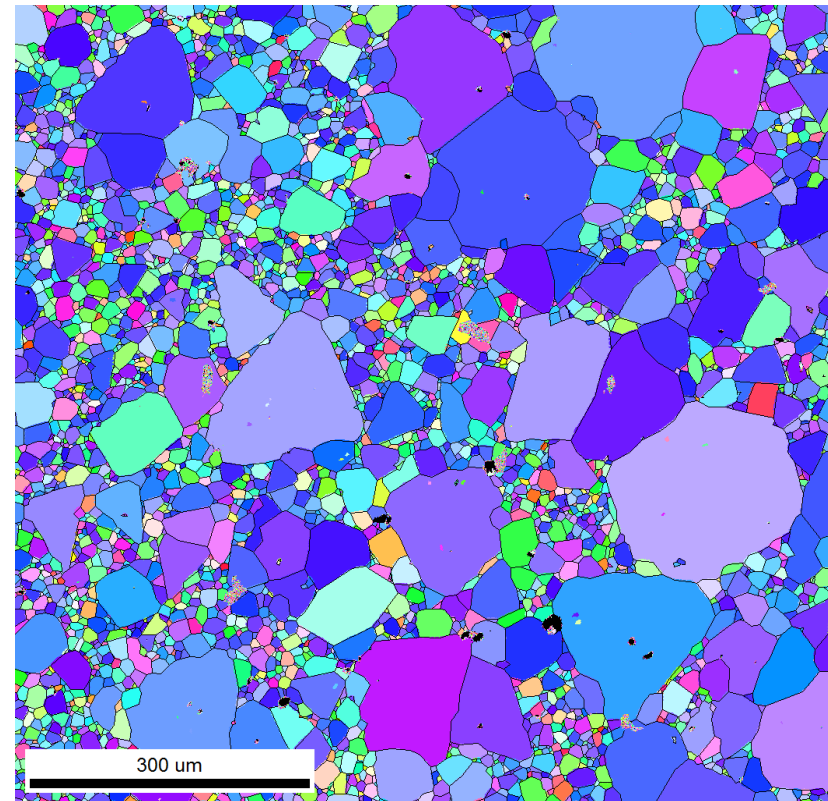
New Phase



Normal Grain Growth (NGG)  
0 hours

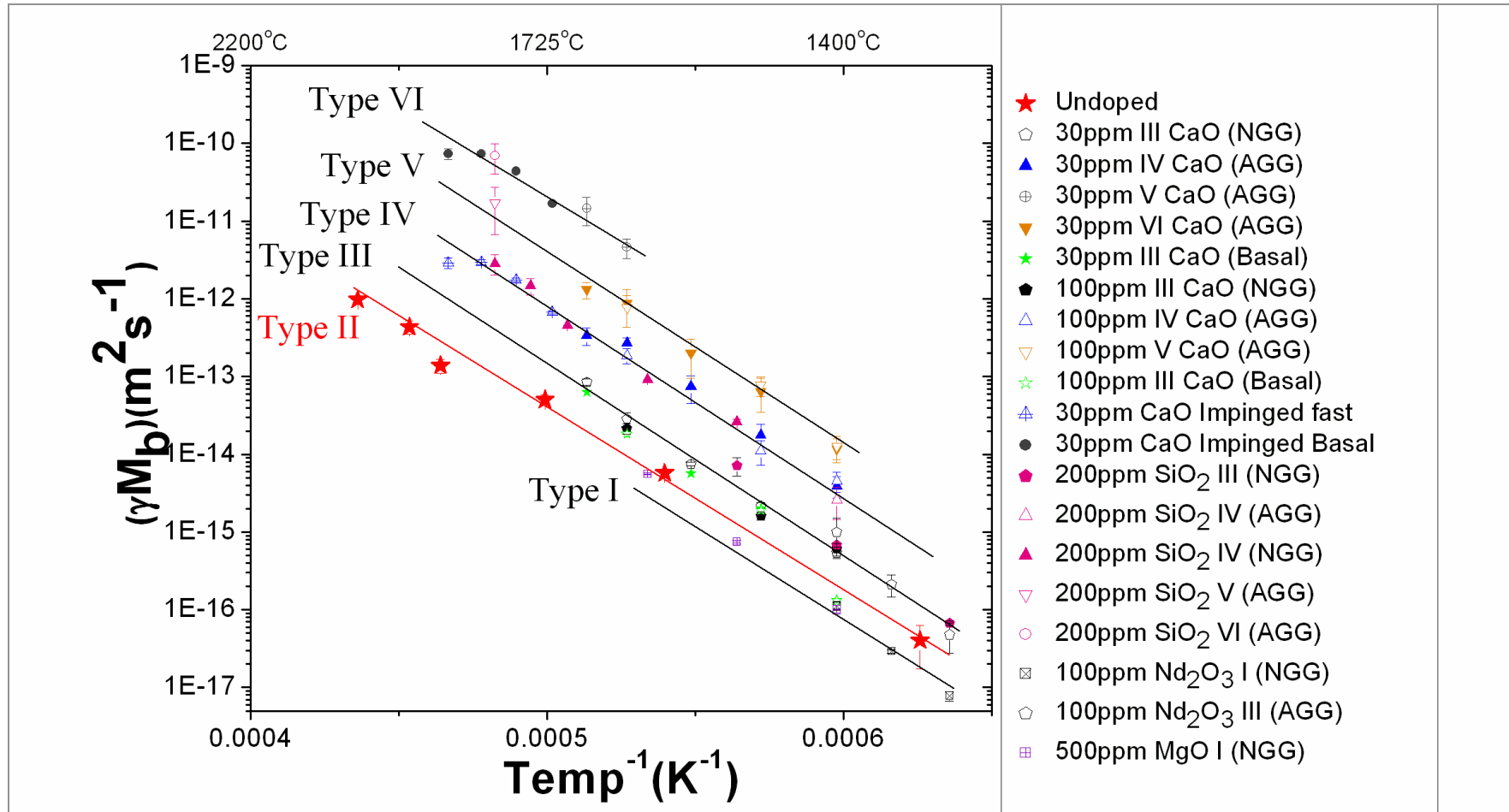


Abnormal Grain Growth (AGG)  
6 hours



- 100 ppm Calcia-doped yttria at 1700°C for 0 and 6 hours in reducing atmosphere
- Fabricated by S. Ma at Lehigh University

# Grain Growth Kinetic Types

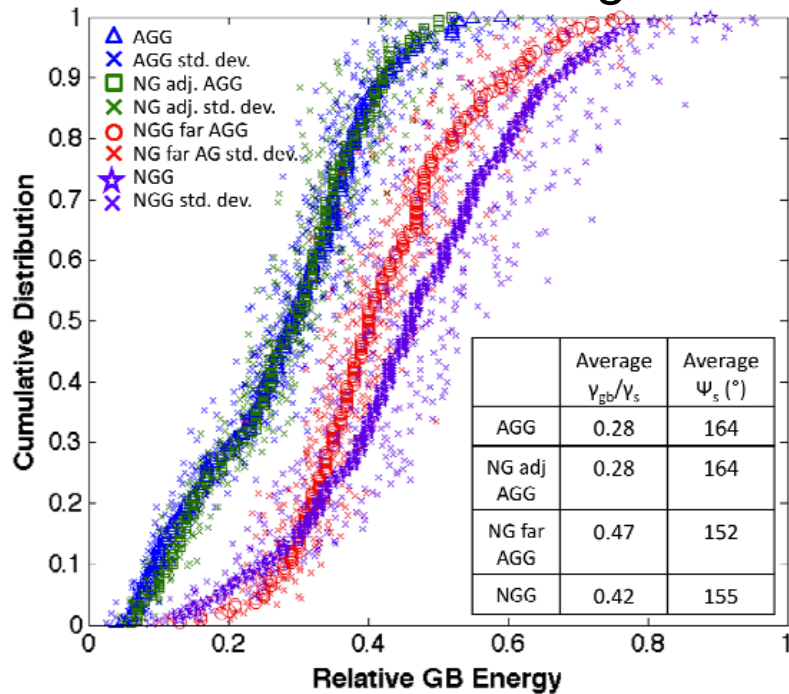


S.J. Dillon, M. Tang, W.C. Carter, M.P. Harmer, "Complexion: A new concept for kinetic engineering in materials science," *Acta Mater.* **55** 6208-6218 (2007).



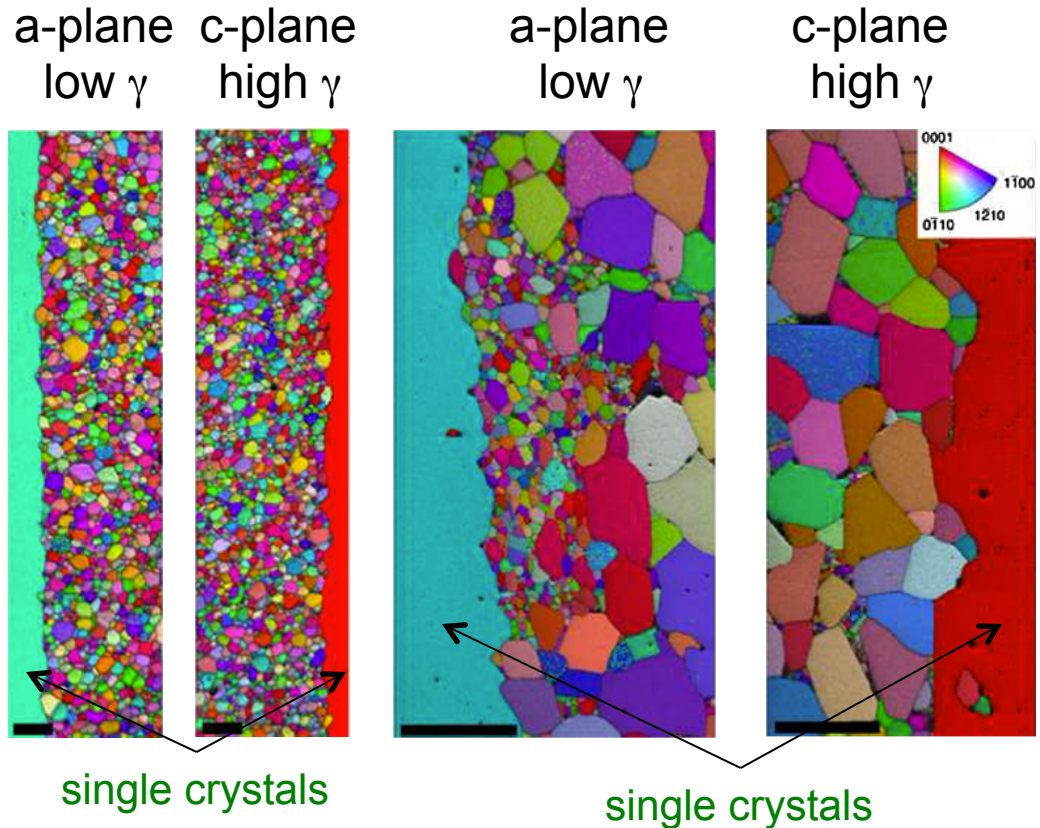
# Complexion Transitions and AGG

Implication: many grain boundaries changed complexion AFTER coming into contact with abnormal grains



Surface dihedral angles

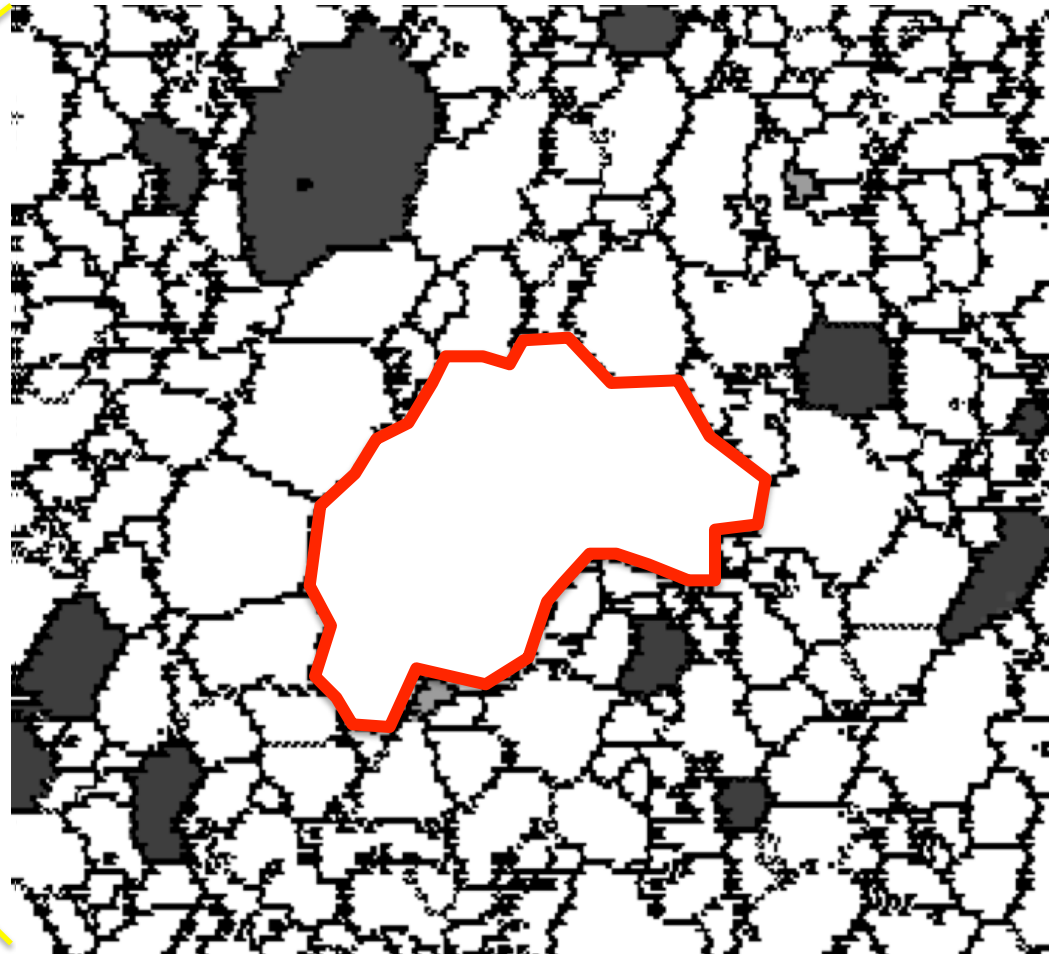
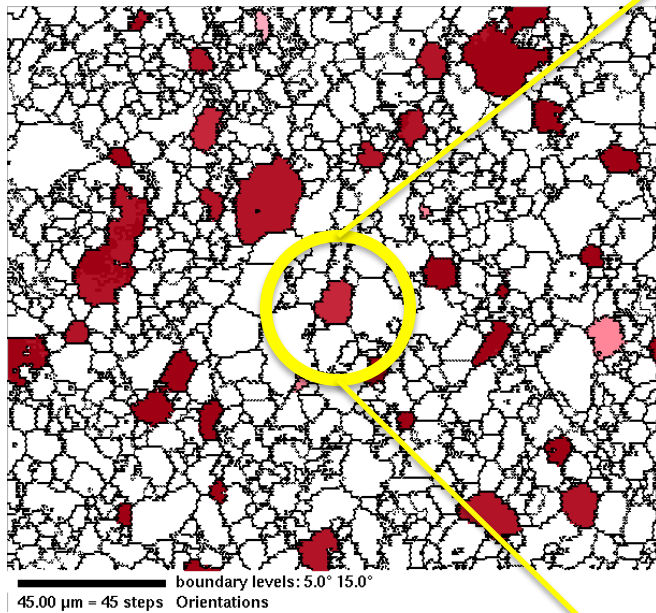
High energy GBs transition more easily, hence we observe AGG more against the single crystal that has a high energy 0001 surface (red color)



Yttrium-doped alumina:  
Bojarski et al., *Mater. Sci. Forum* (2013) **753** 87

Bojarski et al. *Metall. and Mater. Trans. A.* (2012) **43** 3532    38

# Propagation



- Consider the problem of how the transitioned, high mobility boundaries have to propagate.

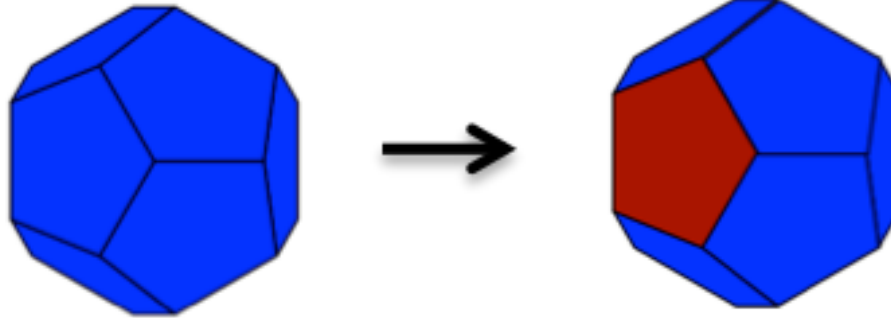


# *Boundary-Based Approach to Modeling AGG with Complexion Transitions*

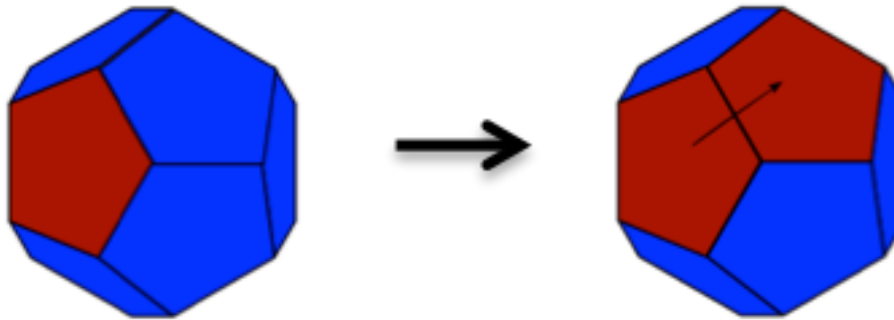
- Over the course of the simulation, transition randomly selected grain boundaries to a high mobility “complexion”.
- Grain boundaries are “special”, as opposed to entire grains.
- How easily can such a process result in AGG?
- Grains with a volume 10x the average ( $\sim 2.66x$  average radius) regarded as abnormal.

### *3 Different Transitions Across TLs*

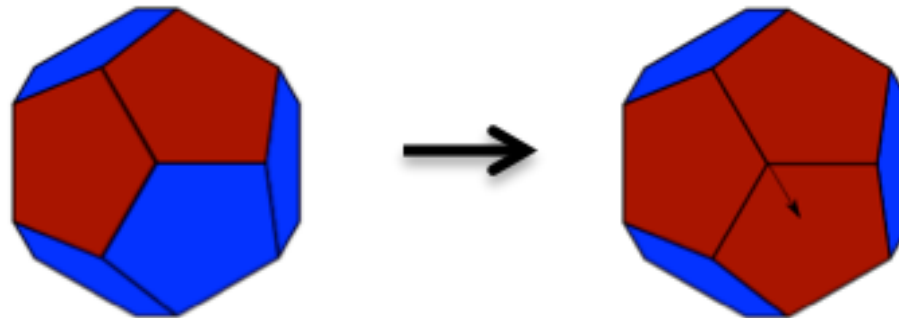
Independent  
"N0" Transition



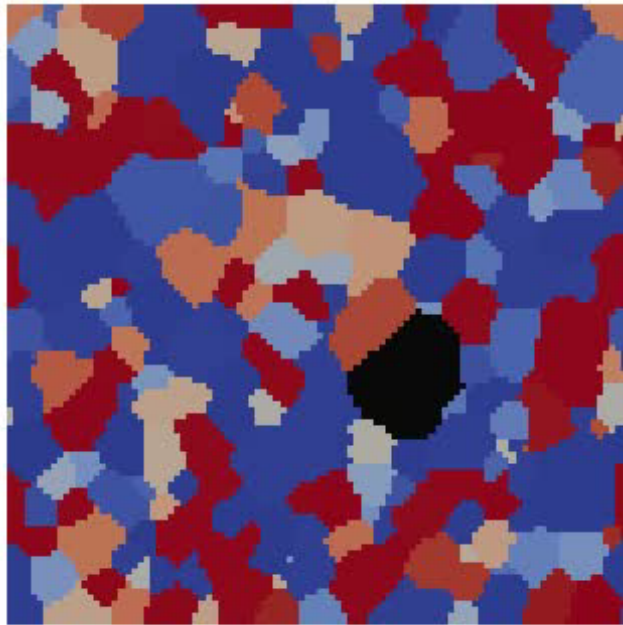
Single Adjacency  
"N1" Transition



Double Adjacency  
"N2" Transition



# *Grain Growth with Independent (N0) + Adjacency (N1) Transitions*

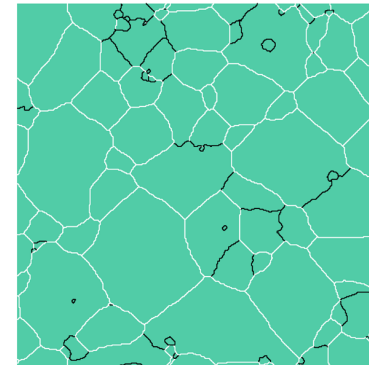
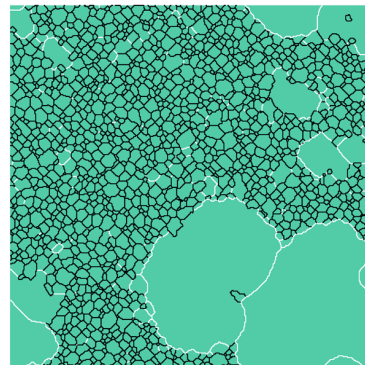
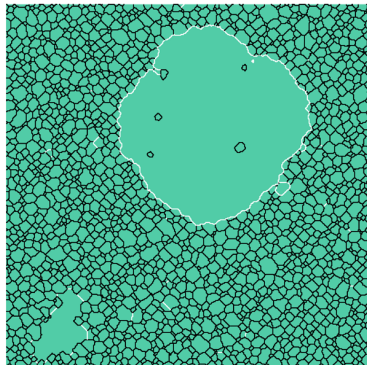


Frazier, W. E., Rohrer, G. S., & Rollett, A. D. (2015), 'Abnormal grain growth in the Potts model incorporating grain boundary complexion transitions that increase the mobility of individual boundaries', *Acta Mater* **96** 390.

# Subgrain Coarsening

- Deformed metals, especially those with high stacking fault energy, will form a subgrain network inside each grain.
- The misorientation across the average subgrain boundary increases steadily with strain.
- Therefore, the likelihood of finding a subgrain with high angle, highly mobile boundaries increases with strain.
- Such a subgrain has the potential to grow abnormally, which can give rise to a new grain – “intragrain nucleation”.
- 2D simulation, theory: Holm, E. A., *et al.* (2003). "On abnormal subgrain growth and the origin of recrystallization nuclei." *Acta materialia* **51**: 2701-2716.
- Complication: “intergrain nucleation” can occur via “strain induced boundary migration”.

Low  
misorient  
ation



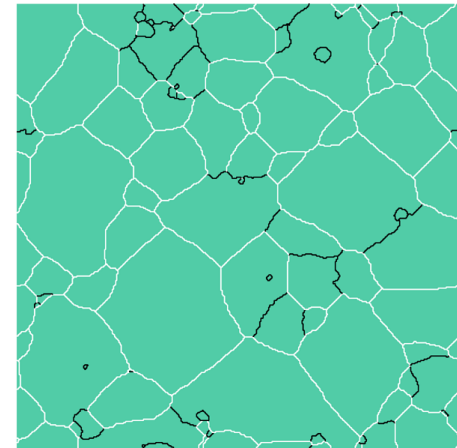
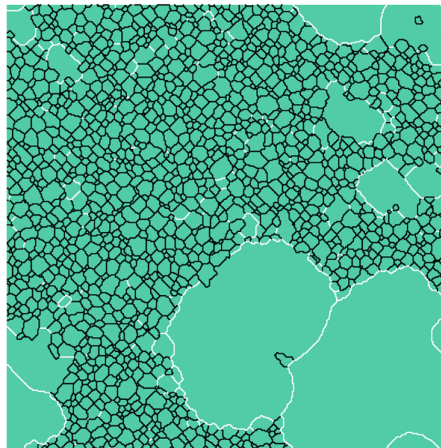
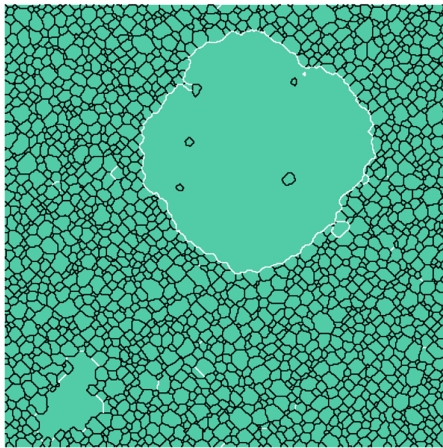
High  
misorient  
ation

# *Anisotropy Dependence?*

- Parametric simulations show that:

isotropic $\gamma$	+	isotropic M	$\Rightarrow$	normal growth
anisotropic $\gamma$	+	isotropic M	$\Rightarrow$	normal growth
isotropic $\gamma$	+	anisotropic M	$\Rightarrow$	abnormal growth
anisotropic $\gamma$	+	anisotropic M	$\Rightarrow$	abnormal growth

- Low densities of highly mobile boundaries are necessary for abnormal growth:



Few high-M boundaries



Many high-M boundaries

Holm *et al.* (2003) *Acta mater.* **51** 2701-2716.



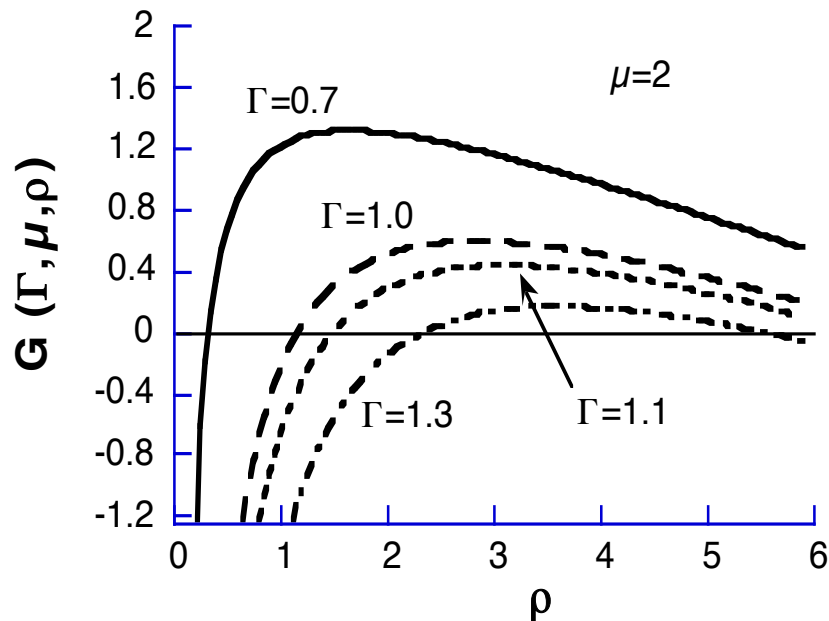
# *Mean field theory for AGG in 2D*

- Hillert originally suggested that any grain with size twice that of the mean,  $R > 2\langle R \rangle$ , would be able to escape and grow abnormally.
- Simulations showed that this was not the case and Thompson *et al.* demonstrated this theoretically by re-analyzing the basic mean field theory; *Acta metall.* **35**: 887-890 (1987).
- Rollett *et al.* (1989) *Acta metall.* **37** 2127, showed that a mobility advantage for the boundary of a grain would allow it to grow abnormally to a multiple of the matrix grain size. Rollett & Mullins (1997) *Scripta mater.* **36** 975, extended von Neumann-Mullins to include energy and mobility (Humphreys used mean-field in his 1997 Acta paper)
- The issue with this approach is, how can an individual grain sustain a mobility advantage while growing through a matrix of multiple orientations?
- 1<sup>st</sup> Answer: subgrain structures can sustain a mobility advantage where a particular outlier subgrain always has a high misorientation, high mobility, perimeter; (AGG) Holm *et al.* *Acta mater.* (2003) **51**: 2701. (Applied to the nucleation of recrystallization) Wang *et al.* (2011), *Acta mater.* **59** 3872.
- 2<sup>nd</sup> Answer: changes in the composition of boundaries (to form different “complexions”) generates perimeters around abnormal grains with sustained high mobility; Frazier *et al.* (2015) *Acta Mater* **96** 390.

## *Philosophy of Approach*

- This development is based on: Rollett, A. D. and W. W. Mullins (1996). “On the growth of abnormal grains.” Scripta metall. et mater. **36(9): 975-980.**
- Analysis confined to 2D because it is possible to integrate the curvature around the perimeter of a grain and relate it to the rate of change of area; not possible in 3D.

# Relative growth rate - summary



$$\langle \dot{\rho} | R_A \rangle = \frac{M_{BB} \gamma_{BB}}{2 \langle R_B \rangle^2} G(\rho, \mu, \Gamma)$$

$$G(\rho, \mu, \Gamma) = \left\{ \mu \Gamma \left( a + (a - 2) \frac{1}{\rho} \right) - \frac{\rho}{4} \right\}$$

$$\rho_+ = 2 \mu \Gamma a + 2 \left[ (\mu \Gamma a)^2 + \mu \Gamma (a - 2) \right]^{1/2}$$

$$\rho_- = 2 \mu \Gamma a - 2 \left[ (\mu \Gamma a)^2 + \mu \Gamma (a - 2) \right]^{1/2}$$

Plot of **relative growth rate** versus relative size for  $\mu = 2$  with four different values for the ratio of grain boundary energies,  $\Gamma = 0.7, 1.0$  (solid line), 1.1 and 1.3. Note that only the curve for  $\Gamma = 1.3$  shows both **upper** and **lower** roots ( $G = 0$ ) but that the other three cases also have upper roots that increase with decreasing  $\Gamma$ . The results predict abnormal grain growth ( $\Gamma > 0$ ) over a range of relative size that decreases with *increasing* boundary energy ratio and *decreasing* boundary mobility ratio.

## *AGG Analysis: Assumptions*

- The theory makes a number of simplifying assumptions.
- Students are assumed to be familiar with the Herring equation.
- Only 2D grain growth is treated, although it is reasonable to expect that theory applies in 3D also.
- Grain boundary properties are assumed to be constant (uniform) everywhere except for the boundaries between certain special grains (type A) and grains in the matrix (type B).
- The special grains share the same energy and mobility on their boundaries.
- The special grains are isolated (no A-A boundaries).

# Microstructure

- Each A grain is surrounded by B grains.
- We are interested in whether the A grain grows faster than the B grains during growth.
- 4-sided example should shrink.

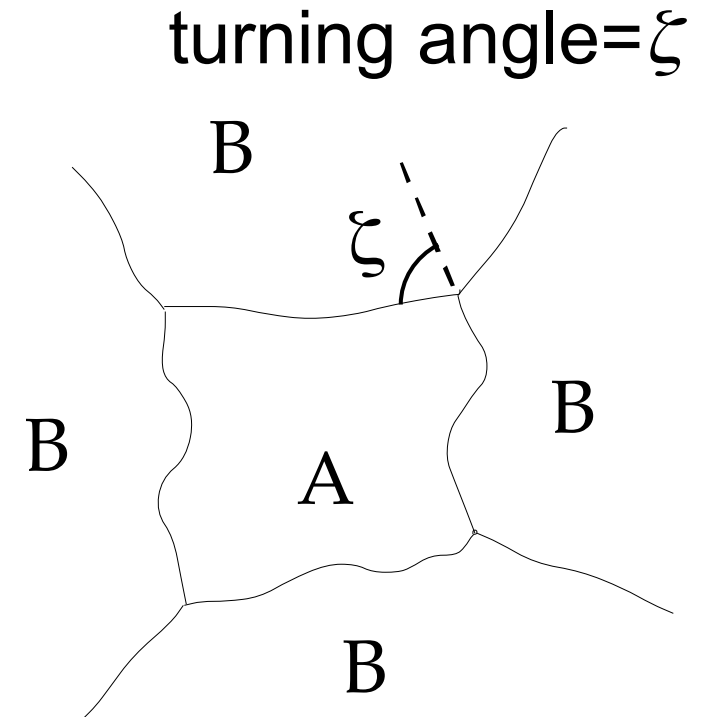


Figure 1.



## *Parameters*

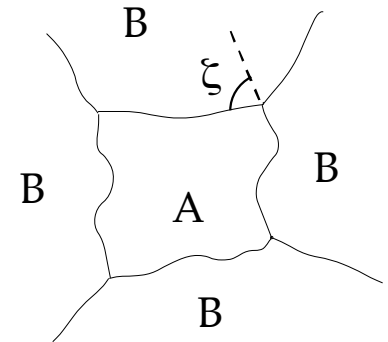
- $\Gamma := \gamma_{AB} / \gamma_{BB}$  in which the  $\gamma$ 's are the boundary energies on the AB and BB boundaries, respectively.
- $\mu := M_{AB} / M_{BB}$  in which the  $M$ 's are the boundary mobilities.
- $A :=$  area of a grain;  $n :=$  number of sides of a grain.
- $S :=$  arc length;  $\beta :=$  angle made by directed tangent to line relative to a fixed reference direction.
- Define a function  $a$ , of the energy ratio:

$$a(\Gamma) = 3\xi / \pi = (6 / \pi) \sin^{-1}(1 / 2\Gamma) < 3$$

## *Turning angle at a vertex*

- Fig. 1 shows an irregular 4-sided A grain surrounded by B grains. The vertices are assumed to be in equilibrium. If torque terms are neglected, the turning angle  $\zeta$  of the tangent to the AB boundary at a vertex is then given by

$$\zeta = 2 \sin^{-1}(1/2\Gamma)$$



- Note the limiting case of wetting of the matrix grain boundaries by the A grain occurs at  $\Gamma=1/2$  or  $\zeta=\pi$ .

## *dA/dt vs. curvature*

- We now derive a relationship between the rate of change of area of the “A” grain, its number of sides, and the equilibrium angles at each vertex. The curvature rule for a two dimensional grain may be written:

$$v = -M\gamma \frac{d\beta}{ds}$$

where  $v$  is the outward velocity in the normal direction, and  $d\beta/ds$  is the curvature.

## *Integrate around the grain*

- If Eq. 2 is integrated around the “A” grain with  $n$  sides of fixed  $M_{AB}$  and  $\gamma_{AB}$ , the left hand side just gives the rate of change of area  $A$  of the grain and on the right, the integral of  $d\beta/ds$  gives  $2\pi - n\xi$ , since there is a discontinuity of the AB tangent angle of  $\xi$  at each of the  $n$  vertices as illustrated in Fig. 1.

$$\frac{dA}{dt} = -M_{AB} \gamma_{AB} (2\pi - n\xi) = \frac{\pi M_{AB} \gamma_{AB}}{3} (an - 6)$$

## *The “n-6” rule*

- The previous equation shows that the rate of area change is constant; if all boundaries are equivalent, as they are for a “B” grain surrounded by “B” grains in the matrix, then  $\Gamma=1$ ,  $a=1$  and the equation reduces to the “n-6” rule for the B matrix grains:

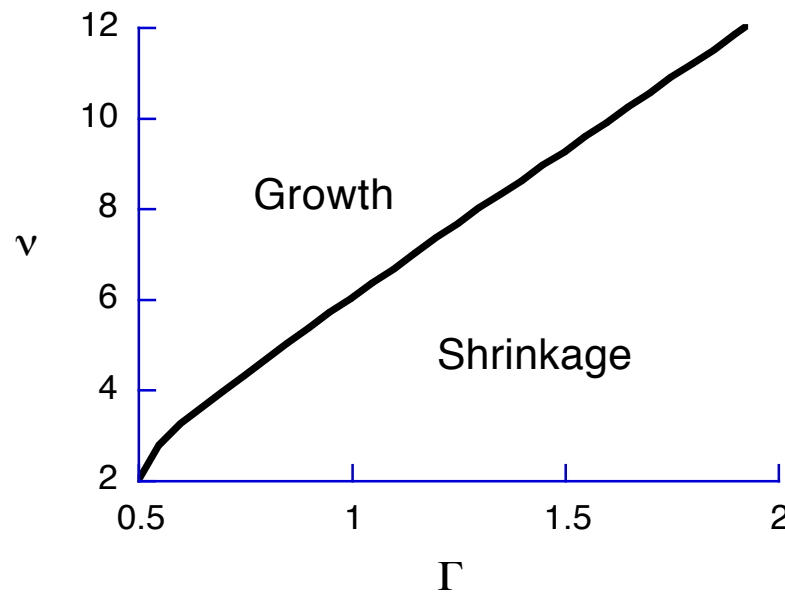
$$\frac{dA}{dt} = \frac{\pi M_{BB} \gamma_{BB}}{3} (n - 6)$$



## Grow or Shrink?

- The equation shows that the A grain will grow if  $n > v = 6/a$  and shrink if the reverse is true. Fig. 2 shows a plot of  $v$  as a function of  $\Gamma$ .

$$v = 6/a = \pi / \sin^{-1}(1/2\Gamma)$$



## *Grow or Shrink? Contd.*

- If  $n > v$  the A grain grows and if  $n < v$  it shrinks. Note if  $\Gamma < 1/\sqrt{3}$ , the A grain grows for any number of sides  $n \geq 3$ , which corresponds to the wetting criterion.
- We now turn to the comparison of the ultimate size of the A grain to that of the B grains. For this purpose, following Thompson et al.† and Rollett et al.\*, we study the time dependence of the ratio  $\rho = R_A / \langle R_B \rangle$  where the  $R$ 's are area-equivalent radii.

† Thompson, C., H. Frost, et al. (1987). "The relative rates of secondary and normal grain growth." *Acta metall.* **35** 887-890.

\* Rollett, A. D., D. J. Srolovitz, et al. (1989). "Simulation and Theory of Abnormal Grain Growth-Variable Grain Boundary Energies and Mobilities." *Acta Metall.* **37** 2127.

## *Growth of A grains*

- Using the rule for differentiating a quotient we have

$$\langle \dot{\rho} | R_A \rangle = \frac{1}{\langle R_B \rangle^2} \left\{ \langle R_B \rangle \langle \dot{R}_A | R_A \rangle - R_A \frac{d\langle R_B \rangle}{dt} \right\}$$

where  $\langle \dot{\rho} | R_A \rangle$  simply means that is averaged over (isolated) A grains of the same  $R_A$  but otherwise possibly of different shape and n, and similarly for  $\langle \dot{R}_A | R_A \rangle$ .

## *Growth of A grains, contd.*

- To evaluate the first derivative in the brackets of the previous equation, we combine Eq. 3 and the expression  $A = \pi R_A^2$  to get

$$\left\langle \dot{R}_A \mid R_A \right\rangle = \frac{M_{AB} \gamma_{AB}}{6 R_A} \left( a \langle n \mid R_A \rangle - 6 \right)$$

For  $\langle n/R_A \rangle$ , the average number of sides of A grains with a fixed  $R_A$ , we use the expression

$$\langle n/R_A \rangle = 3r + 3$$

which is linear in the size of the A grain and gives the limit 3 as  $R_A$  becomes very small; it approximates the number of circular B grains that would fit on the circumference of the A grain

## *Growth of A grains, contd.*

- Combining these equations:

$$\langle \dot{R}_A | R_A \rangle = \frac{\mu \Gamma M_{BB} \gamma_{BB}}{2 \langle R_B \rangle} \left( a + (a - 2) \frac{1}{\rho} \right)$$

- Now we need something to predict the coarsening rate in the matrix (the “B” grains), for which we turn to Hillert’s classical grain growth theory.

## Hillert's theory

- Assume that the presence of A grains does perturb the B matrix; the theory may be obtained by combining two ingredients: the “ $n-6$ ” rule, expressed in area equivalent radius form and averaged over all B grains of radius  $R_B$ :

$$\langle \dot{R}_B | R_B \rangle = \frac{M_{BB} \gamma_{BB}}{6R_B} \left( \langle n | R_B \rangle - 6 \right)$$

and the linear relation sides(size):

$$\langle n | R_B \rangle = 3R_B / \langle R_B \rangle + 3$$



## *Hillert's theory, contd.*

- Abbruzzese et al.† found that this relationship is experimentally supported. It also satisfies the Euler\* requirement that  $\langle n \rangle = 6$ . Combining Eqs. 11 and 12 with standard coarsening theory, one obtains the Hillert result

$$\frac{d}{dt} \langle R_B \rangle = \frac{M_{BB} \gamma_{BB}}{8 \langle R_B \rangle}$$

† Abbruzzese, G., I. Heckelmann, et al. (1991). "Topological foundation and kinetics of texture controlled grain growth." *Textures and Microstructures* **14-18**: 659-666.

\*Courant, R. and H. E. Robbins (1941). What is Mathematics, Oxford University Press.

## *Abnormal Growth: main result*

- Combining equations gives the following:

$$\langle \dot{\rho} | R_A \rangle = \frac{M_{BB} \gamma_{BB}}{2 \langle R_B \rangle^2} G(\rho, \mu, \Gamma)$$

$$G(\rho, \mu, \Gamma) = \left\{ \mu \Gamma \left( a + (a - 2) \frac{1}{\rho} \right) - \frac{\rho}{4} \right\}$$

The sign of G is the same as that of  $\langle \dot{\rho} | R_A \rangle$

## *Finding a limiting (abnormal) size*

- Think of the result as a quadratic equation and consider which way the relative size is changing: for there to be a *fixed* relative size ( $\rho$ ), there must be a “restoring force”.
- Thus, for a stable  $\rho$  to exist, corresponding to a fixed ratio of the A to B grain size as growth proceeds, there must be a positive root  $\rho$  of the quadratic equation  $G=0$  at which  $\partial G/\partial \rho < 0$ , so that the sign of  $\langle \dot{\rho} | R_A \rangle$  is positive
- The mathematical condition for real roots of  $G=0$  to exist is

$$\mu \geq (2 - a) / \Gamma a^2$$

## *The positive root: max. size*

- Physically  $\mu$  must also be positive. If the previous condition is not satisfied,  $G < 0$  for all  $\rho$  (the Eq. above shows  $G < 0$  for large  $\rho$ ) so that under these conditions the “A” grain would shrink and disappear. If the condition above is satisfied, it is easily shown that the upper root, given by

$$\rho_+ = 2\mu\Gamma a + 2\left[(\mu\Gamma a)^2 + \mu\Gamma(a - 2)\right]^{1/2}$$

is then the stable one. If

$$1/2 < \Gamma \leq 1/\sqrt{3} \quad (3 > a \geq 2),$$

then  $G > 0$  for any (positive)  $\rho < \rho_+$  so that any A grain in this range will grow toward the stable  $\rho_+$ .

## *Minimum size for abnormal growth*

- If, however,  $\Gamma > 1/\sqrt{3}$  ( $a < 2$ ), the initial value of  $\rho$  must lie in the range  $\rho_- < \rho < \rho_+$  for growth toward  $\rho_+$  to occur, where  $\rho_-$  is given by

$$\rho_- = 2\mu\Gamma a - 2\left[(\mu\Gamma a)^2 + \mu\Gamma(a-2)\right]^{1/2}$$

if  $\rho < \rho_-$ ,  $G < 0$  so shrinkage and disappearance of the A grain would occur. In the special case that the condition above is an equality, which represents a double-root curve in the  $(\mu, \Gamma)$  plane (e.g.  $\mu = \Gamma = a = 1$  as discussed by Thompson et al.), then  $\rho_+ = \rho_- = 2(2 - a)/a$ . In this case  $G$  is never positive so grain A would again ultimately disappear.

## *Asymptotes*

- Note also that one only expects the relative size to approach the asymptote rather slowly under experimental conditions. If the range of  $\rho$  over which  $G > 0$  is small then fluctuations in the growth rate, due for example, to fluctuations in the number of neighbors, may cause  $\dot{\rho}$  to become negative for long enough to cause  $A$  to disappear. Note also that one only expects the relative size to approach the asymptote rather slowly under experimental conditions.



## *Details*

- The case of  $a < 2$  ( $\Gamma > 1/\sqrt{3}$ ) is illustrated in the following figure which shows a plot of  $G$  as a function of  $\rho$  for  $\mu = 2$  and several values of  $\Gamma$ . There are two positive roots of  $G = 0$ . The effect of decreasing  $\Gamma$  is to expand the range over which  $G$  is positive. The meaning of  $G > 0$  or  $\langle \dot{\rho} | R_A \rangle > 0$  is that the average growth rate of the A grain will exceed that of the mean size of the matrix so that the expected value of  $\rho$  will increase until it reaches the stable upper root of  $G = 0$ . Note that this analysis addresses only the average value of  $d\rho/dt$ . If the range of  $\rho$  over which  $G > 0$  is small then fluctuations in the growth rate, due for example, to fluctuations in the number of neighbors, may cause to become negative for long enough to cause A to disappear.

## Relative growth rate - plot

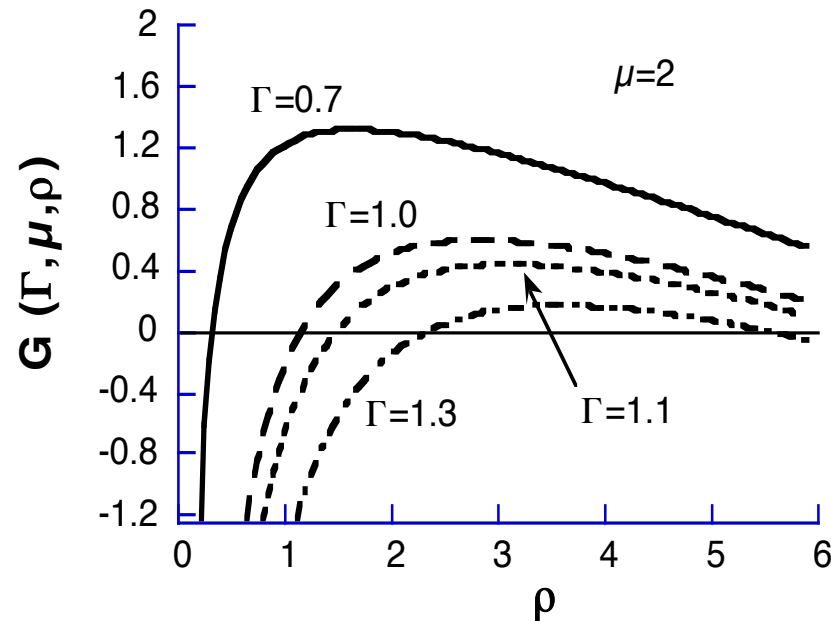


Figure 3. Plot of relative growth rate versus relative size for  $\mu=2$  with four different values for the ratio of grain boundary energies,  $\Gamma=0.7$ , 1.0 (solid line), 1.1 and 1.3. Note that only the curve for  $\Gamma=1.3$  shows both upper and lower roots ( $\rho=0$ ) but that the other three cases also have upper roots that increase with decreasing  $\Gamma$ . The results predict abnormal grain growth ( $G>0$ ) over a range of relative size that decreases with increasing boundary energy ratio.

## *Contours in the $(\mu, \Gamma)$ plane*

- The next figure shows the  $(\mu, \Gamma)$  plane with regions of  $\rho_+$  (stable root) delineated: no real roots exist in the upper left triangle whereas two roots exist in the lower right triangle ( $\Gamma > 1/\sqrt{3}$ ). Over the range  $0.5 < \Gamma \leq 1/\sqrt{3}$ , only one positive root exists ( $\rho_-$  is negative), and for  $\Gamma \leq 0.5$ , wetting occurs. Several contours of constant relative size are shown; these were calculated by setting  $G=0$  in Eq. 14a, and solving for  $\mu$  with fixed values of  $\rho$ . Also shown is the curve (thick line) along which the upper and lower roots are equal; this was calculated from Eq. 16 with an equality. Each contour of constant  $\rho$  touches this line at a point for which  $\rho_+ = \rho_-$ ; for  $\mu$  and  $\Gamma$  less than this point, the contour describes the branch for  $\rho_+$ ; conversely, for  $\mu$  and  $\Gamma$  larger than this point, the contour describes the branch for  $\rho_-$ . In the region of two positive roots, each  $\mu, \Gamma$  pair is intersected by two contours; the difference between  $\rho_+$  and  $\rho_-$  defines the range of relative size over which abnormal growth is likely to occur. [Eq. numbers refer to the Scripta metall. Paper]

# Contours in the $(\mu, \Gamma)$ plane: plot

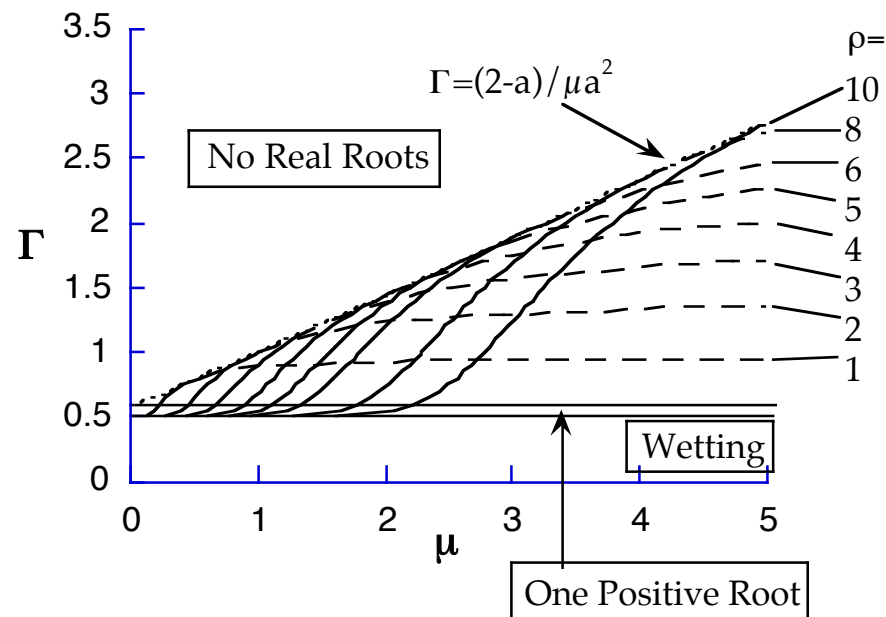


Figure 4. The  $\mu, \Gamma$  plane with regions of stable  $\rho$  delineated. For  $\Gamma < 0.5$ , wetting occurs; for  $0.5 \leq \Gamma \leq 1/\sqrt{3}$ , only one positive root exists; below the double root curve (dotted line) and for  $\Gamma > 1/\sqrt{3}$  two positive roots exist. Contours of constant  $\rho_+$  (solid curves) and  $\rho_-$  (dashed curves) have been drawn; the difference between the  $\rho_+$  and  $\rho_-$  values at any point in the two root region defines the range of relative sizes over which abnormal growth can occur.

## *Abn. Gr. Gr.: Conclusions*

- Abnormal growth is promoted by high mobility of the abnormal grain relative to the matrix.
- Abnormal growth is constrained by high energy of the abnormal grain.
- A combination of high mobility and high energy could occur in a sub-grain structure with a few misoriented subgrains.
- Complex dependence of abnormal growth revealed by contours in the  $(\mu, \Gamma)$  plane.

# *Extending AGG to nucleation of primary recrystallization*

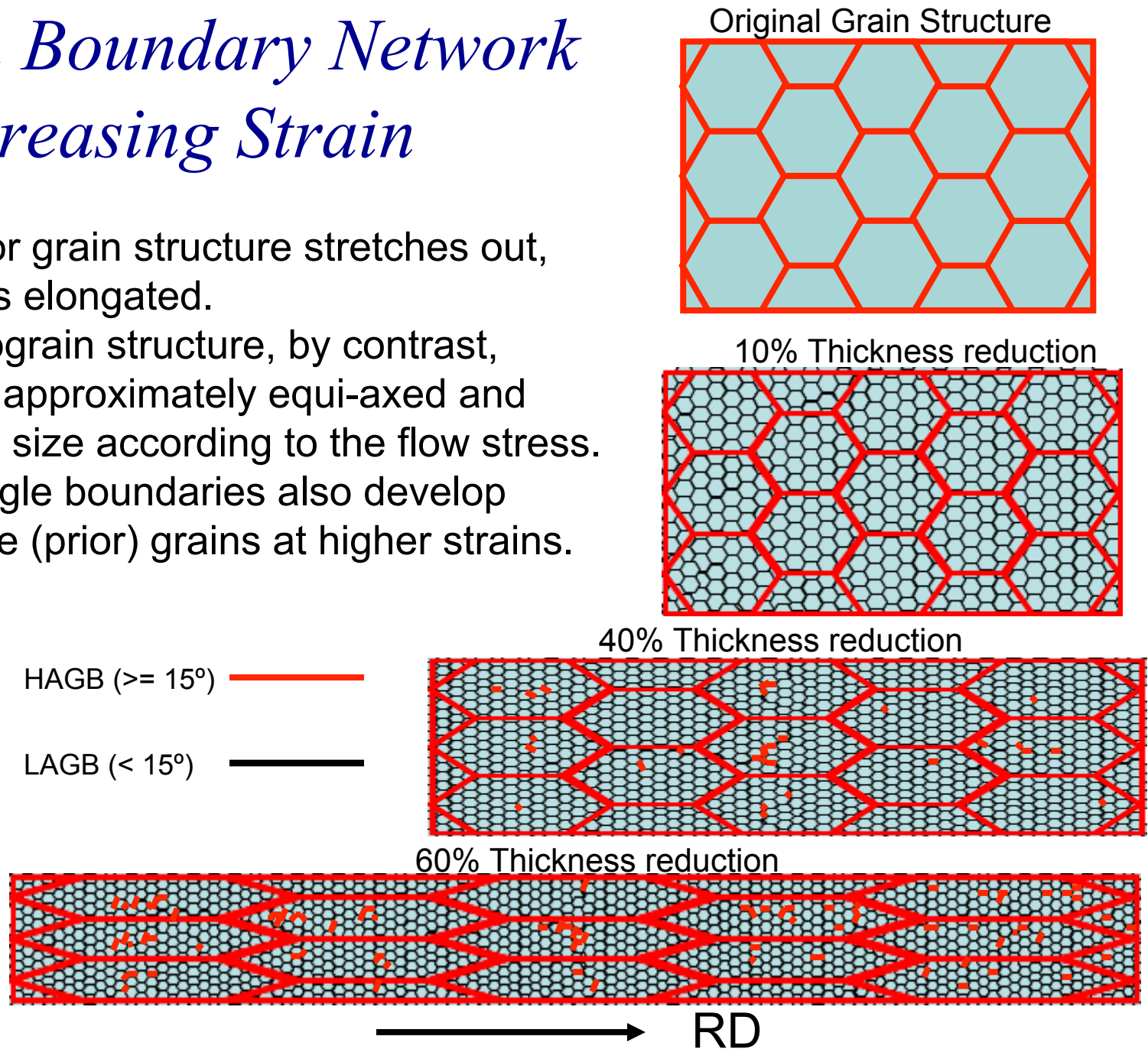
- Since deformed metals develop dislocation cell structures with accumulating strain, it is reasonable to ask what happens during annealing.
- Polygonization is the process by which dislocation cells evolve into subgrain structures. Cahn [Cahn, R. W. (1950), *Proceedings of the Physical Society of London A*, **63**, 323-336] postulated many years ago that this process could continue with certain individual subgrains growing abnormally and thereby acting as "nuclei" for primary recrystallization.
- Wang et al. extended the simulation of AGG in subgrain structures by combining its results (in terms of the frequency of generation of abnormal grains) with constitutive information about subgrain misorientations available in the literature and showed that the dependence of recrystallized grain size on prior strain was in reasonable agreement with the literature.
- It is important to note that primary recrystallized grain size is, to first order, only dependent on the prior strain and not sensitive to annealing temperature. This confirms that the process of recrystallization is determined by the prior strain history, even if the rate (kinetics) of recrystallization depend on temperature via the rate sensitivity of grain mobility.

Wang et al. (2011), *Acta mater.* **59** 3872.

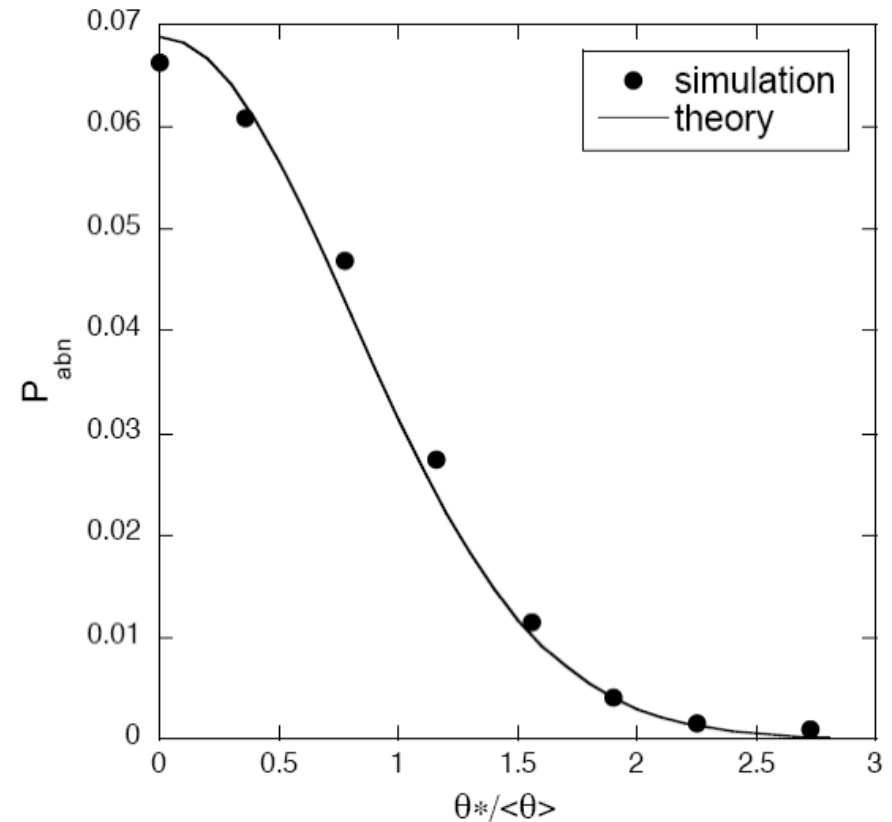
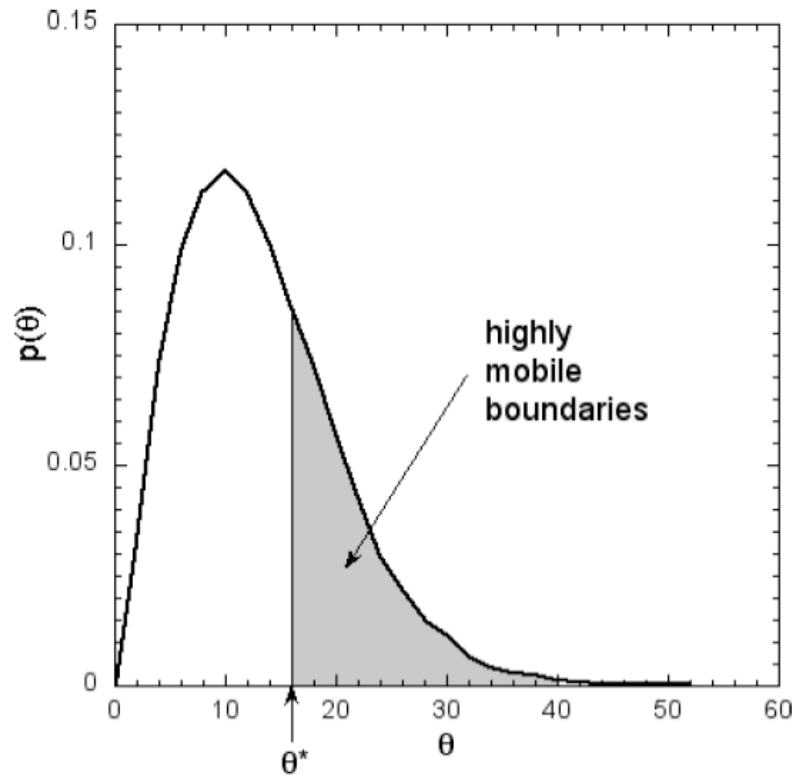


# Grain Boundary Network at Increasing Strain

1. The prior grain structure stretches out, becomes elongated.
2. The subgrain structure, by contrast, remains approximately equi-axed and changes size according to the flow stress.
3. High angle boundaries also develop within the (prior) grains at higher strains.



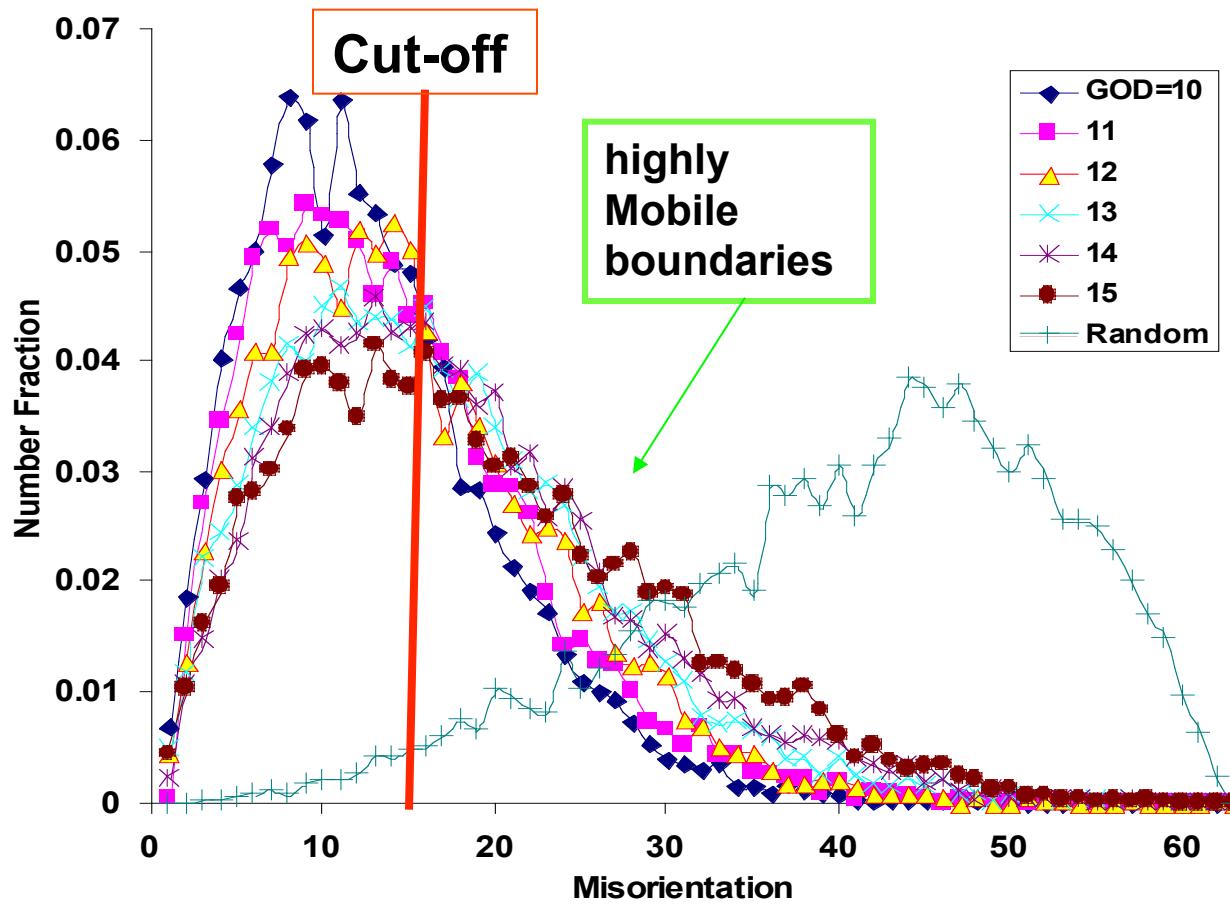
## Holm Theory



Mobility anisotropy is changed by varying critical angle ( $\theta^*$ ) defining a jump in mobility.

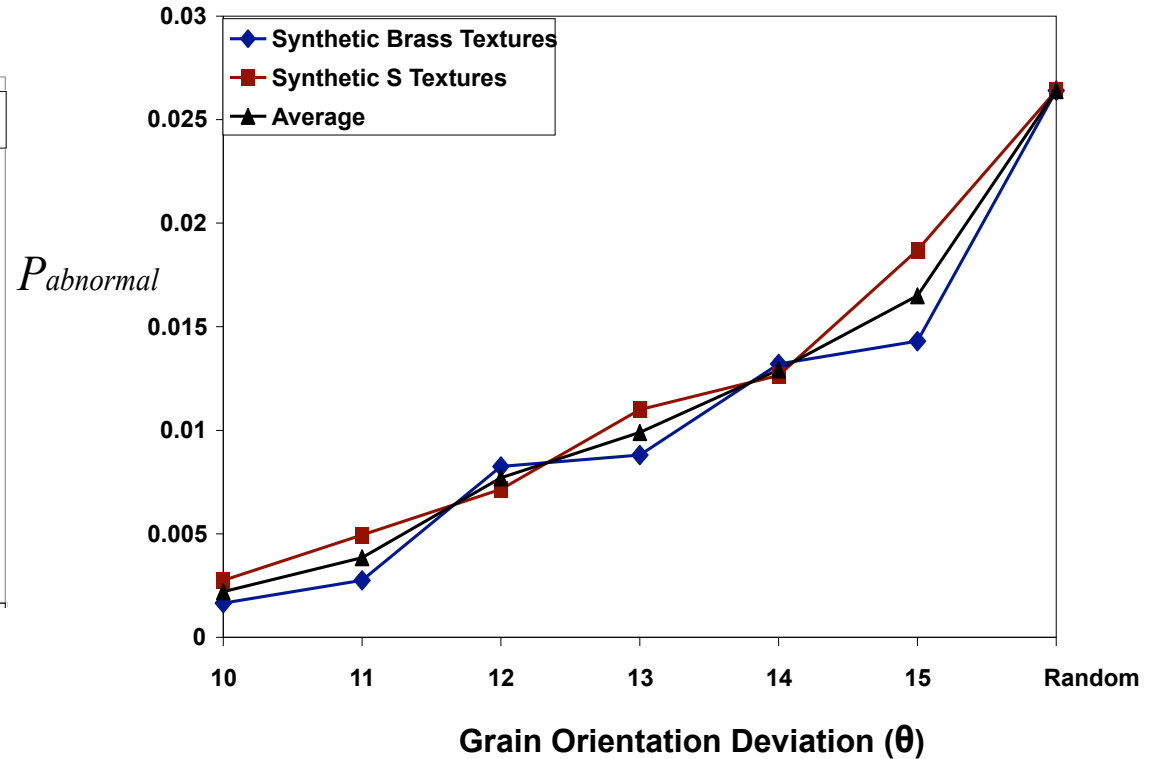
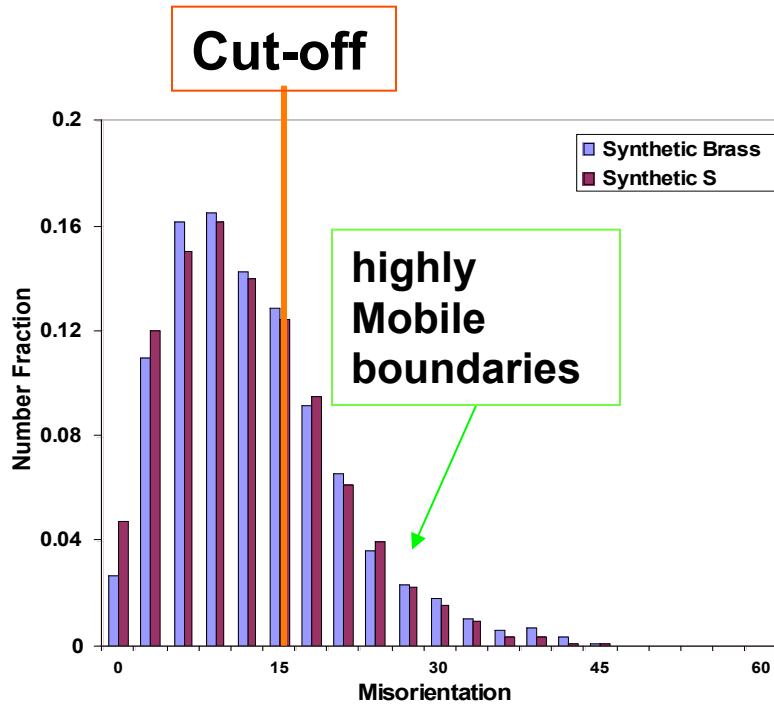
$$P_{abn} = C \exp \left[ -\frac{\pi}{4} \left( \frac{\theta^*}{\langle \theta \rangle} \right)^2 \right]$$

# *MDF Comparison*



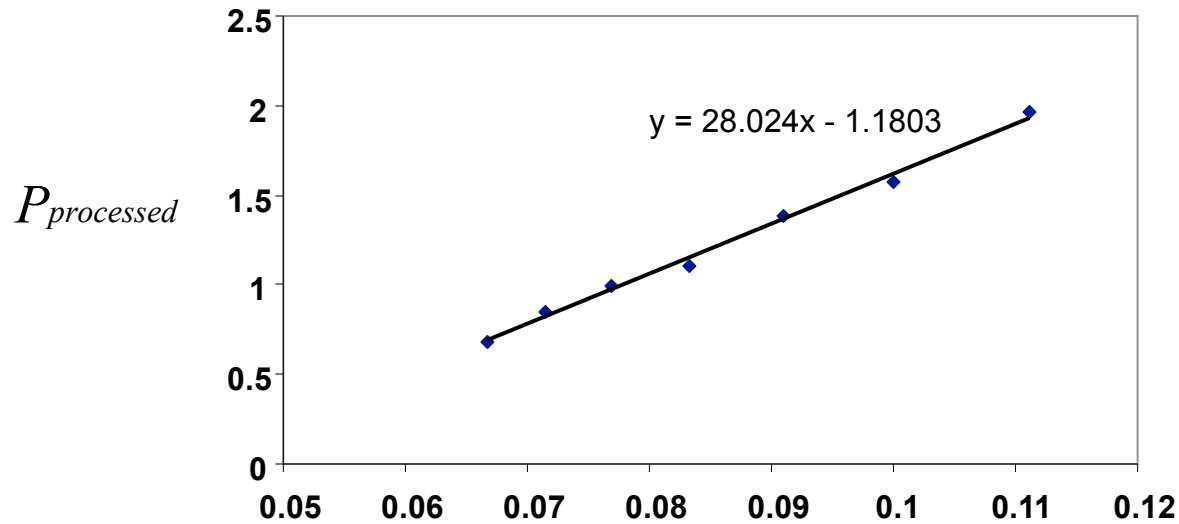
*Note: Misorientation calculation is based on only nearest neighbors in a 3D voxelized structure.*

# 3D Simulation Results



Average over 2 textures is based on the similar MDFs for synthetic Brass/S textures.

# Abnormal growth Modeling



$$P_{processed} = \sqrt{\ln\left(\frac{P_{random}}{P_{abnormal}}\right)} \quad \frac{1}{\theta}$$

$$P_{abnormal} = P_{random} \exp\left(-\left(\frac{C_1}{\theta} - C_2\right)^2\right)$$

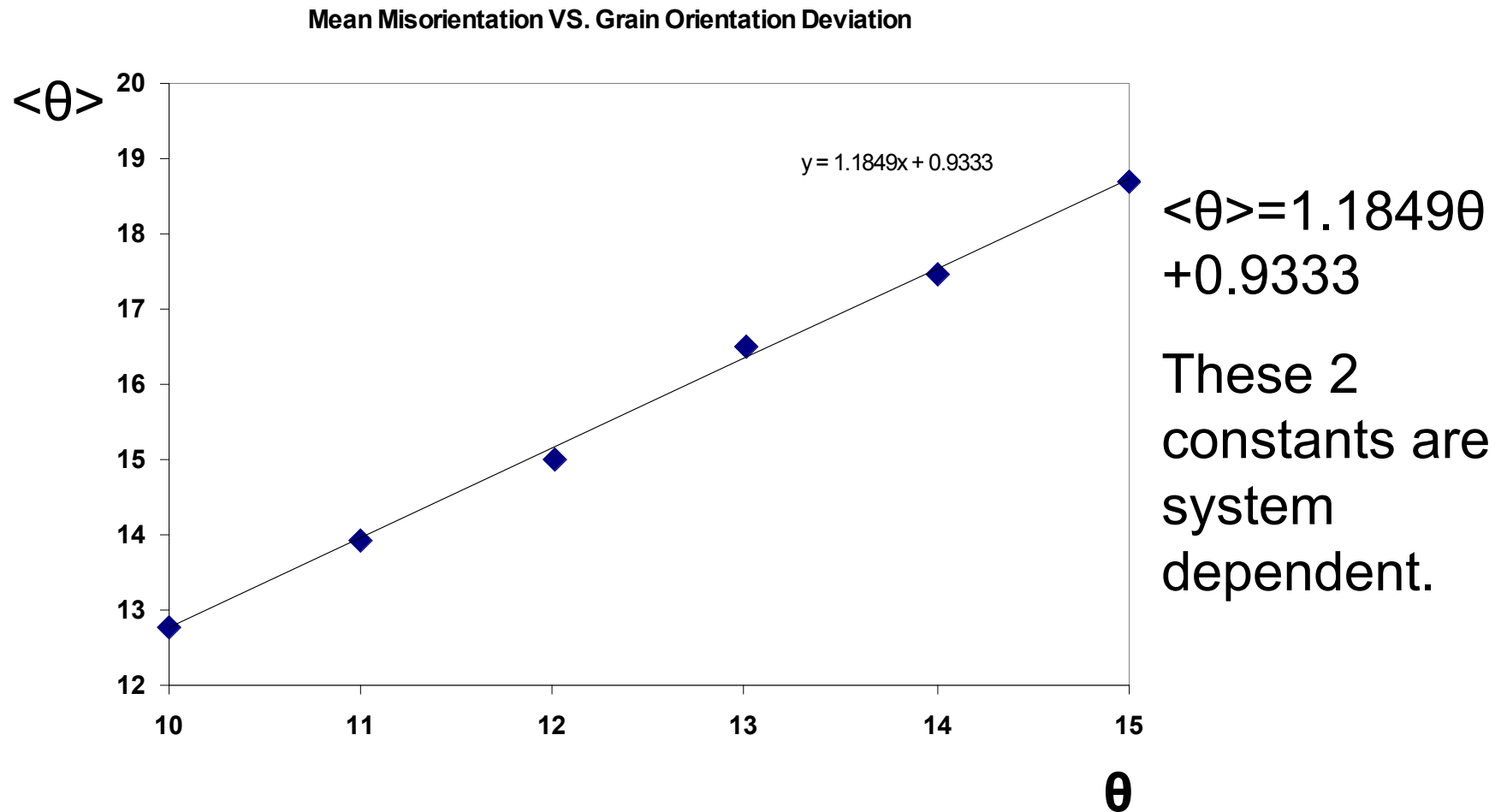
$C_1$  and  $C_2$  are constants,  
28.0 and 1.18 respectively.

Wang *et al.* (2011), *Acta mater.* **59** 3872.

Application conditions:

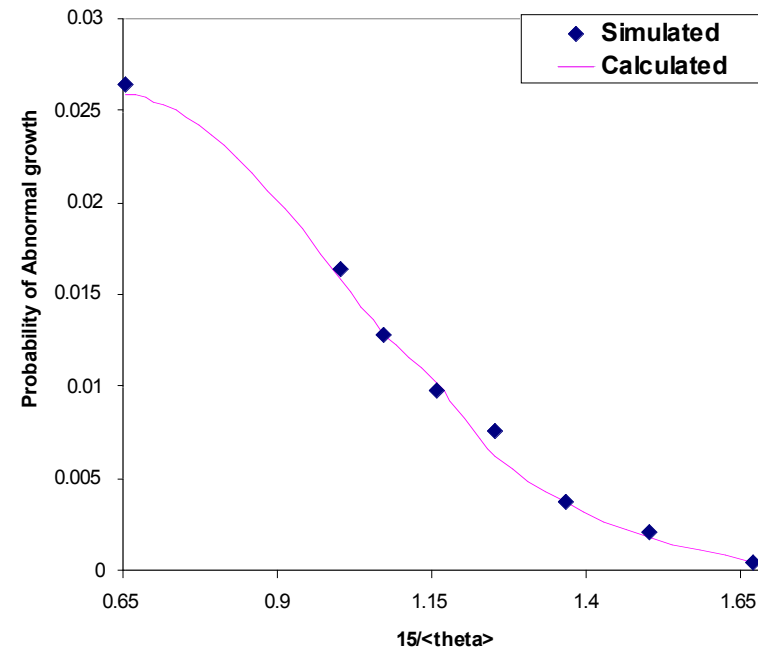
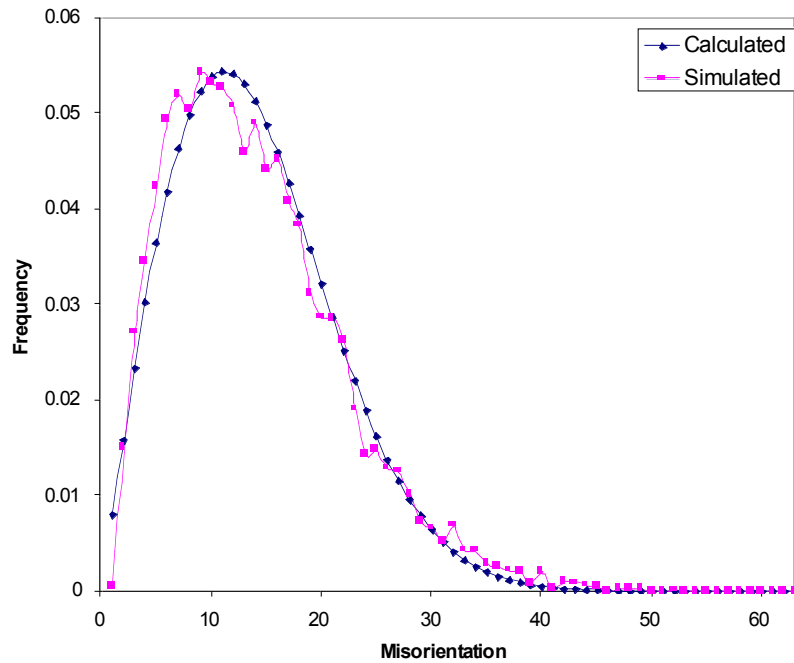
- Strong texture
- One single component

## Relation between GOD & Mean Misorientation





# Model by Wang et al.



$$f(\theta) = c \frac{\theta}{\langle \theta \rangle} \exp \left[ -\frac{\pi}{4} \left( \frac{\theta}{\langle \theta \rangle} \right)^2 \right]$$

$$P_{nucleation} = 0.026 \exp \left( -\left( \frac{28.024}{0.84 \langle \theta \rangle - 0.79} - 1.1803 \right)^2 \right)$$

M.A. Miodownik, P. Smereka, E.A. Holm and D.J. Srolovitz, *Proc. Roy. Soc. Lond.* **A457** 1807 (2001)

## Application *to* Nucleation

$$\langle \theta \rangle = k\sqrt{\varepsilon}$$

Where k is a constant,  $\sim 1.50^\circ$  for incidental subgrain boundaries (IDBs) and  $\sim 7.21^\circ$  for geometrically necessary boundaries (GNBs).

$$\varepsilon = \frac{2}{\sqrt{3}} \ln\left(\frac{o.thickness}{f.thickness}\right)$$

$\varepsilon$  is Von Mises strain.

$$P_{nucleation} = 0.026 \exp\left(-\left(\frac{33.36}{k\sqrt{\varepsilon} - 0.94} - 1.1803\right)^2\right)$$

$$\langle \theta \rangle = 11.5^\circ$$

Based on data: 90% thickness reduction and GNBs.

$$P_{nucleation} = 0.00052$$

D.A. Hughes et al. *Phys. Rev Lett.* **81** 4664 (1998)

Wang et al. (2011), *Acta mater.* **59** 3872.

## Grain Size (after Recrystallization) Model via AsGG

$$V_{grain} = \frac{V_{subgrain}}{P_{nucleation}(\epsilon)}$$

← Subgrain size model      ← Nucleation mode

$$D_{predicted} = \sqrt[3]{V_{grain}(\epsilon)}$$

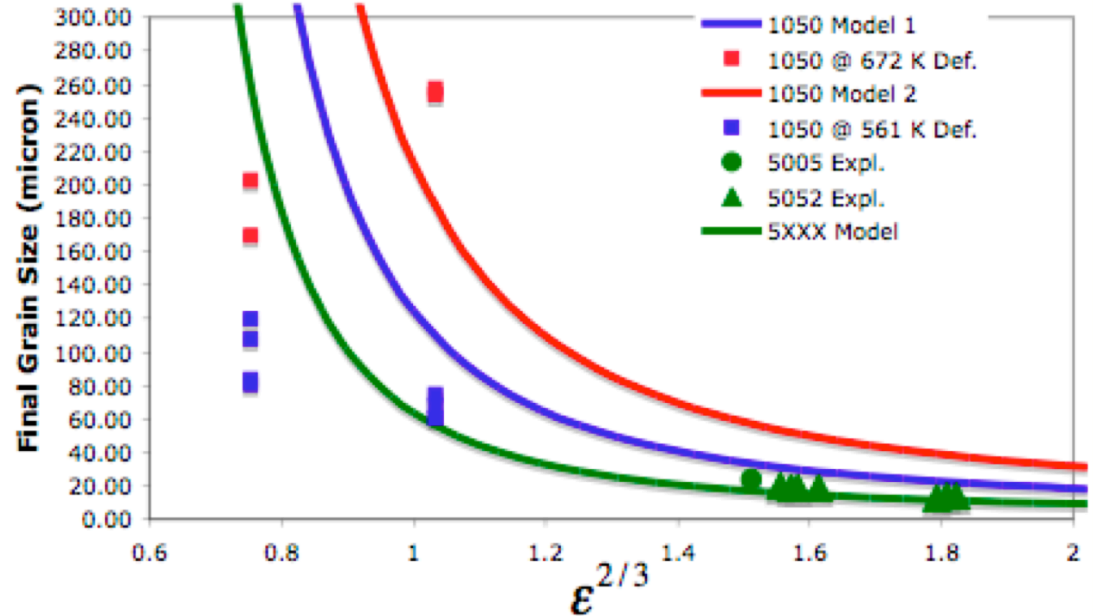
Based on the subgrain size (a constant) calculated from the flow stress model

1050 Model 1: 672 K (Def. T), 5/s (strain rate)

1050 Model 2: 561 K (Def. T), 50/s (strain rate)

5XXX Model: 623 K (Def. T), 50/s (strain rate)

Wang *et al.* (2011). "Modeling the recrystallized grain size in single phase materials." *Acta mater.* **59** 3872-3882.



AA 5XXX: 1.1% Mg, 97% Al, other alloying elements and impurities.

AA1050: Commercial purity aluminum.

AA5052: J.J. Nah *et al.* *Scripta Materialia* **58** (2008) 500-503

AA1050: J.P. Suni, H. Weiland, R.T. Shuey. *Materials Science Forum* 2002; **408 - 412**: 359.

D.A. Hughes *et al.* *Phys. Rev Lett.* **81** 4664 (1998)

## Questions (1)

1. If a given grain has a perimeter that has a higher *mobility* than the boundaries in the surrounding (matrix) grains, what effect does this have on the probability of AGG?
2. If a given grain has a perimeter that has a higher *energy* than the boundaries in the surrounding (matrix) grains, what effect does this have on the probability of AGG?
3. What contradictory effects can impurities have in promoting AGG?
4. What is the main effect of second phase particles on grain boundary migration?
5. What is the main effect of second phase particles on grain growth kinetics?
6. What effect do pores have on grain growth?
7. In what way are pores different from (most) second phase particles?

## *Questions (2)*

1. What is “relative size” in the context of AGG?
2. What does an analysis of relative size reveal in terms of mobility and energy ratios?
3. What impact does abnormal growth in subgrain networks have on primary recrystallization?
4. Why is the dependence of average GB misorientation on plastic strain important?
5. Why is the subgrain size as a function of flow stress important?
6. How does abnormal subgrain growth help to explain the fact that recrystallized grain size depends on prior strain (and deformation conditions such as deformation temperature and strain rate) but not on annealing temperature?

## *Summary*

- The kinetics of abnormal grain growth can be described with a mean field theory that considers the behavior of an exceptional grain. Upper and lower limits to relative size are found, so we expect bimodal grain size distributions.
- Abnormal grain growth in a limited range of orientations (subgrains) occurs when a small minority of grains have misorientations large enough to give their perimeters high mobility.
- AGG can also occur if the boundaries of a grain undergo a transition to high mobility, e.g. impurity segregation leading to a transition in the GB structure.
- AGG demonstrated to occur in the presence of particle pinning, provided that the grain size is smaller (but not too much smaller) than the Smith-Zener limit. If a higher than random fraction of particles is present on the boundaries, then this raises the probability of AGG.

# *Supplemental Slides*



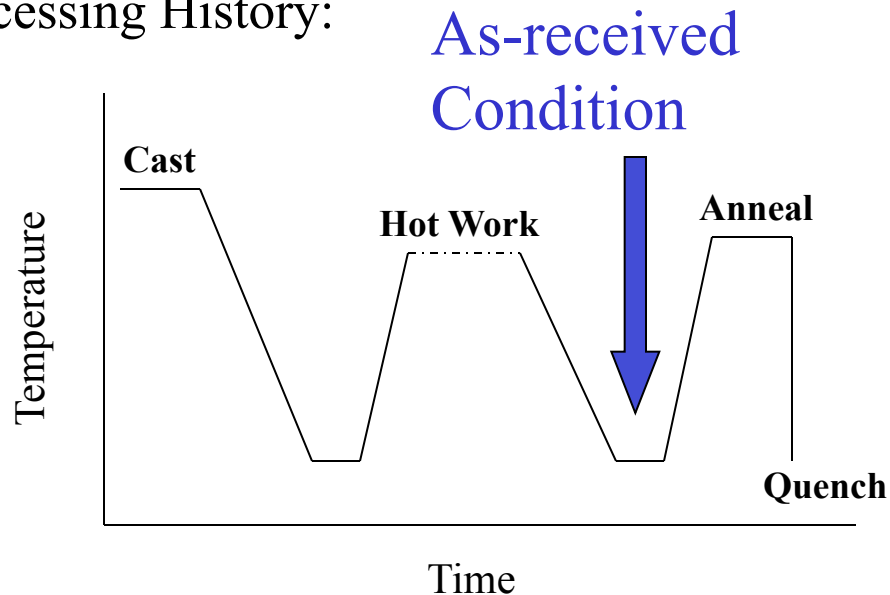
## Waspaloy: Experimental

**Waspaloy** is a high strength, nickel base, precipitation-hardening alloy.

Waspaloy Composition:

Al	B	C	Nb	Co	Cr	Fe	Mo	Mn	Ni	Ti	Zr
1.34	0.01	0.04	0.06	13.5	19.8	0.79	4.25	0.04	Bal.	2.98	0.05

Processing History:



**Effect of High Temperature:**

1.  $\gamma'$  dissolves
2. Only [MC] type carbides are present.
3. Complex alloy is essentially reduced to 2 phases:  
Matrix + Carbides

Roberts, PhD thesis CMU (2007)

Sims and Hagel, *The Superalloys*, Wiley: New York (1972), p. 577.

Jackman, Canada and Sczerzenie, *Superalloys 1980*, TMS: Warrendale, p. 365

Annealing Temperature =  
1100°C (above the  $\gamma'$  solvus)

## Particle/Boundary Stereological Relationship

The number fraction of particles on grain boundaries was measured and predicted for the (1) initial and (2) annealed conditions (i.e. 1100°C/1h).

**Predicted:** 
$$\frac{(N_A)_b}{N_A} = \frac{8}{\pi} r L_A$$

**Observed:** 
$$\frac{(N_A)_b}{N_A} = \frac{n_{gb}}{n_{gb} + n_{bulk}}$$

Assumptions:

- (1)  $N_S = N_A$
- (2) spherical particle
- (3) uniform spatial distribution

Definitions:

$(N_A)_b$  = # of particles on boundaries

$N_A$  = # of particles

$r$  = particle radius

$L_A$  = grain boundary trace per unit area

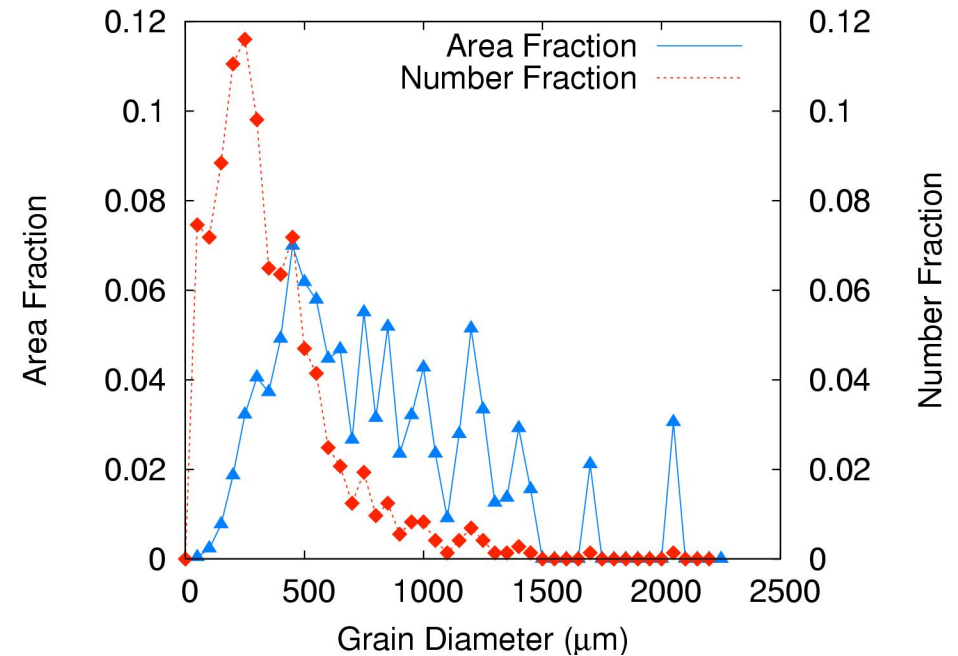
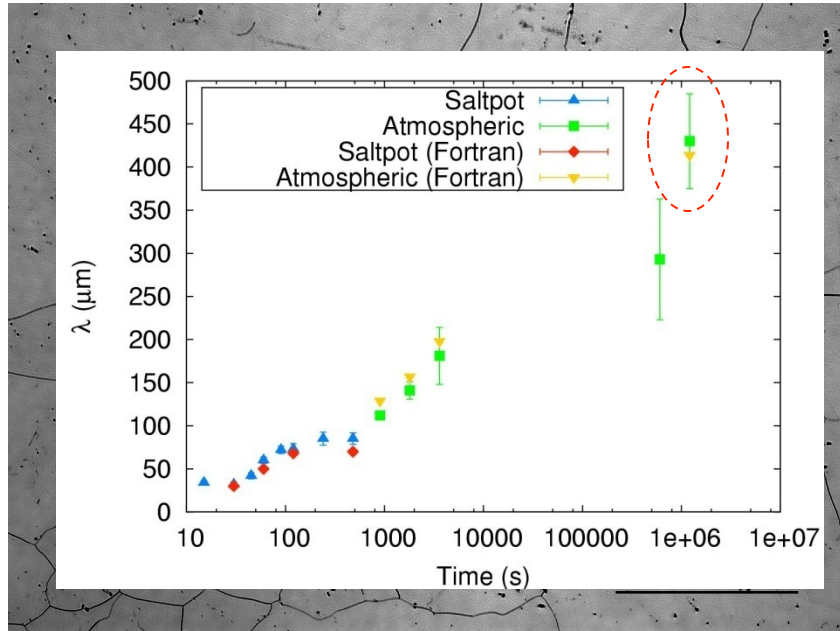
The fraction on boundaries decreased in agreement with theoretical calculations; however, both experimental conditions showed higher fractions than predicted from random intersections.

History	Expected	Observed
As-received	0.23	0.61
1100°C/1h	0.07	0.19

Roberts, PhD thesis  
CMU (2007)

Larger than expected fractions on boundaries may explain why the limiting grain size is commonly less than the Smith-Zener limit.

# Abnormal Grain Growth in Waspaloy



To obtain a pinned microstructure, the material was annealed for an extended period of time; however, abnormal grain growth (AGG) occurred at long annealing times (1100°C/2wk).

What is the *cause of AGG* in this material?

*Texture?* The orientation and misorientation were random, implying that texture does not initiate or control AGG.

*Particles?*

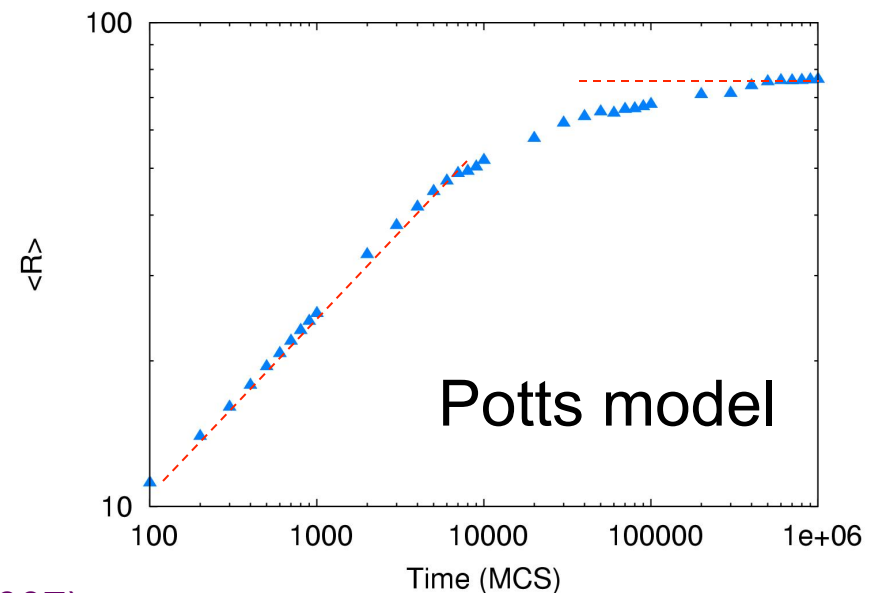
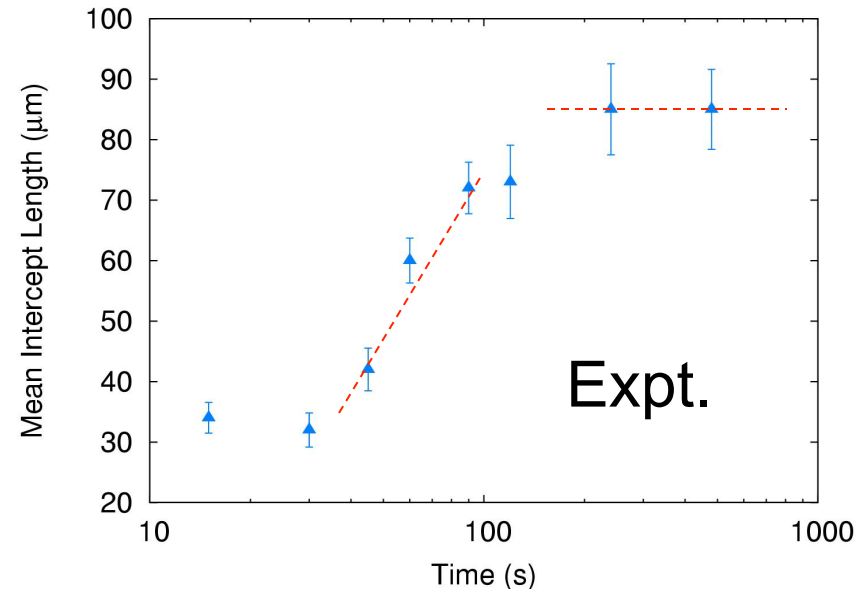
*Size Advantage?*

## Comparison of Expt. w/ Simulation

Experiment and simulation show qualitative agreement of the observed growth trends.

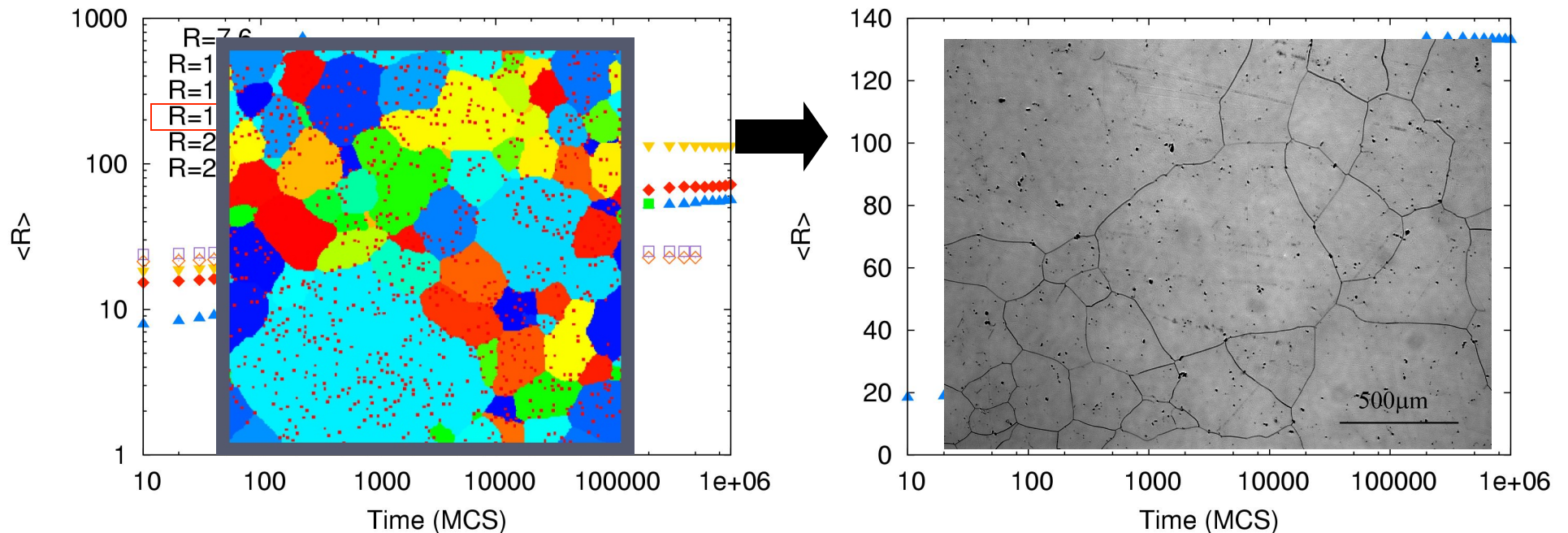
Note:

The nickel alloy increased its mean grain size by a factor of  $\sim 2.5$  while the simulations exhibited factors greater than 3.



## Comparison of Expt. w/ Simulation

A transition from NGG to AGG was observed in both the simulations and experiment.



Initiation of AGG was caused by grain size advantage and/or non-random particle distributions on grain boundaries. More specifically, if the grain size is smaller than the Smith-Zener limit, but the structure is pinned by the larger-than-random density of particles on boundaries (to match expts.), then it is possible for a large grain to escape and become “abnormal”.

Simulation: isotropic GB properties; temperature = 1.5; particles size = 27 voxels; volume fraction of particles = 6%, 70% of particles were located *on boundaries*; image taken at 100,000 MCS.

Roberts, PhD  
thesis CMU  
(2007)

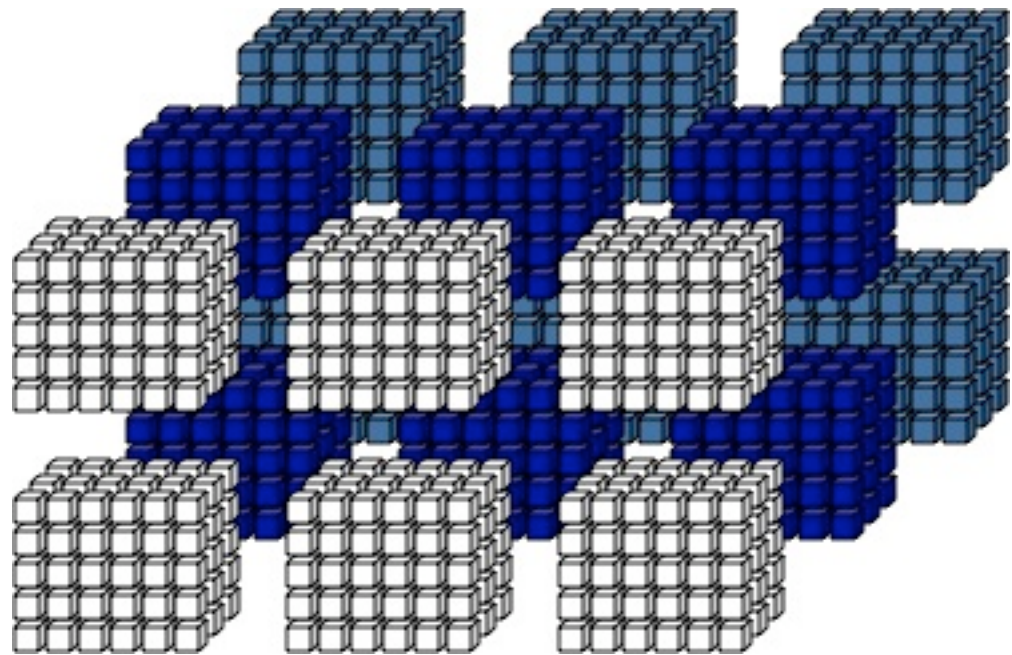
# Software

- Materials people have, collectively, invested substantially in software development.
- CMU philosophy: unless there exists an obvious opportunity for commercialization, it is better to make software freely available.
- CMU makes its tools for serial and parallel algorithms for Monte Carlo, phase field, and level set models of grain growth, as well as particle dissolution. We have already made many of our 3D microstructure analysis tools available on the web.
- CMU software is distributed over a number of websites.
  - <http://code.google.com/p/mbuilder/> : Microstructure Builder
  - <http://matforge.org/cmu/> : MMSP package
  - <http://latir.materials.cmu.edu/websvn>
  - <http://mimp.materials.cmu.edu/research/downloads.html>
  - [http://neon.materials.cmu.edu/rollett/texture\\_subroutines](http://neon.materials.cmu.edu/rollett/texture_subroutines)



*MMSP is a library of functions that  
manipulate parallel uniform grids*

- Written in C++ using MPI
- Open-source, extensible
- Parallelism mostly hidden
- Most serial algorithms written in C or C++ can be quickly parallelized
- Primarily intended for numerical modeling



*Grid data subdivided  
across an array of 18  
processors*



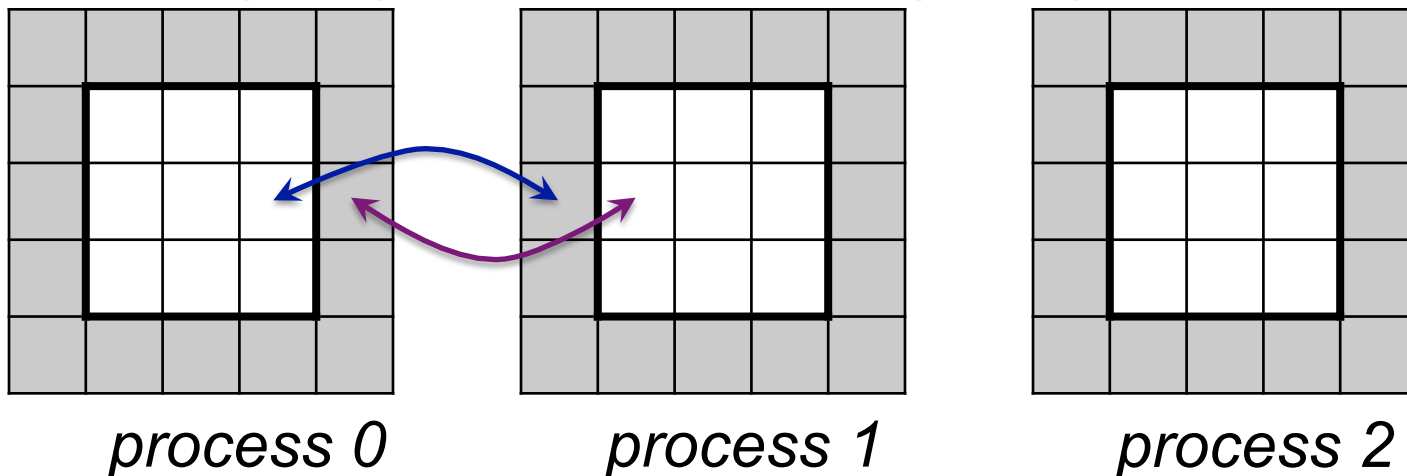
# *An MMSP grid is a distributed array*

## ***Distributed:***

Each MPI process “owns” its own segment of the array, and “shares” ghost buffers

This permits the creation of **very large grids** which can be accessed at the same time by **many processors** on any system with MPI installed (either shared or distributed memory architectures).

*ghost buffers (grey); original domain (white)*



# *An MMSP grid is a templated array*

## ***Templated:***

An MMSP grid can store *any type of data*.

An MMSP grid is *N-dimensional*, where N is any positive, non-negative integer.

This permits **tremendous versatility in the data structure** used to represent information at each point in the domain, and also enables **dimension-independant coding**

## ***Supported data types:***

- Any POD data type: `int`, `float`, `double`, etc.
- Any STL container: `std::vector`, `std::map`, `std::list`, `std::string`, `std::complex`, etc.
- MMSP built-in data types, such as **arrays**, **matrices**, **sparse vectors**, **sparse matrices**, **tensors**, etc.
- Advanced users can create their own data types as well.

## *When to use MMSP*

- . . . when the required computations are **data-intensive** (large domains) so that data parallelism makes sense
- . . . when the workload is **evenly distributed** across the domain (or approximately so)
- . . . when you have access to a **large computing system** (with either shared or distributed memory) and on which MPI has been installed
- . . . when your computation requires a **complicated data type** (such as vector, sparse vector, or sparse tensor data) at every node in your grid

---

*Other options exist, such as global arrays:*

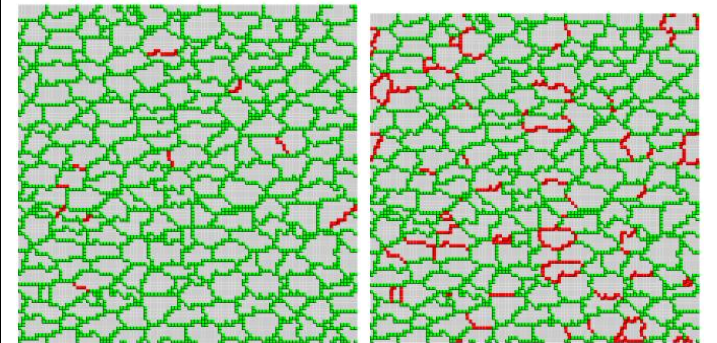
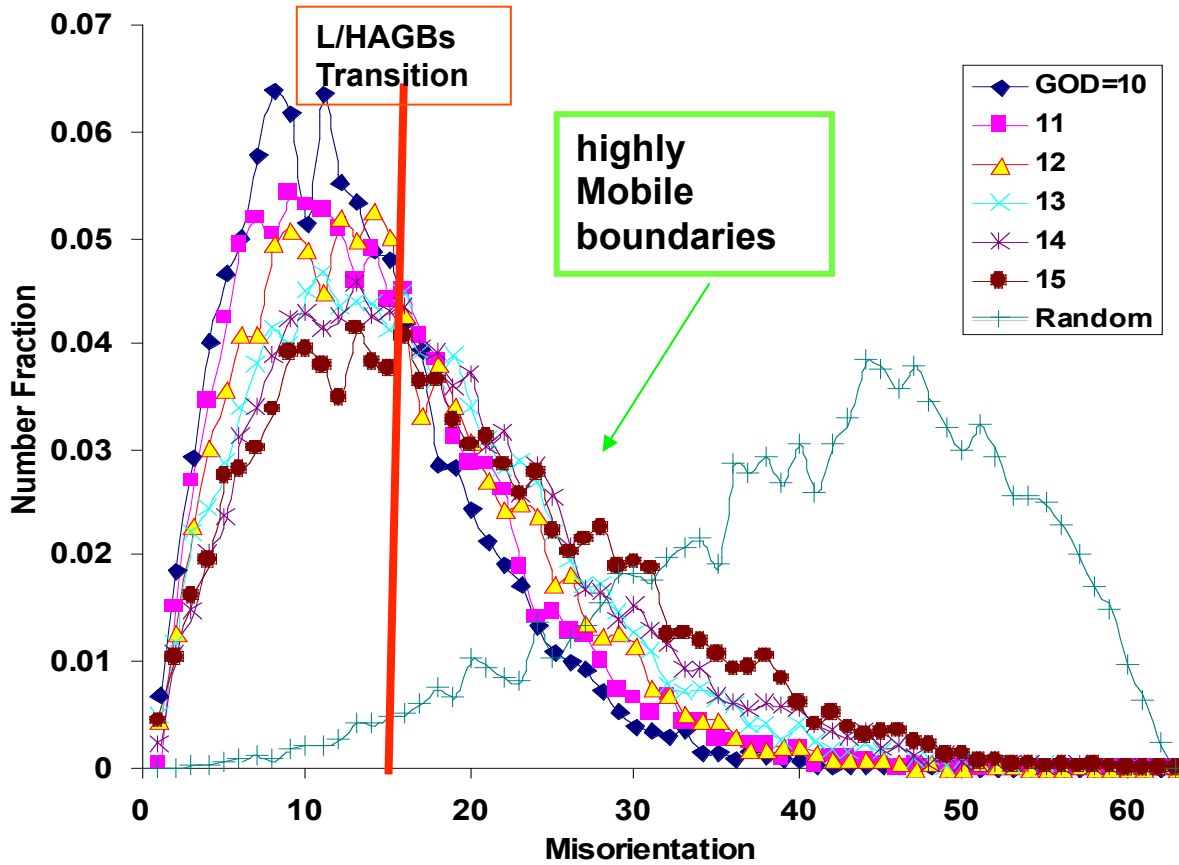
<http://www.emsl.pnl.gov/docs/global/>

*MMSP is not compatible with some excellent software utilities (such as PETSC; <http://www.mcs.anl.gov/petsc/petsc-as/> )*

## *Adapting MMSP for AGG*

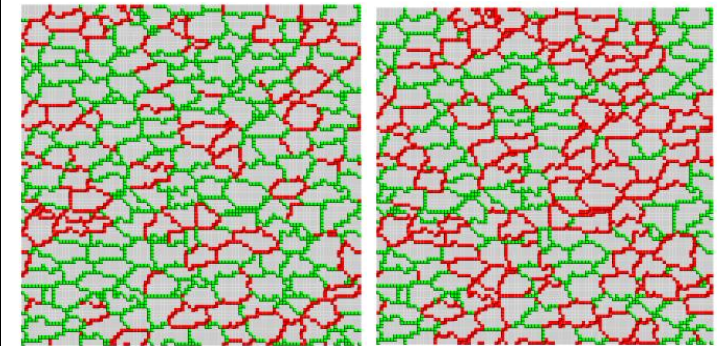
- Use the Potts model (Q-state Ising) for simplicity and efficiency
- Moderately large domains run in minutes on a single CPU
- Run isotropic grain growth until small, compact grain structure developed
- Use microstructure from previous run as input; declare a small ( $\sim 10$ ) grains as abnormal grains; assign their perimeters as having low energy and high mobility  
allow the system to evolve
- Measure the results
- Eventually, repeat in phase field to permit dependence of energy, mobility on boundary normal (e.g. to capture the faceted growth observed in yttria)

# Synthetic Textures (One Component)



5°

8°



12°

15°

— HAGBs (< 15°)

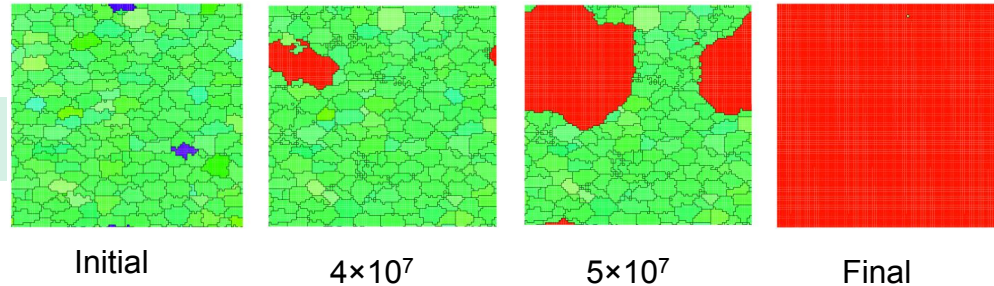
— LAGBs (< 15°)

$$GROD = \frac{1}{N} \sum_i^N (G_i G_{average}^{-1})$$

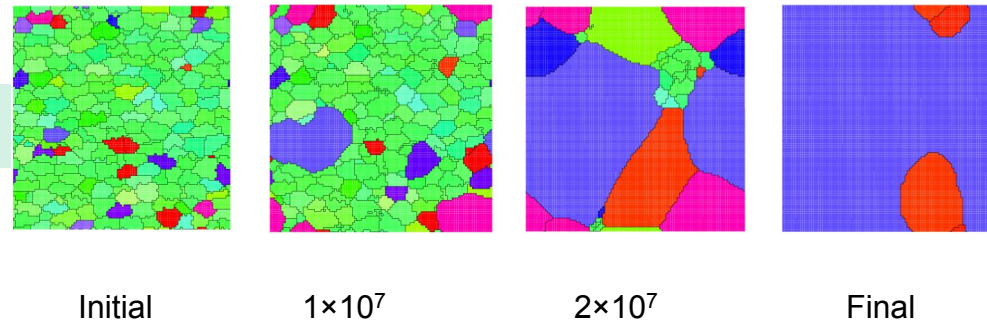
Note: Misorientation calculation is based on only nearest neighbors in a 3D voxelized structure.

## *AsGG - Brass Component*

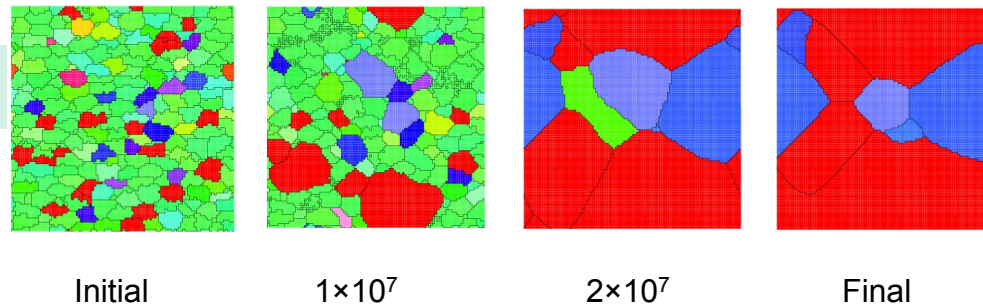
8° GROD of Brass



12° GROD of Brass



15° GROD of Brass



The number of abnormally large grains (ALG) increases as deviation increases.

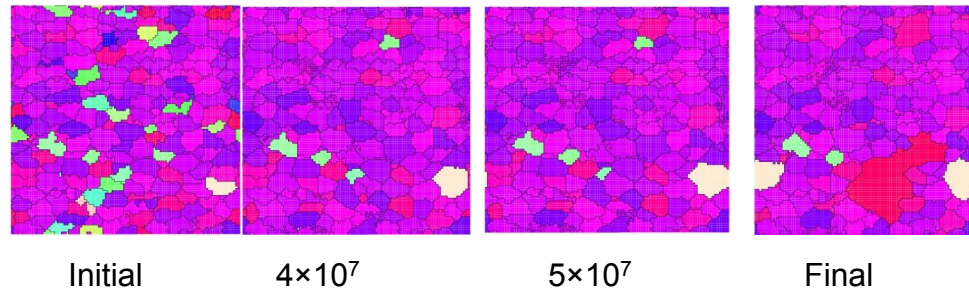
Time

**AGG** has occurred when a minority of grains grow much larger than the majority (“matrix”). An “abnormal grain” is defined as one that is  $> 8X$  initial average volume.

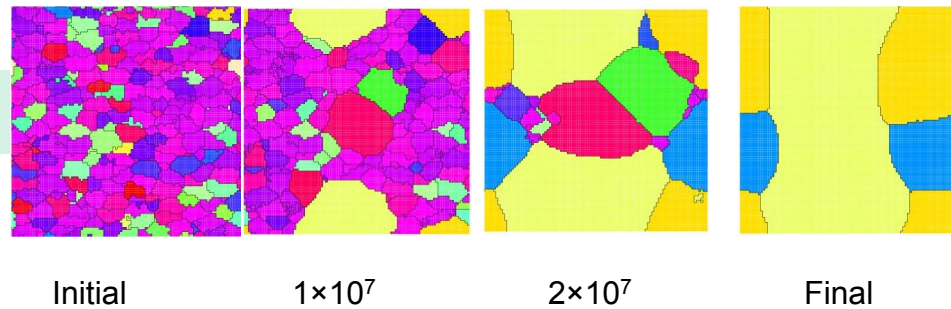


# *AsGG - S Component*

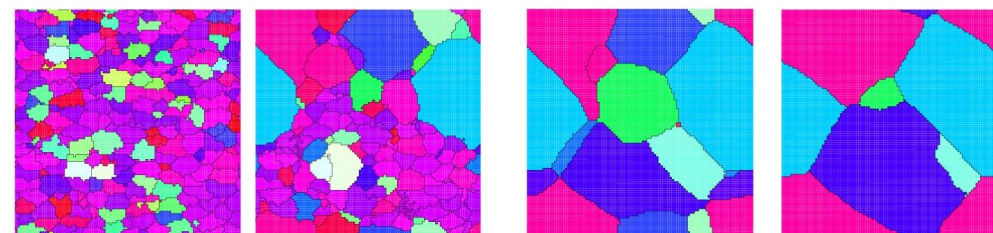
8° GROD of **S**



12° GROD of **S**

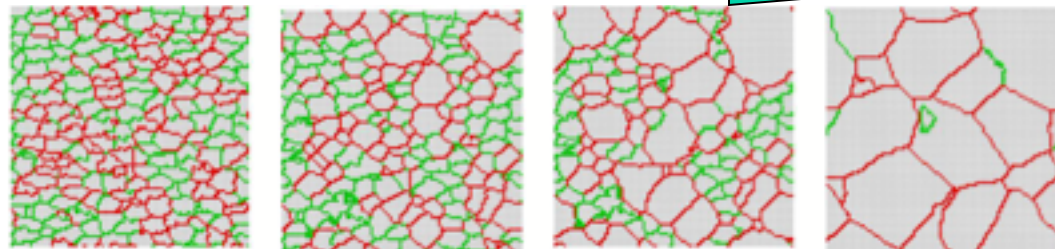


15° GROD of **S**



The number of abnormally large grains (ALG) increases as deviation increases.

**AGG** has occurred when a minority of grains grow much larger than the majority ("matrix"). An "abnormal grain" is defined as one that is  $> 8X$  initial average volume.



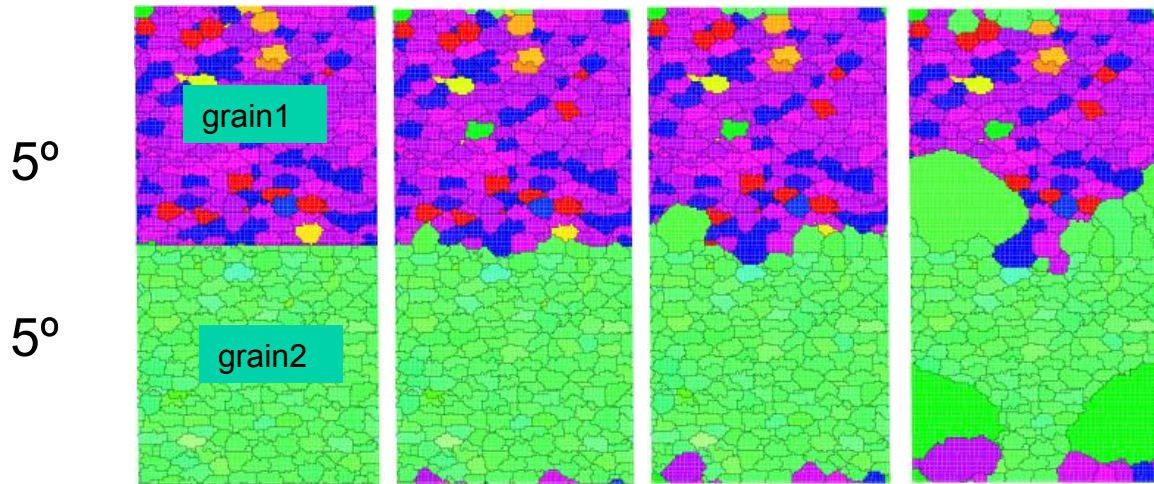
— HAGBs ( $\geq 15^\circ$ )

— LAGBs ( $< 15^\circ$ )

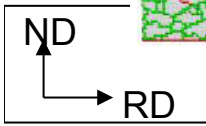
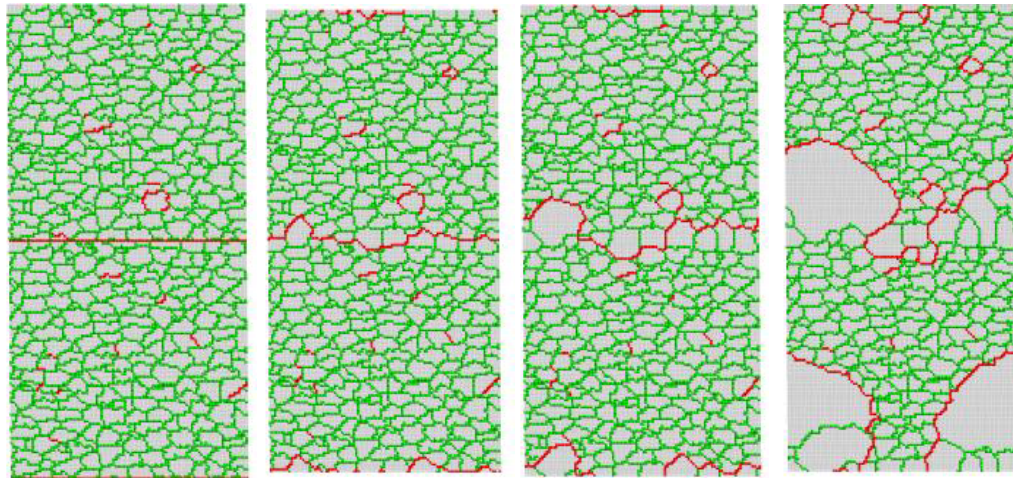


100

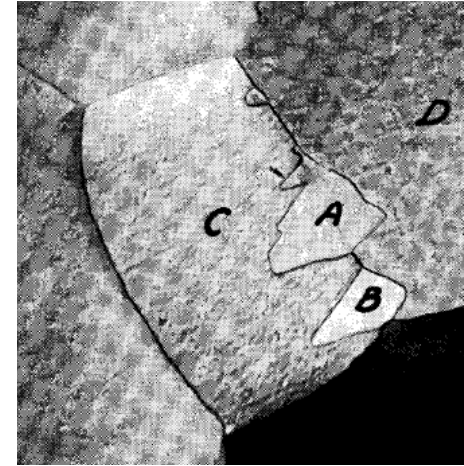
# SIBM



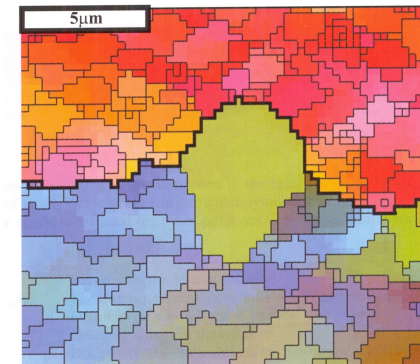
Initial  $2 \times 10^5$  Steps  $5 \times 10^6$  Steps  $9 \times 10^6$  Steps



Components: **Brass** Bunge Angles: 35,45,0 **S** : 123,27,221



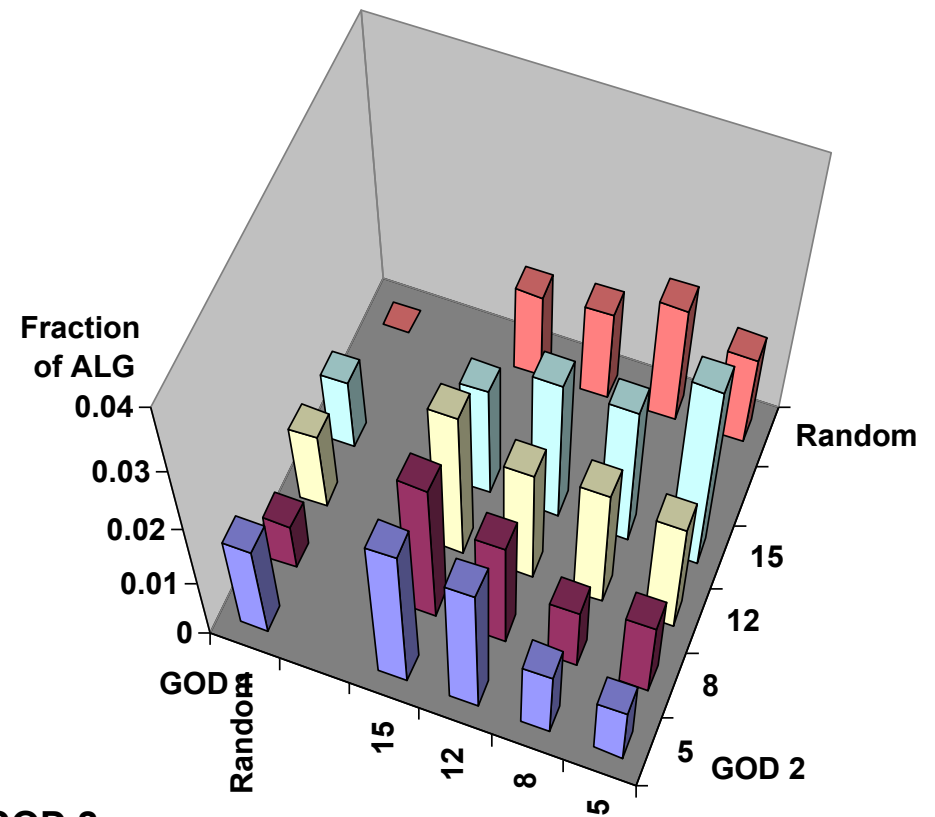
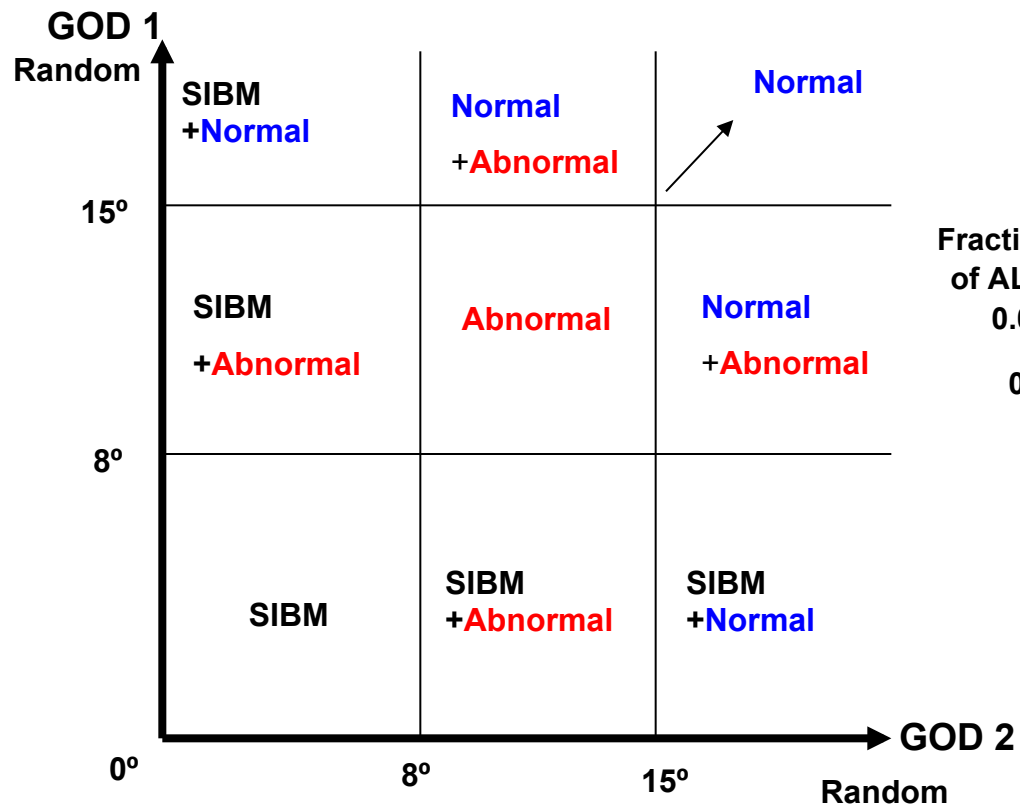
1. Nucleation at HAGB after 20% thickness reduction in aluminum. New grain A,B are growing between deformed grain C,D.



2. EBSD Map showing SIBM in Al-0.1 wt% Mg, cold rolled 20% and annealed at 300°C. HAGBs are black and LAGBs are grey.

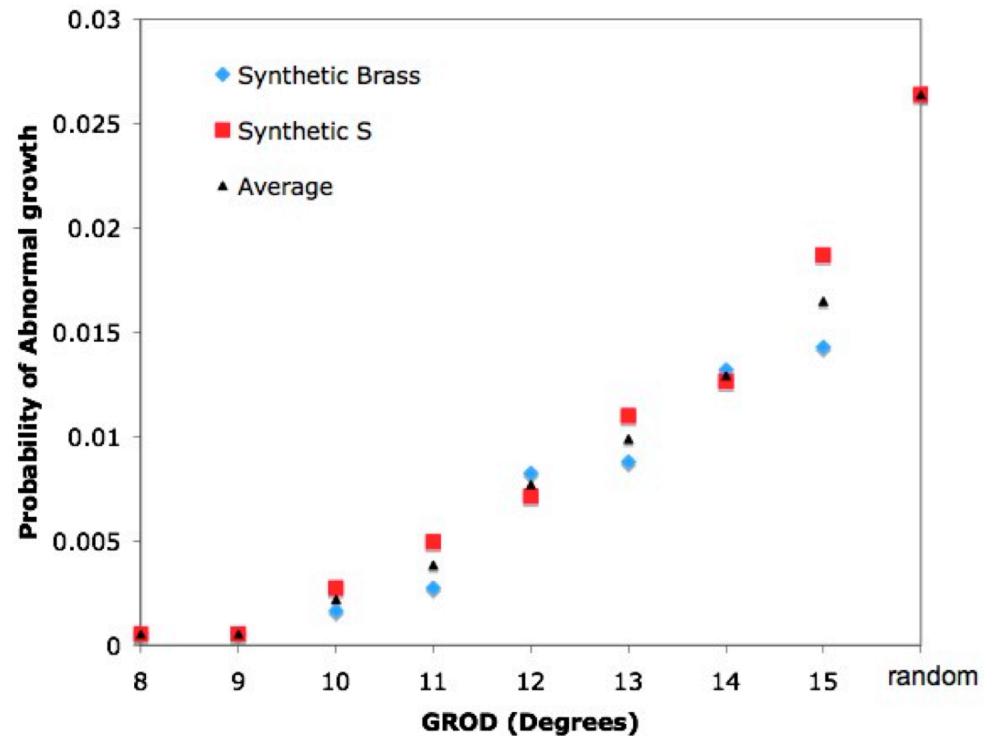
1. Beck PA, Sperry PR.. *J. Applied Physics.* (1950); **21**:150-152  
 2. P.J. and Humphreys, F.G. (2003), *Acta Mater.* **51**.

# Subgrain Coarsening - Map



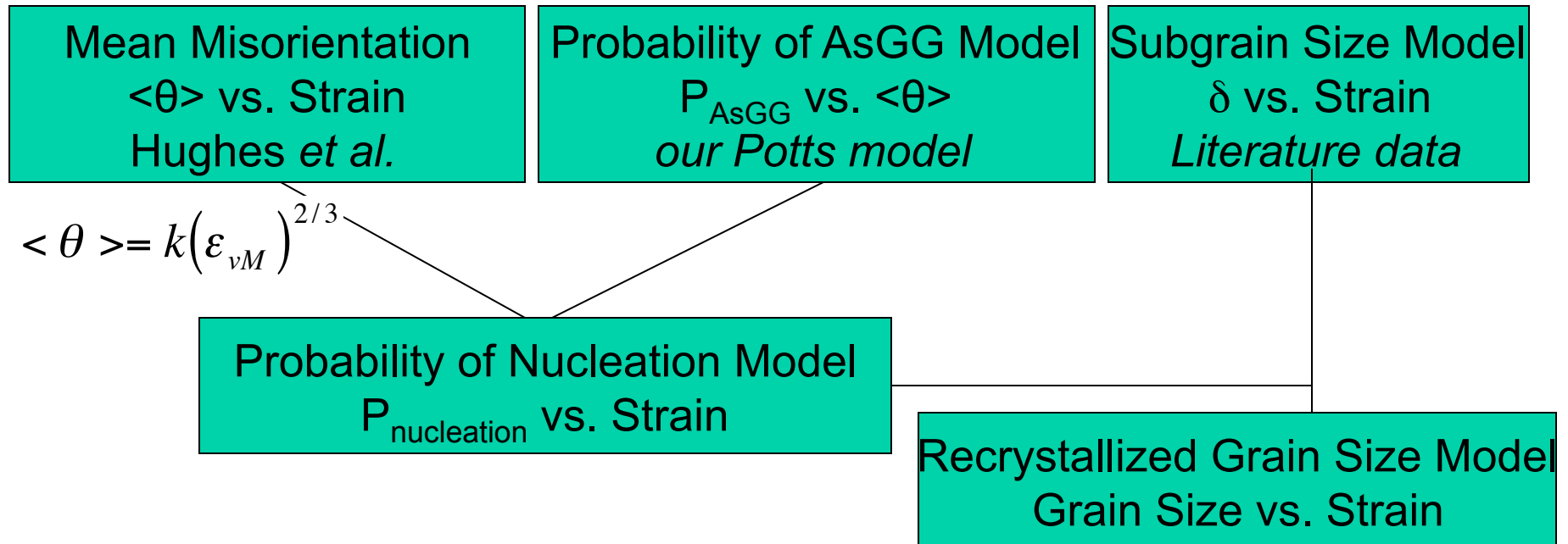
Note: based on studies of Brass and S texture components. An ALG is a (sub)-grain which is 8 times greater in volume than the average at  $10^6$  MCS.

# Summary of Simulation



- Both AsGG and SIBM was successfully simulated using 3D Monte Carlo method. The 3D digital materials model physical textures with variable orientation spread, which is correlated with the mean misorientation.
- Which recrystallization nucleation mechanism operates depends on the orientation spread. For example, when both grains have orientation spreads (GROD values) smaller than  $5^\circ$ , SIBM is dominant.

# *Recrystallized Grain Size based AsGG*



**We need a functional form for  $P_{AsGG}$  vs.  $\langle \theta \rangle$ :**

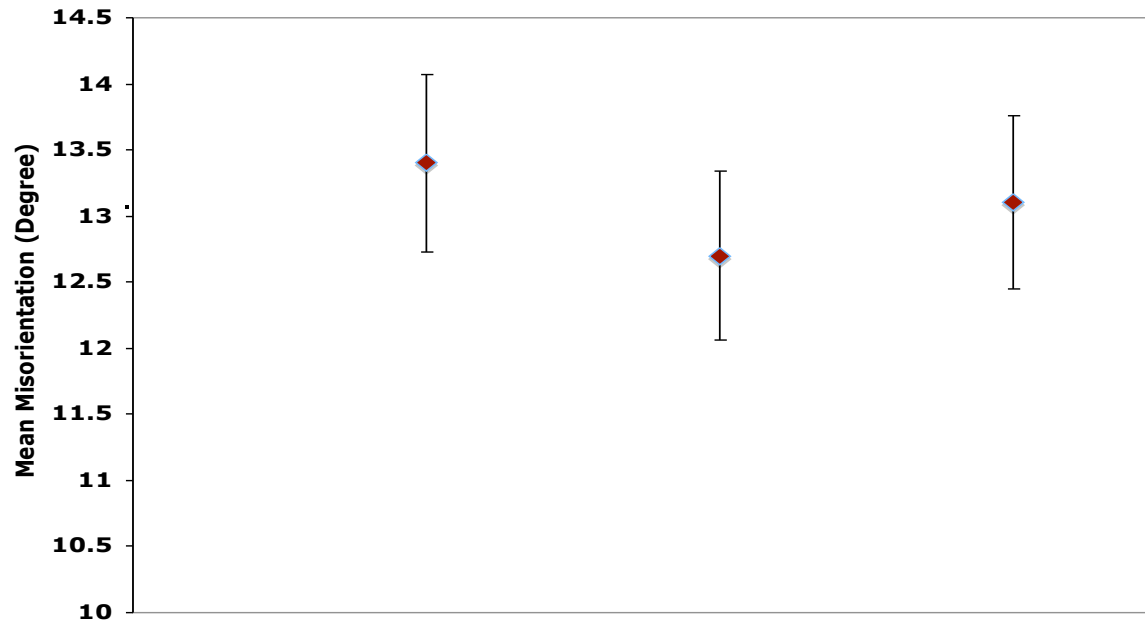
Model 1: Regression analysis of the probability of AsGG against  $\theta$  (GROD).

Model 2: Regression analysis of the probability of AsGG against  $15/\langle \theta \rangle$ .

Model 3: Exponential function found by plotting the scaled probability of AsGG against  $1/\theta$ .

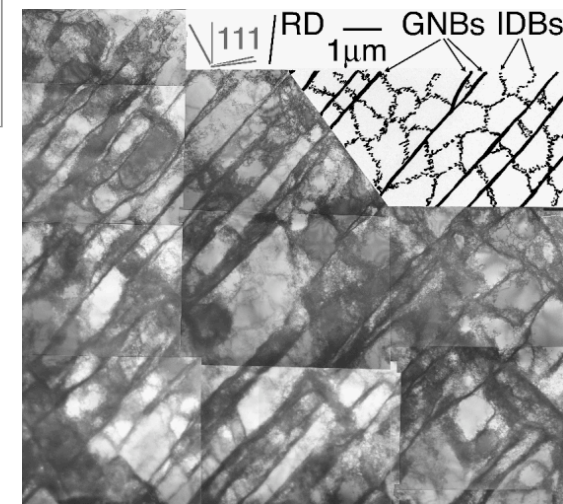


# Mean Misorientation Validation



EBSD data Average  $\langle \theta \rangle = 13.1^\circ$

Hughes's equation  
is valid!



**AA5005 data: 90% thickness reduction and GNBs.**

**Hughes's Observation:**

$$\langle \theta \rangle = k \sqrt{\varepsilon_{vM}} \quad \varepsilon_{vM} = \frac{2}{\sqrt{3}} \ln \left( \frac{\text{Original thickness}}{\text{Final thickness}} \right)$$

Where  $k$  is a constant,  $\sim 1.50^\circ$  for incidental subgrain boundaries (IDBs) and  $\sim 7.21^\circ$  for geometrically necessary boundaries (GNBs).

$\varepsilon_{vM}$  is von Mises strain.

TEM micrograph showing the arrangement of dislocation boundaries developing in pure Ni deformed to a rolling reduction of 20%.

# Subgrain Size Models

## Shear Stress Model

$$\delta = bK(\tau/G)^{-r}$$

$\tau$  : shear stress  
 $G$  : shear modulus

$$\gamma_{slip\ system} = \frac{\gamma_{shear}}{\langle M_{torsion} \rangle} = \frac{\epsilon_{v.m.}}{\langle M_{tension} \rangle}$$

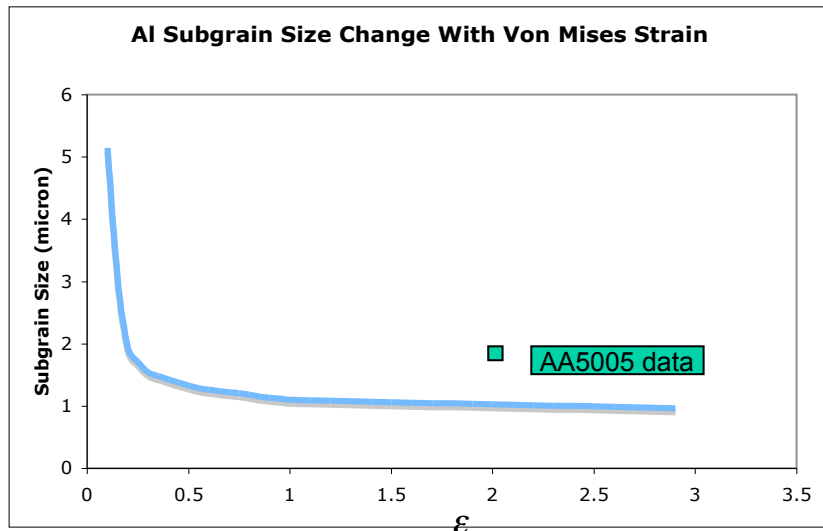
$$\epsilon_{v.m.} = 3.07 \times \frac{\sqrt{3}}{2.7} \gamma_{shear}$$

Burgers vector :  $b = 2.86 \times 10^{-10} m$

$K=10, r=1$

### Steps:

1. von Mises strain is converted to shear strain.
2. Shear stress is found from the shear stress-strain curve.
3. Insert shear stress into the subgrain size equation.
4. Plot subgrain size as a function of v.M strain.



Timothy J. Ginter, Farghalli A. Mohamed, *Journal of Materials Science* 17 (1982) 2007-2012  
 D.A. Hughes et al. *Phys. Rev Lett.* 81 4664 (1998)

## Flow Stress Model

$$\bar{\sigma} = \frac{1}{\alpha} \ln \left\{ \left( \frac{Z}{A} \right)^{\frac{1}{n}} + \sqrt{\left[ \left( \frac{Z}{A} \right)^{\frac{2}{n}} - 1 \right]} \right\}$$

Zener-Hollomon Parameter  
 $Z = \dot{\epsilon} \exp\left(\frac{\Delta H}{RT}\right)$

Alloy	Def. Temp (K)	$\alpha$	$\dot{\epsilon}$ (1/s)	$\Delta H$ (J)	$\ln A$	n	Stress (Mpa)	$\delta$ (Subgrain Size) ( $\mu m$ )
1050	561	0.037	50	15688	26.69	3.84	31.71	2.34
1050	672	0.037	5	15688	26.69	3.84	12.77	5.82
1050	561	0.037	5	15688	26.69	3.84	26.29	2.83
1050	672	0.037	50	15688	26.69	3.84	18.54	4.01
5XXX	623	0.051	50	16549	23.56	2.74	46.70	1.59
5XXX	623	0.051	5	16549	23.56	2.74	39.13	1.90
5XXX	623	0.051	10	16549	23.56	2.74	41.40	1.80

Assumption: The strain rate and deformation temperature for 5XXX (5000 series) alloy are based on typical industry process parameters.

T. Sheppard, M.A. Zaidi, P.A. Hollinshead, N. Raghunathan. *Structural Evolution During The Rolling of Aluminium Alloys*. In: Chia E, H., McQueen HJ, editors. *Microstructural Control in Aluminium Alloys: Deformation, Recovery and Recrystallization* New York, USA, 1985. p.19.

# Subgrain Size Models

## Flow Stress Model

$$\bar{\sigma} = \frac{1}{\alpha} \ln \left\{ \left( \frac{Z}{A} \right)^{\frac{1}{n}} + \sqrt{\left[ \left( \frac{Z}{A} \right)^{\frac{2}{n}} - 1 \right]} \right\}$$

Zener-Hollomon Parameter

$$Z = \dot{\epsilon} \exp\left(\frac{\Delta H}{RT}\right)$$

Alloy	Def. Temp (K)	$\alpha$	$\dot{\epsilon}$ (1/s)	$\Delta H$ (J)	$\ln A$	$n$	Stress (Mpa)	$\delta$ (Subgrain Size) ( $\mu\text{m}$ )
1050	561	0.037	50	156888	26.69	3.84	31.71	2.34
1050	672	0.037	5	156888	26.69	3.84	12.77	5.82
1050	561	0.037	5	156888	26.69	3.84	26.29	2.83
1050	672	0.037	50	156888	26.69	3.84	18.54	4.01
5XXX	623	0.051	50	165499	23.56	2.74	46.70	1.59
5XXX	623	0.051	5	165499	23.56	2.74	39.13	1.90
5XXX	623	0.051	10	165499	23.56	2.74	41.40	1.80

Subgrain size obtained from standard relationship between flow stress and subgrain size.

Assumption: The strain rate and deformation temperature for 5XXX (5000 series) alloy are based on typical industry process parameters.

T. Sheppard, M.A. Zaidi, P.A. Hollinshead, N. Raghunathan. *Structural Evolution During The Rolling of Aluminium Alloys*. In: Chia E, H., McQueen HJ, editors. *Microstructural Control in Aluminium Alloys: Deformation, Recovery and Recrystallization* New York, USA, 1985. p.19.



# Grain Size (after Recrystallization) Model via AsGG

$$V_{grain} = \frac{V_{subgrain}}{P_{nucleation}(\epsilon)}$$

← Subgrain size model  
← Nucleation model

$$D_{predicted} = \sqrt[3]{V_{grain}(\epsilon)}$$

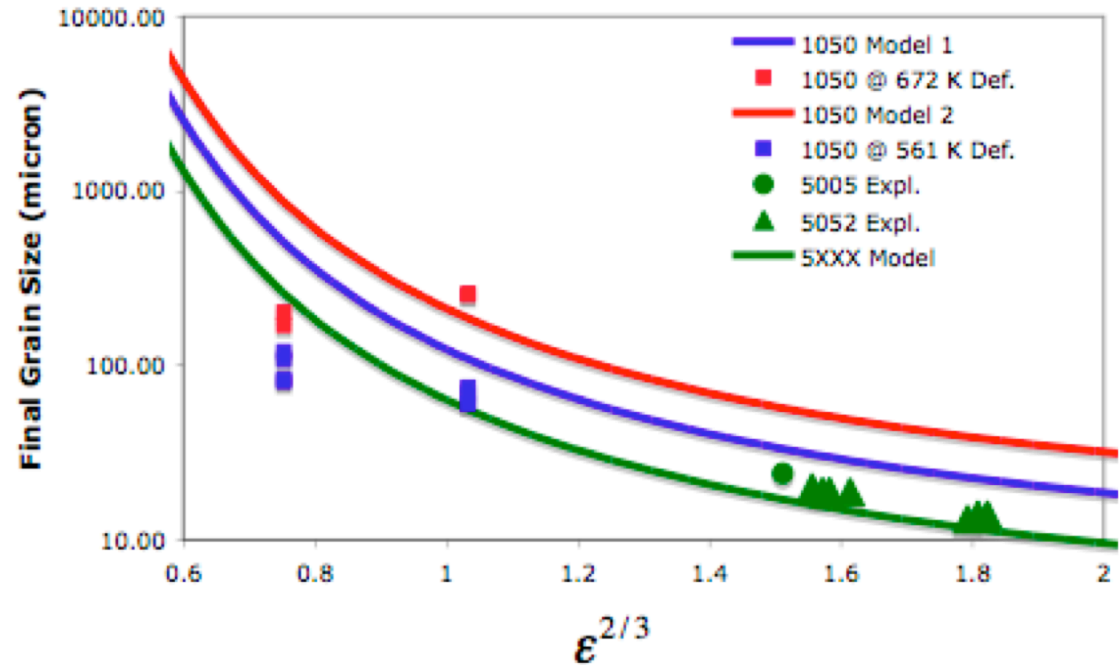
Based on the subgrain size (a constant) calculated from the flow stress model

1050 Model 1: 672 K (Def. T), 5/s (strain rate)

1050 Model 2: 561 K (Def. T), 50/s (strain rate)

5XXX Model: 623 K (Def. T), 50/s (strain rate)

log-scale grain size



AA 5XXX: 1.1% Mg, 97% Al, other alloying elements and impurities.

AA1050: Commercial purity aluminum.

AA5052: J.J. Nah et al. *Scripta Materialia* **58** (2008) 500-503

AA1050: J.P. Suni, H. Weiland, R.T. Shuey. *Materials Science Forum* 2002; **408 - 412**: 359.

D.A. Hughes et al. *Phys. Rev Lett.* **81** 4664 (1998)